School of Mining Engineering



UNIVERSITY OF THE
WITWATERSRAND,
JOHANNESBURG

OPTIMISING THE USE OF THREE-DIMENSIONAL DATA TO LOWER GOLD GRADE DILUTION BY CONTROLLING STOPE WIDTH IN THE MINING OF ULTRA-DEEP COMPLEX ORE BODIES.

Anne-Marie Olivier

A research dissertation submitted to the Faculty of Engineering and the Built Environment, University of the Witwatersrand, Johannesburg, in partial fulfilment of the requirements for the degree of Master of Science in Engineering.

Johannesburg, 2023

DECLARATION

I declare that this report is my own, unaided work. I have read the University Policy on Plagiarism and hereby confirm that no plagiarism exists in this report. I also confirm that there is no copying, nor is there any copyright infringement. I willingly submit to any investigation in this regard by the School of Mining Engineering and I undertake to abide by the decision of any such investigation.



_____ 09 January 2023

Signature of Candidate Date

ABSTRACT

Excessive hanging wall or footwall dilution in narrow, tabular gold mines affects the payability of the mine. Three-dimensional (3D) scanning of stope faces is an option for quickly creating face maps to incorporate into a mine's digital map. As this would make data capturing less time-consuming, the geology team now has more time to guide production regarding stopping width specifications and possibly reduce associated dilution. Unfortunately, Mponeng Mine's current 3D scanner is bulky, expensive and unavailable for direct use by the geology team.

Mponeng Mine investigated more convenient alternatives for 3D scanning of stope faces. Since March 2020, certain Apple products have incorporated a LiDAR scanner. The iPad Pro scanner, with a scanning range, of five metres, was tested in the mine mock-up at the University of the Witwatersrand. A 3D-printed iPad holder was created, holding a compact yet powerful LED light. DigiMine tunnels and stopes were scanned using this hardware and a variety of software. The 3D Scanning App supplied with the iPad Pro was found adequate for the identified purposes. Underground testing was then carried out in the ultra-deep stopes of the Mponeng Gold Mine. These scans can be geo-referenced into the mine's existing digital models. In addition, they can capture the contacts of the ore body. However, the iPad Pro is not waterproof, and the large screen makes it susceptible to damage. So, the mine is now testing LiDAR-equipped iPhone 13 Pro as a more robust, compact option.

ACKNOWLEDGMENTS

The contribution of Senior Lecturer Dr C. Birch is appreciated. Thank you to Mponeng Mine's team from Harmony Gold for assisting and supporting the testing of this technology and for making time and technology available to conduct the test work.

R.E. Olivier for editing the document.

I am grateful for all the support on my journey.

TABLE OF CONTENTS

DECLARATION i

ABSTRACT ii

ACKNOWLEDGMENTS iii

LIST OF FIGURES i

LIST OF TABLES vii

LIST OF SYMBOLS ix

LIST OF ABBREVIATIONS x

INTRODUCTION 1

1.1 Problem Statement 4

1.2 Justification for Research 5

1.3 Previous Work 6

1.4 Research Methods 6

1.5 Sources of Data 8

1.6 Structure of the Research Report 8

GEOLOGICAL THREE-DIMENSIONAL MODELLING 11

1.7 Section Overview 11

1.8 Manual Visualisation 16

1.9 Computer 3D Modelling 18

1.10 Section Summary 31

THREE-DIMENSIONAL SCANNING 32

1.11 Section Overview 32

1.12 Scanning methods 42

1.13 Case Studies 61

1.14 Section Summary 72

RESEARCH METHODOLOGY 73

1.15 Section Overview 73

1.16 Deliberation of Devices and Methods 75

1.17 Data Collection and Analysis 116

1.18 Section Summary 121

RESULTS AND OBSERVATIONS 123

1.19 Section Overview 123

1.20 Apple iPad Pro 11-inch in the DigiMine at Wits 123

1.21 Apple iPhone Pro Max in On-Surface Conditions 137

1.22 Underground Stope Scanning 146

1.23 Section Summary 168

MINE THREE-DIMENSIONAL SCANNING WORKFLOWS 169

1.24 Section Overview 169

1.25 Geological Scanning Workflow 169

1.26 Production Scanning Workflow 171

1.27 Section Summary 172

CONCLUSIONS AND RECOMMENDATIONS 174

1.28 Introduction 175

1.29 Summary of Chapters 176

1.30 Research Observations..... 177

1.31 Research Contributions..... 179

1.32 Recommendations for Future Research Work 180

1.33 Conclusions 181

REFERENCE LIST 183

LIST OF FIGURES

Figure 1-1: Location of Mponeng Mine, South Africa 2

Figure 2-1: Filled block model framework 12

Figure 2-2: Block model blocks rotated to Z-axis (Modified) 13

Figure 2-3: Unrotated blocks (Modified) 14

Figure 2-4: 3D geological model created with Leapfrog modelling software 20

Figure 2-5: Geology modelled in 2D using drawings and tables of raw data 22

Figure 2-6: A Geologist busy mapping a panel using the traditional method. 23

Figure 2-7: Mapping sheet that informs the production team 24

Figure 3-1: Manually operated arm and strip 3D scanner 33

Figure 3-2: Typical laser triangulation system comprises a laser source . 35

Figure 3-3: 3D laser scanning of land, buildings and objects 36

Figure 3-4: Structured optical light scanners 37

Figure 3-5: Cross-sectional view of a 12K SLM modulated light scanner 38

Figure 3-6: Modulated light scanner - 1x12288 Linear Array Liquid Crystal on Silicon scanner 39

Figure 3-7: Computerized tomography (CT) scan 40

Figure 3-8: SIGNA 7.0T, a magnetic resonance imaging (MRI) scanner . 41

Figure 3-9: Summary of the different scanning methods 42

Figure 3-10: Concept of image sectioning 43

Figure 3-11: Camera offset geometry 44

Figure 3-12: Line JK is normal to AB 45

Figure 3-13: Illustration of a very dense point cloud with errors and resulting mesh 46

Figure 3-14: Illustration of less dense point cloud with errors and resulting mesh 46

Figure 3-15: Leica BLK2GO Imaging laser scanner..... 47

Figure 3-16: ZEB Revo RT - Real-Time handheld scanner 48

Figure 3-17: Marker on a scanned image. 49

Figure 3-18: The principle of tacheometric Laser Scanning..... 50

Figure 3-19: The different types of tacheometric scanners 51

Figure 3-20: Leica RTC360 Laser Scanner 52

Figure 3-21: RIEGL VZ-6000 laser scanner..... 53

Figure 3-22: Camera field of view relationship..... 54

Figure 3-23: F-number to focus depth relationship 55

Figure 3-25: Point cloud of a scanned building 57

Figure 3-26: Picked points are shown as A0, A1 and A2 in 3D and in a table CloudCompare software 58

Figure 3-27: Reference point coordinates..... 59

Figure 3-28: End scan at the scan start point 60

Figure 3-29: East Kalimantan Province..... 61

Figure 3-30: Compared point cloud difference between DTMs..... 63

Figure 3-31: Measurement of discontinuity spacing..... 66

Figure 3-32: Delineation of significant discontinuity planes for export and capture in the Acquire geotechnical database 67

Figure 3-33: Excel face mapping report sheet from Acquire geotechnical database 68

Figure 3-34: Schematic data flow for geotechnical face mapping data at Sishen Mine 69

Figure 3-35: Terrestrial laser scanner using a vehicle-mounted set-up (left) and a high-resolution point cloud for use in face mapping (right)..... 70

Figure 4-1: The Occipital Structure Sensor (Mark II)) 77

Figure 4-2: Apple iPad Pro 11-inch..... 78

Figure 4-3: iPhone 12 Pro..... 79

Figure 4-4: Total Station N7..... 82

Figure 4-5: TS07 3” R500 Total Station 83

Figure 4-6: Face section from Deswik Mapping application..... 85

Figure 4-7: Brass spad with numbered copper disc..... 86

Figure 4-8: Occipital Structure Sensor (Mark II)..... 88

Figure 4-9: OBJ file open in Microsoft 3D Builder 91

Figure 4-10: File structure of a PLY file format..... 93

Figure 4-11: An object in a PLY file format with colour attributes assigned to each vertex format 94

Figure 4-12: Scanned object and room by the ‘Scanner’ application 95

Figure 4-13: Scanned room by ‘Room capture’ application 98

Figure 4-14: The iPhone accelerometer axes 101

Figure 4-15: Scanned object by the Scaniverse application 105

Figure 4-16: Polycam 3D scanned model with measurements 108

Figure 4-17: Focus3D X 330 laser scanner 110

Figure 4-18: Stone pillar that was created with LiDAR Mode and Photo Model 111

Figure 4-19: Selection of the most suitable scanners and applications for the research. 117

Figure 5-1: Leapfrog Geo Model of the Wits Mine Tunnel showing UG1 and UG2 stratigraphy as well as the fault and dyke relationship..... 124

Figure 5-2: The Wits DigiMine control room and life-size mining stope . 124

Figure 5-3: Initial scan of stope panel at DigiMine before light-fitting modification; iPad using SiteScape to export Polygon Model File at University of the Witwatersrand in May 2021. 126

Figure 5-4: Image of ‘Mobile LED Video Light with Smartphone Bracket' 127

Figure 5-5: Ultimaker S5 printer 128

Figure 5-6: The back view of the iPad Pro 11-inch holder was designed using Shapr3D software. 129

Figure 5-7: Front view photograph of iPad Pro 11-inch holder during printing. 130

Figure 5-8: Cross-section through the stope panel of DigiMine scanned after light-source insufficiency was mitigated; with iPad at the University of the Witwatersrand in May 2021 131

Figure 5-9: 'Polygon Model File' of stope area in the DigiMine exported to CloudCompare to assess iPad scanning using the SiteScape application during May 2021. 132

Figure 5-10: 'Polygon Model File' format of a portion of crosscut at the DigiMine to assess iPad scanning using the SiteScape application during May 2021, illustrating geological features. 133

Figure 5-11: 'Object File' format of the crosscut at the DigiMine exported to Deswik CAD to assess iPad scanning using the '3D Scanner' application during May 2021, illustrating geological features. 135

Figure 5-12: 'Object File' format processed in Deswik CAD showing Multislice lines of the crosscut at the DigiMine (as black lines) in Deswik CAD to assess iPad Pro scans using the '3D Scanner' application in May 2021. 136

Figure 5-13: HILTI PD-I distometer 138

Figure 5-14: Rooms scanned with the 3D Scanner App on iPhone Pro. 141

Figure 5-15: Enlargement of 1m mark measured from the face of the DigiMine tunnel. 142

Figure 5-16: Bottom view of the '3D Scanner App' scan captured in the DigiMine tunnel. 143

Figure 5-17: Visible ground formation in the 113-68-East 5 stope panel. 147

Figure 5-18: Sampling report for 113-68-East 5. 150

Figure 5-19: 20cm measured CW of the VCR in the 113-68-East 5 stope panel. 151

Figure 5-20: 113-68 East 2 panel of the VCR. 153

Figure 5-21: Scan accurate to within 20 cm. 154

Figure 5-22: Survey point (target) that was placed below the survey peg. 155

Figure 5-23: Mapping report of the 113-68 East 2 panel of the VCR. 157

Figure 5-24: The 120-80 E1A panel of the CLR. 158

Figure 5-25: Tributary area requirements for rockfall conditions 159

Figure 5-26: Stope plan view indicating minimum distance behind the face 160

Figure 5-27: Mapping report of the CLR's 120-80 E1A panel from 15 September 2021. 162

Figure 5-28: Mapping report of the CLRs from 7 October 2021. 164

Figure 5-29: Sampling report of the panel of the CLRs 120-80 E1A from 8 November 2021. 166

Figure 5-30: Mapping report of the CLR's 120-80 E1A panel from 12 November 2021. 167

Figure 6-1: Geological Scanning Workflow. 170

Figure 6-2: Production Scanning Workflow. 172

LIST OF TABLES

Table 3-1: Volume calculation using Global Mapper and Surfer 64

Table 4-1: Object File Format 90

Table 4-2: 3D software that supports PLY file format..... 92

Table 4-3: Scanned models exported to 3D file formats. 104

Table 4-4: Supporting file formats - Deswik CAD for viewing scans 114

Table 4-5: CloudCompare supported file formats 115

Table 5-1: Distometer measurements..... 139

Table 5-2: Distometer versus scan - dimension comparison and variance in rooms measured. 140

Table 5-3: Accuracy test results from the 3D Scanner application (.OBJ). from DigiMine. 144

Table 5-4: Measurements from 113-68-East 5 stope panel of the VCR. 149

Table 5-5: Volume calculation of 113-68-East 5 stope panel of the VCR. 152

LIST OF SYMBOLS

Centimetre	cm
Cubic metres (Volume)	m^3
Degrees	°
Dollar	$
Gold	Au
Grams per tonne	g/t
Inches	"
Kilogram per cubic metre	kg/m^3
Megapascal	MPa
Metres	m
Millimetres	mm
Parts per million	ppm
Percentage	%
Rand	R
Three-dimensional	3D

LIST OF ABBREVIATIONS

Allocated Stoping Width	ASW
Carbon Leader Reef	CLR
Channel Width	CW
Computer-Aided Design	CAD
Digital Terrain Model	DTM
Explosion protected	Ex
Global Navigation Satellite System	GNSS
Harvest with Advanced Regeneration	HARP
Identification Application	ia
Inertial Measurement Unit	IMU
Infrared	IR
Light Detection and Ranging	LiDAR
Magnetic Resonance Imaging	MRI
Mineral Resource Estimation	MRE
Mineral Resource Management	MRM
Red Green Blue	RGB

Simultaneous localisation and mapping	SLAM
Stoping Width	SW
Structured Query Language	SQL
Subscriber Identity Module	SIM
Tool Command Language	TCL
University of the Witwatersrand	Wits
Ventersdorp Contact Reef	VCR

INTRODUCTION

This research project was initiated to identify orebody dilution in an ultra-deep South African gold mine. Mponeng Mine is southwest of Johannesburg (shown in Figure 0-1) and mines the Ventersdorp Contact Reef (VCR) and Carbon Leader Reef (CLR). The narrow, tabular stopes are currently over 3,500 metres (m) below the surface. The VCR is highly variable as it forms an unconformity with the underlying sediments of the Witwatersrand Supergroup. The orebody is typically 120 cm thick and dips approximately 18 degrees towards the south.

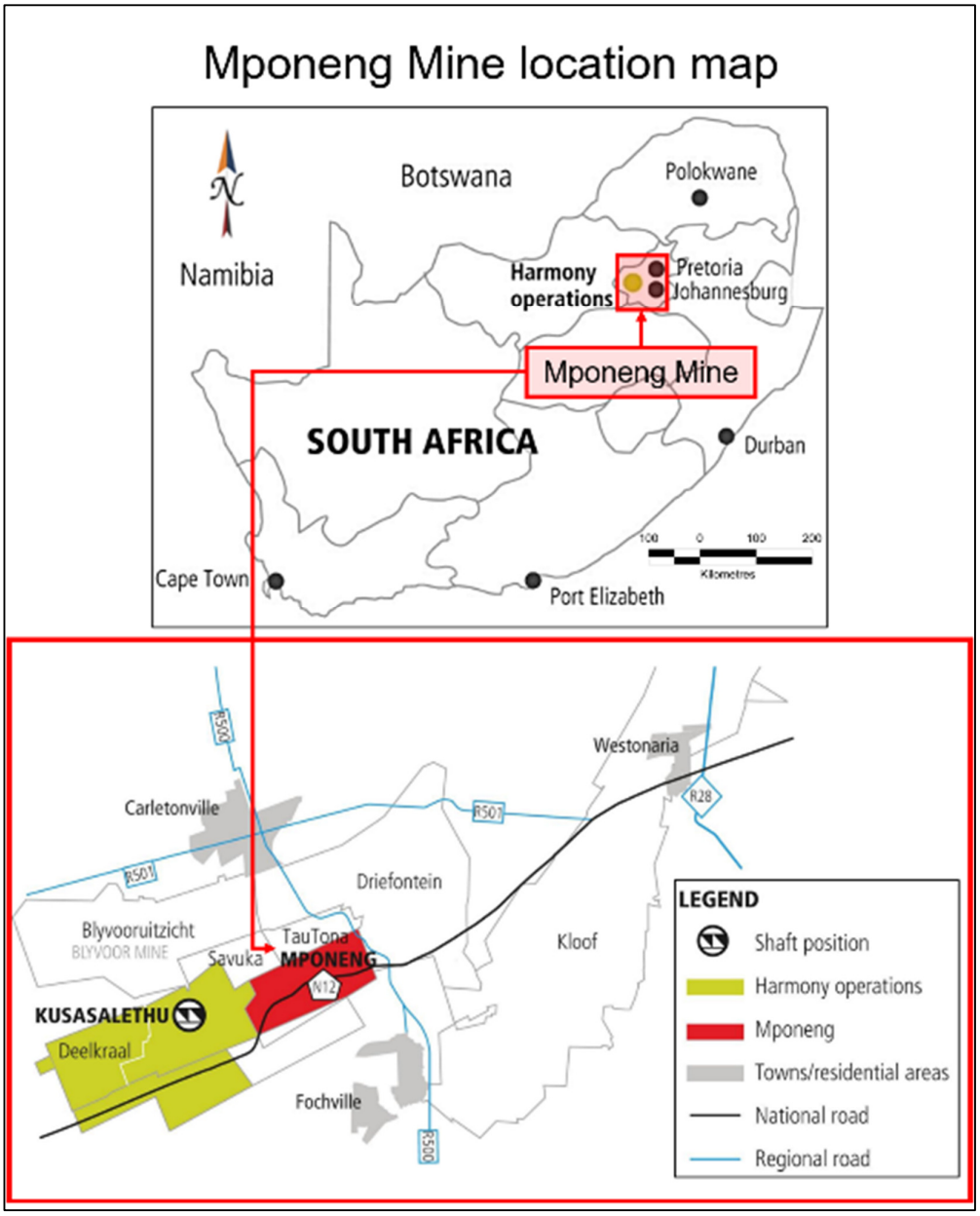


Figure 0-1: Location of Mponeng Mine, South Africa (Harmony Gold Mining Company Limited., 2020).

Predicted virgin stresses, at these depths, are between 95 MPa and 135 MPa with a rock density of 2700 kg/m³ (Malan & Basson, 1998). Predicted virgin stresses create challenges concerning the practical support of workplaces. The rolling of the reef occurs on the strike and dip of the ore

body (Roberts & Schweitzer, 1999). For this reason, mining heights need constant adjustments to avoid grade dilution. Other mining operations that mine in the same region and under similar circumstances, for example, Kloof Gold Mine, may benefit from the research results (Manzi, et al., 2014).

Mine planning requires three-dimensional (3D) spatial measurements of the orebody. Currently, on Mponeng Mine, the mine survey, geology and valuation departments gather this information on a regular grid. However, this information was unavailable in a format easily incorporated into the mines' 3D model. The research aims to investigate how to best supply dynamic 3D information to the underground mine planning department and highlight any excessive dilution. Light detection and ranging (LiDAR) has proved to be a technology that will assist with gathering and disseminating 3D information concerning the orebody.

Mineral resource management (MRM) is the information hub for extracting minerals in underground mining (Blaauw & Trevarthen, 1987). Limited information on the ore body may influence mining decisions. Therefore, exploring more innovative mining techniques could increase precision and decrease the lag in relaying information about dilution is essential. One way to do this is by utilising and optimising dynamic 3D details.

1.1 Problem Statement

Orebody/reef dilution affecting the grade destroys the economic value of mining operations. In addition, unwanted waste mining causes dilution, affecting the ore grade and increasing the mining and processing costs (Rogers & Kanchibotla, 2013). For this reason, Mponeng Mine strives to reduce dilution by controlling the stoping width (SW). As a result, Mponeng Mine's SW was, on average, 12% greater than the allocated stoping width (ASW) for the past ten years (AngloGold Ashanti, 2020).

With the information available, it is possible to make informed decisions. There may be room for the MRM department at Mponeng Mine to optimise the 3D data they supply to the production team. Currently, geologists and samplers capture information at the stope face. Geologists and samplers then provide the production team with a report showing the results in the form of a plan and a section view of only one panel on a sheet of A4 paper. This report may sufficiently guide the production team in the short term. Unfortunately, this information is unavailable for monthly planning in a holistic 3D view. The MRM department cannot verify this non-integrated information internally. As found in other Harmony Gold Mines, the geological sections are not copied and included in the monthly planning sessions. As the VCR ore body's complexity poses challenges in effectively controlling SW, Mponeng Mine faces challenges in reducing associated grade dilution. Grade dilution is the result of mining unwanted waste material. This translates to added waste tonnes needing transportation to the plant for

processing. Additional waste tonnes result in increased production and processing costs, with a concomitant reduction in profitability.

The research hypotheses show that integrated 3D data from samplers, geologists and mine surveyors can help the production team better manage SW control to reduce grade dilution.

1.2 Justification for Research

“Some gold loss and dilution will always occur during blasting and transporting broken ore” (Xingwana, 2016, p. 149). Gold loss and ore dilution are evident in sampling results from Mponeng Mine. However, sampling results show that it is possible to increase the average gold grade by 31% if the recommended SW is honoured (AngloGold Ashanti, 2020). Improving ore grades has added benefits such as reducing support costs.

Currently, the mine has a LiDAR scanner available from the mine survey department on Mponeng Mine. However, this instrument is bulky and unsuitable for use in stopes, prevalent on the mine. This research report explored simple, low-cost solutions that will allow for 3D scanning by geologists, valuation officers and production personnel. The aim is to provide the underground mine planning department with more frequent 3D dynamic information.

1.3 Previous Work

The MSc candidate had the privilege of taking part as a co-author in a publication that inspired, developed alongside, and received a contribution from work done in this MSc research project. The leading author, C. Birch, presented findings from the research paper "*Narrow, Tabular Stope 3D Scanning in Deep-Level Gold Mines Using An iPad Pro LiDAR"* at the 2022 International Multidisciplinary Conference of Engineering Technology (IMCET) in Turkey. The work complements this research project's purpose, specifically to explore the potential of implementing 3D scanning to map faces and develop a workflow that could improve associated reconciliation. Correspondingly, the work was supported by Wits and on-site investigations performed at Mponeng Mine.

1.4 Research Methods

Research design: The research methodology aimed to investigate using a cost-effective 3D LiDAR scanner for underground use. The research design comprises both a quantitative and a qualitative method. The quantitative portion short-lists scanning technology. The qualitative portion focused on the quality of the scans and the value that the 3D scanner offers. This involved the following steps:

- Stock-taking exercise to short-list suitable hardware and software;
- The literature survey process supports the evaluation of the short-listed hardware and software.

The following criteria were applied in short-listing and then identifying the choice of scanner for the experimental underground conditions of narrow tabular mining:

- Ease of use;
- Accuracy and quality of scanners;
- Cost of 3D scanners and software. The compatibility of software considers the currently used software of Mponeng mine. Price played an essential role since the project was in the test phase; and
- Test short-list of scanners and software.

The aim was to test what influence light may have on the quality of scans. Hence, the intention was to try these scanners at DigiMine at the University of the Witwatersrand. The DigiMine at the University of Witwatersrand is a simulated environment of an underground gold mine where scanners were utilised for the following:

- Comparing and analysing the quality of the scans captured;
- The best quality scanner and the sensor were to be tested underground at Mponeng Mine;
- Through practical observation of geological practices, original data was collected by 3D LiDAR scans of stope panels, using built-in features of the iPad Pro for comparisons;
- Comparing and analysing the quality of the scans captured at Mponeng Mine; and

- Decide what scanning applications would be best suited to the research study in the future.

1.5 Sources of Data

The 3D LiDAR scanning process used the following data sources:

- 3D scans of stope panels;
- Mponeng Mine's survey peg database;
- Data/information used from Mponeng Mine;
- Mine survey actuals measured;
- Sampling results; and
- Geological mapping.

Data capturing applied the following procedures:

- Capture time, date, and workplace names for each scan; and
- Create relevant workflows for both geological scanning and production scanning.

1.6 Structure of the Research Report

Chapter 1 is the introduction with the research background and the problem statement. Chapters 2 and 3 are the literature review, focusing on

background knowledge and geological modelling and 3D scanning case studies, respectively. Chapter 4, the research methodology, consists of the following points:

- Further literature survey content about current mine survey equipment on Mponeng Mine;
- The appraisal of potential scanners; and
- Justifies considerations for subsequent experimental procedures (thereby lending itself to initiating the qualitative portion of the research method).

Chapter 5 is the quantitative short listing of scanning technology and the reporting of preliminary testing in the DigiMine on the West Campus of the University of the Witwatersrand. DigiMine is a mock mine with a control room. The simulated mine has a life-size tunnel that imitates geological features on the sides of the tunnel. This mock mine also has a life-size narrow reef stope and lamp room. (University of the Witwatersrand, 2020). Chapter 5 compares underground observations of the following on-site manual measurements:

- iPad Pro scans with measurements processed in Deswik CAD (data obtained on the same date in the presence of the MSc candidate); and
- Mponeng Mine's sampling team performed mining survey measurements.

Chapter 6 presents the new projections of a Geological and a Production Scanning Workflow, incorporating the chosen scanning technology and allowing a baseline suggestion for future optimisation. Chapter 7 summarises the research conclusions and recommendations for furthering this research of reducing dilution, which is currently associated with the inherent limitations in informational flow between geological and production departments on the Mponeng Mine.

GEOLOGICAL THREE-DIMENSIONAL MODELLING

1.7 Section Overview

Geologists create a geological model from the core extracted from geological boreholes. Geological boreholes reveal, among other things, the ore body's physical characteristics in terms of size, shape, geological structures and geo-mechanical properties of ore and waste rock (Pandey, 2022). The ore body features determine which mining method can be applied to mine safely and economically.

Geological mapping is a manual process that traces contacts between different rock formations, often on other planes. This manual process enables the geologist to project and interpret geological features. In turn, this led to a better understanding of the ore body.

3D modelling computer systems, for example, Datamine, Leapfrog, MineRp and Deswik, were introduced in the mining sector to visualise and understand the complexity of ore bodies. With Datamine software packages, namely Strat3D and Fusion, it is possible to create 3D block models. South African mines, and Mponeng Mine, in particular, have adopted computerised 3D modelling.

Geological 3D block models are rectangular 3D X Y Z grid systems. Figure 0-1 illustrates a filled block model framework where “N” is the number of blocks in the framework. A block origin defines the cell positions within the block model framework (Poniewierski, 2019).

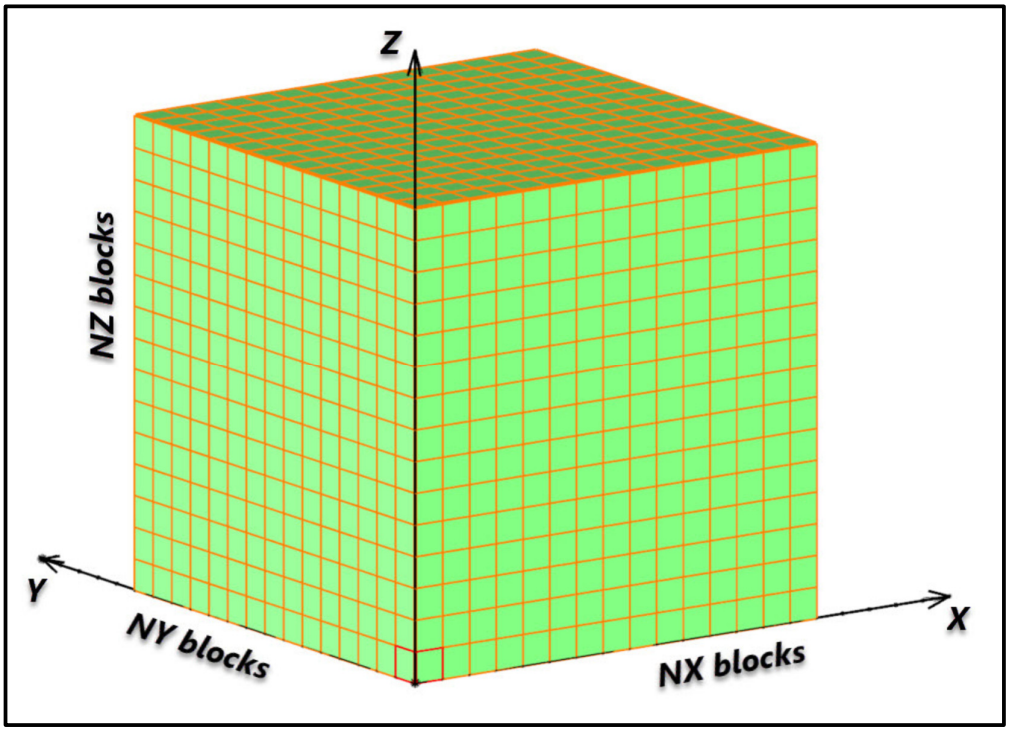


Figure 0-1: Filled block model framework (Poniewierski, 2019).

Grade dilution can start with the 3D block model creation process. 3D block models are created as rotated or unrotated models. A rotated model rotates cells according to the coordinate system (Poniewierski, 2019). For example, Figure 0-2 illustrates a stratified orebody dipping or plunging. Waste from the host rock does not dilute rotated block model cells (Poniewierski, 2019).

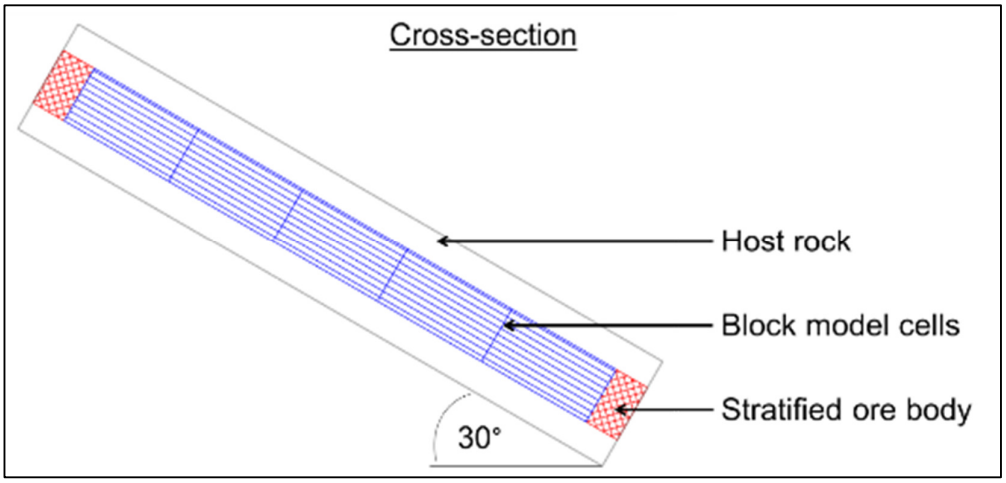


Figure 0-2: Block model blocks rotated to Z-axis (Modified) (Poniewierski, 2019).

Figure 0-3 shows a standard orthogonal unrotated block model applied to a stratified ore body that is dipping or plunging. With this unrotated block model, grade dilution occurs as the grade value of the block model cells is diluted by the waste from the surrounding host rock (Poniewierski, 2019).

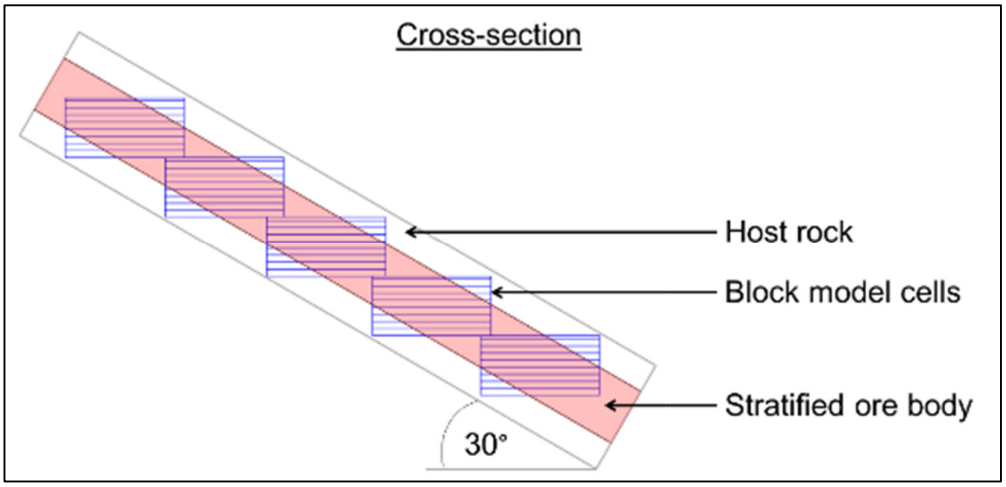


Figure 0-3: Unrotated blocks (Modified) (Poniewierski, 2019).

Each block in the 3D model represents a particular value of width, grade, tonnes and geological entity of the ore body. An ore body model must satisfy the following four conditions:

- The parameters of the chosen model should allow estimation;
- The model must be able to provide an answer to a relevant question;
- The model must be compatible with data; and
- An experienced geologist should very or check the model's predictions (Pandey, 2022).

The 3D geological model guides the mineral resource estimation (MRE) and classification process. Mine planners also use it to plan excavations at an accurate mining height for minimal grade dilution. The following geological aspects are used to generate the 3D geological model:

- Exploration drilling;
- Sampling;
- Geological mapping;
- Interpretation of geological features; and
- Ore grade (Chanderman, et al., 2017).

Gold deposit in Mali

"The workflow adopted in this study is based on a gold deposit containing an oxide zone (oxides) and a deeper sulphide zone (sulphides) comprised of unweathered (fresh rock) material, located in southwestern Mali. Exploring the potential for additional oxide resources is thus a natural step to increase the life of the mine" (Chanderman, et al., 2017, p. 189). The gold deposit is located on the West African craton in the Malian portion of a Paleoproterozoic inlier known as the Kedougou-Kenieba window (Chanderman, et al., 2017).

In Mali, using 3D geological modelling and geostatistical evaluation techniques enabled the resource estimation of a gold deposit to increase by 7200 ounces. Stochastic approaches to ore body modelling and estimation should be considered to fully characterise the geological uncertainty (Chanderman, et al., 2017). This information is based on 3D geological modelling and geostatistical evaluation techniques as informed by newly drilled advanced grade-control holes.

Gemfields Resources PLC in Zambia

Accurate ore body modelling depends on accurate drilling information. If drill hole practices do not support the uniqueness of the ore body, precise estimation of tonnes and grade will not be possible. Research indicates that it is challenging to sample economic concentration zones. Examples of such challenges can be seen with the Kagem emerald deposit of Gemfields Resources PLC in Zambia. The MRE process depends on available results of bulk samples and historical production statistics for reporting on the volume of economic talc-chlorite-tremolite magnetite (SRK Consulting (UK) Limited, 2012). This paper stresses the importance of accurate ore body modelling to estimate tonnes and grades accurately. Dynamic 3D LiDAR scanning may positively contribute to this cause.

1.8 Manual Visualisation

Over the years, geologists have used different methods to represent an ore body visually. Geologists must communicate geological information effectively between departments (Donnelly, 2008).

Traditional geological mapping is a manual process that traces contacts between different rock formations, groups, types and planes. The geologist would take measurements with a tape and clinometer along a single centre line that runs across the width of a stope panel or against the sidewall of a development excavation. A clinometer measures the dip and strike of the

reef and fault plane (Lisle, et al., 2011). This information is then drawn and projected on a plan and section view.

A representation of the ore body was often constructed from layering transparent Perspex sheets. Geological sections were drawn onto individual Perspex sheets that were joined together to create a physical model of the ore body. Over the years, as 3D laser cutting technology developed, it became possible to create plastic models from digital data (Lisle, et al., 2011).

As technology developed, geologists used cameras to photograph stope faces while mapping. These photographs were a reference in writing geological reports (Lisle, et al., 2011).

Notably, time at a particular face is always limited and would seldomly exceed 30 minutes. Therefore, the geologist must capture as much information about the stope as possible with maximum efficiency and accuracy. In complex ore bodies, the grade may fluctuate over short distances and for this reason, it is also vital to map geology regularly. The mining process can be more efficient and cost-effective when a well-designed grade control programme is applied. Developing a value-adding grade control programme may be well received by stakeholders (Dominy & Platten, 2012).

1.9 Computer 3D Modelling

Data given directly or indirectly to a specific location is known as “spatial data”. Geospatial data is often about a geographical area (Information Commissioner's Office, 2015). Geometric data is global data mapped on a two-dimensional flat surface (Zola & Fontecchio, 2021). Geographic data is information mapped around a sphere. Most often, the globe is planet Earth. Geographic data highlights the latitudinal and longitudinal relationships relative to a specific object or location. A global navigation satellite system (GNSS) is a familiar example of where geographic data is fully implemented (Zola & Fontecchio, 2021). Geological subsurface models are based on rock units' spatial distribution and deformation. The geologist maps information about rock types, contacts and depositional or magmatic flow features. In summary, the geologist maps the following structures:

- Folding - dip, strike, deformation, the orientation of grains;
- Joints – attitude, size, open or closed; and
- Faults - look for slickensides, fault gouge, breccia and visible displacements (Balasubramanian, 2017).

The uncaptured geological information about a stope face is accepted as lost after the stope face has advanced. Regular mapping of stope faces provides a complete picture of the ore body's behaviour. The greater the distance between mapping data, the greater the interpretation required of the geologist. The data needed to estimate local grade, and undertake

optimal SW, is provided by the mapping and sampling of these exposures (Dominy & Platten, 2012). Geological mapping information assists the geologist when they recommend the maximum SW of a stope panel.

Leonida (2016) reported from an interview with the chairman of the mining software firm Maptek that ‘spatial modelling’ is a concept that has been already accepted and incorporated since the late 1970s. In the 1990s, however, mining became revolutionised by what is now called ‘3D modelling’. Computing capabilities and enhanced software produced user interfaces that present the data and allow user interaction within the 3D space. (Leonida, 2016). Maptek now uses Silicon Graphics technology initially used for movies and entertainment in the mid-1990s (Leonida, 2016).

Christchurch, New Zealand-based ARANZ was founded in the early 2000s. ARANZ started its operations with 3D medical imaging technology that supported accurate information for medical diagnostics. In 2004, geological science was the first to apply this technology. The software enabled faster, dynamic processing of data. As a result, the software became better known as Leapfrog Geo and has impacted mineral resources positively by enabling better decision-making. Seequent acquired ARANZ Geo in 2018 (Seequent Limited, n.d.). Figure 0-4 is an example of a 3D model of an orebody created with Leapfrog Geo software (Orefind, 2017).

According to borehole data, Figure 0-4 depicts the different attributes associated with the 3D model. These attributes may include the following:

- Variables;
- Mineral grades;
- Contaminant concentrations;
- Geomechanically properties;
- Characteristics;
- Lithology;
- Mineralogy; and
- Coordinates (University of the Witwatersrand, n.d., p. 14).

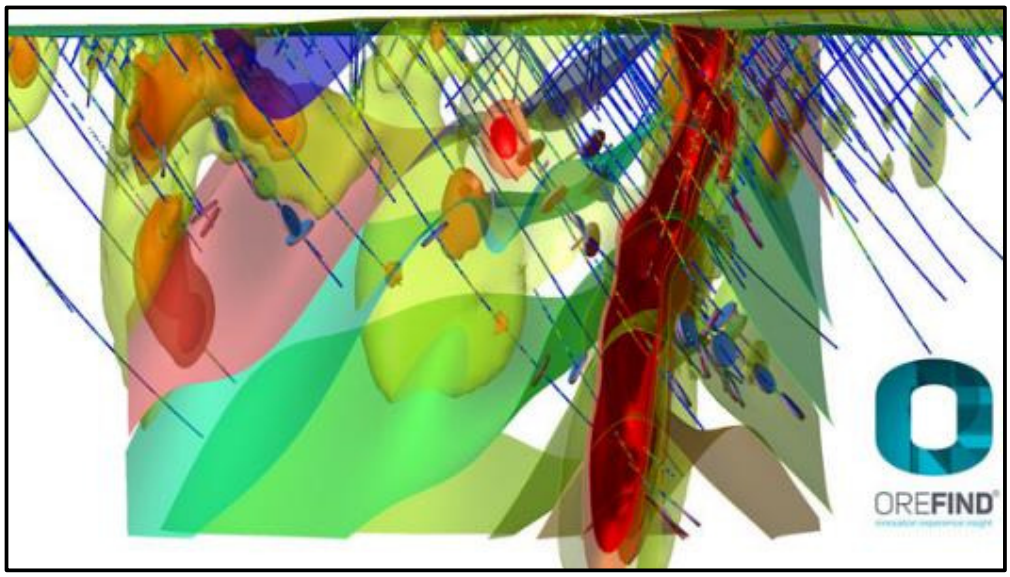


Figure 0-4: 3D geological model created with Leapfrog modelling software (Orefind, 2017).

Datamine software has provided time-saving automation and ease-of-use digital mining technology to the mining industry since 1981 (Datamine,

2022b). MineMapper 3D is part of Datamine's Fusion Suite, which enables the geologist to capture mapping digitally while at the workplace. This mapping then informs mine planning and modelling systems of the characteristics of the orebody and ore grade (Datamine, 2022a).

Surpac was initially developed in Perth, Western Australia, by its founder Bebb in 1978 (Mining Patch Associates, 2017). By the late 1990s, Surpac was used primarily for non-seam or layered mining projects. In the mid-1990s, Surpac introduced the tool command language (TCL), which contains macros that allow users to automate repetitive activities. In later years, Surpac joined forces with Minex Company and Gemcom Software. Since 2012, these groups have been part of Dassault Systems (Mining Patch Associates, 2017).

The 1960s marked the beginning of 3D models. At that stage, 3D modelling was reserved only for computer engineering and automation professionals. Instead, they worked with mathematical models and data analysis (Architectural CGI, 2016). One of the pioneers of 3D graphics is Sutherland, the creator of Sketchpad. This revolutionary program helped create the first 3D objects and significantly made 3D what it is today. Along with his colleague, Evans, Sutherland opened the first department of computer technologies at the University of Utah (Architectural CGI, 2016).

Before this computerised technology became available, geologists were entirely dependent on mapping and modelling in 2D, using drawings and

tables of raw data. Figure 0-5 illustrates Geology modelled in 2D using drawings and tables of raw data (Leonida, 2016).

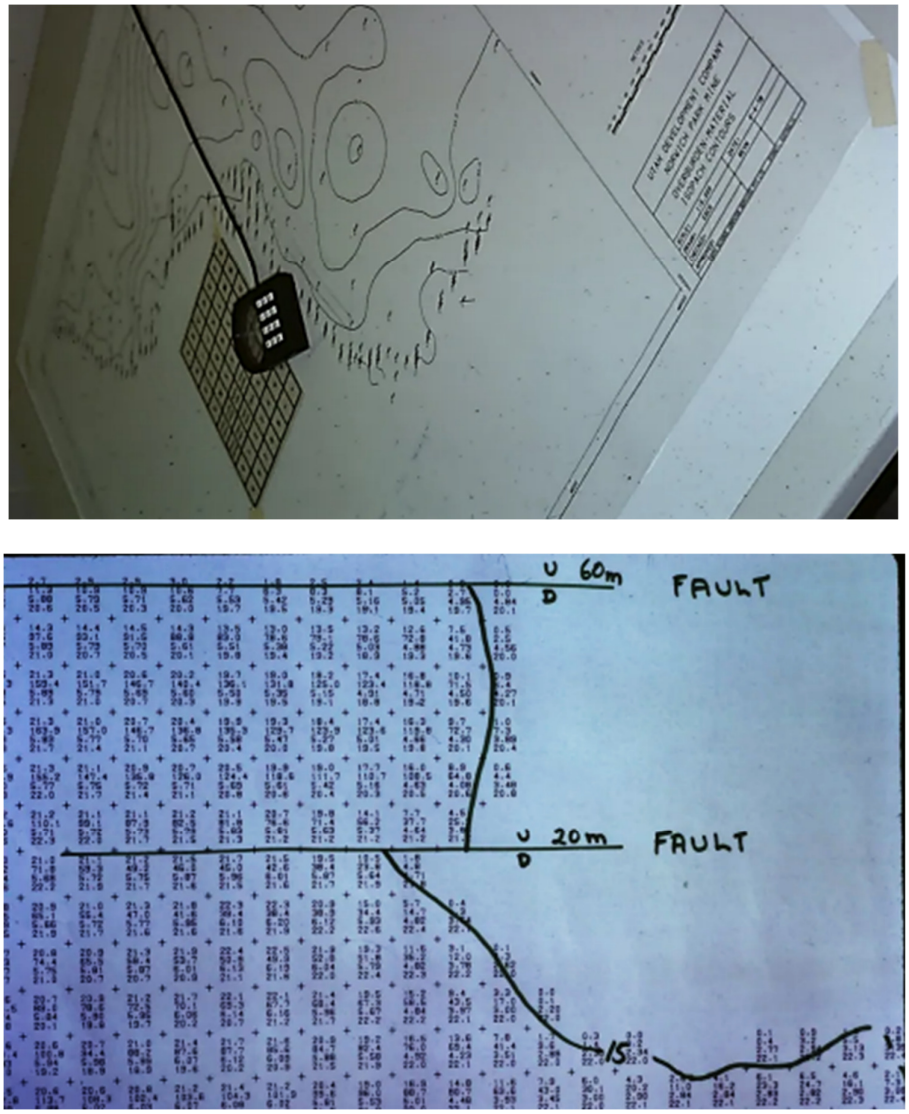


Figure 0-5: Geology modelled in 2D using drawings and tables of raw data (Leonida, 2016).

Due to its variability, the currently available 3D modelling technology enables geologists to understand an ore body's behaviour and the entire mine's performance, due to its variability (Leonida, 2016).

Currently, the geologists working on Mponeng Mine do manual stope mapping using tapes and a clinorule. Figure 0-6 shows a geologist mapping a stope panel at Mponeng Mine.



Figure 0-6: A Geologist busy mapping a panel using the traditional method.

Figure 0-7 is an example of a typical plan and section view of a mapping sheet that informs the production team of the following:

- SW measured;
- CW measured;
- If there is reef in the hanging wall or reef in the footwall; and
- The ASW.

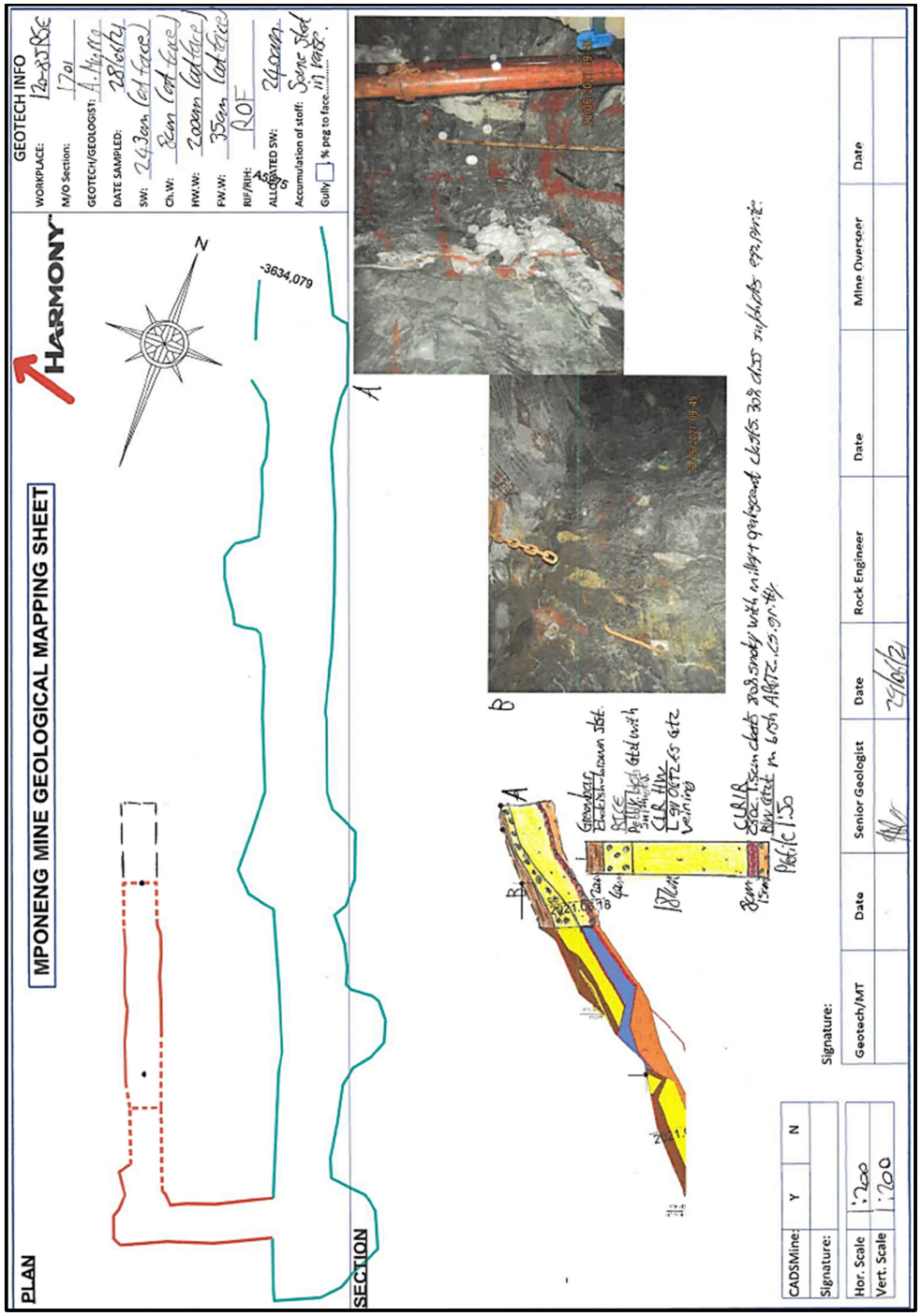


Figure 0-7: Mapping sheet that informs the production team (Mponeng Mine, 2021).

The mapping is plotted on elevation in Deswik CAD software. Interpretations enable a 3D geology view of lines and polygons with very little data.

Geologists at Mponeng Mine assign the following attributes to lines and polygons:

- Reef type;
- Mining level;
- Raise line number;
- The grain size of rock formation;
- Colour;
- Rock type;
- Stratigraphic position; and
- Stratigraphic colour.

Geologists at Mponeng Mine use Fusion software from Datamine to create 3D geological models from the above-mentioned geological mapping, sampling and drill hole data.

The geology department is the custodian of the 3D geological and grade models for a mine. 3D modelling is crucial in evaluating an ore deposit to guide production in the mine planning process. 3D modelling software has been used successfully to model thin tabular reef deposits. Although negative perceptions about the accuracy of computer-generated 3D geological models exist, these perceptions have been critiqued as baseless and said to generally stem from a misunderstanding of software applications (Johnstone, 2003). Multi-dimensional modelling software should

complement traditional mapping techniques, thereby improving the professional output of geologists in the mining industry (Johnstone, 2003).

A study at Namibia's Navachab Gold Mine showed that 3D implicit modelling reduces user-based modelling bias by generating open or closed surfaces. It uses geochemical, lithological, and structural data without requiring manual digitisation or linking. Instead, mathematical interpolation is used to visualize patterns and trends in large drillhole datasets. This research also proposed that examining existing drillhole datasets using 3D implicit modelling is a powerful tool for spatial analysis of mineralisation patterns. Furthermore, when used in conjunction with fieldwork, this approach can potentially improve the structural understanding of various ore deposits (Vollgger, et al., 2015).

Mponeng Mine, previously owned by AngloGold Ashanti, was acquired by Harmony in October 2020 (Harmony, 2022). After the holding period of three months elapsed, Harmony implemented new systems and software at Mponeng Mine. Harmony's software was upgraded across various mines to meet the requirements of the different software companies. Consequently, block model calculations were processed much faster. In addition, 3D block modelling enables the combination of separate data sets that can be analysed and updated. As a result, the block models are more realistic and can be updated based on information from ongoing drilling (Fallara, et al., 2006).

Traditional wireframing requires a good understanding of the ore body and demands more significant manual labour and interpretation of the ore body. On the other hand, implicit geological modelling involves a single mathematical function capable of determining the structural composition of the ore body. Therefore, the mathematical function decreases the time needed for creating 3D block models (Birch, 2014).

Geological modelling software used in South African mines

The most common block models in the mining industry are Datamine, Vulcan, Surpac, Micromine and MineSight (Poniewierski, 2019). The British Geological Survey developed the G-EXEC relational database management system in the 1970s. “The G-EXEC system consisted of an integrated collection of applications built around a relational database engine. The first was operational in 1973 and served the needs of its geological users for over ten years” (Resources Computing International Ltd, n.d.). Datamine has used the G-EXEC system since its establishment in 1981 (Poniewierski, 2019). Datamine software is used for accurate resource modelling and reporting for large and small deposits on all commodities (Datamine, 2021c).

Surpac clusters identical blocks until further grouping is impossible. The effect is smaller model sizes. Surpac uses an exact method for sub-blocking, resulting in parent blocks in fractions of a half, quarter, eighth and so forth. It is also necessary to specify the sub-blocking size during block

model creation. The actual division of parent blocks only occurs when more detailed data is required. The result is that a Surpac block model always uses the minimum blocks possible.

For this reason, a Surpac block model can be much smaller than a Datamine block model. Conversion between Surpac and Datamine block models is possible when the data is available in comma-separated values (CSV) format. A CSV “file is a text file with a specific format which allows data to be saved in a table structured format” (Google, 2022). It is possible to convert a Surpac block model into Datamine format using Deswik software (Poniewierski, 2019).

MineSight block models use a whole block modelling system, meaning no sub-celling is present. This method allows extensive mines to be modelled within computing memory and storage limitations at the time. In addition, this method identifies the percentages of the block within geological domain contacts. Sub-blocking/sub-celling have been available in MineSight since 2013, which generates an additional file associated with the 3D block model for sub-blocked items and areas (Poniewierski, 2019).

Here are the differences between the different types of block models:

- How sample grades are interpolated/ extrapolated into a block used to populate the blocks within a block model;

- It may be possible to estimate within a block; for example, it is possible to estimate the magnitude of a sample by weighing four sampled points placed around it; and
- The physical constructed blocks represent the size and rotation of blocks (Poniewierski, 2019).

The following are different types of geological block models:

- Inverse distance models;
- Ordinary Kriged models;
- Linear versus non-linear methods;
- Multiple Indicator Kriged models;
- Localised indicator Kriging / Uniform conditioning;
- Conditional Simulation models;
- Gridded seam models; and
- Harvest with Advanced Regeneration (HARP) models (Poniewierski, 2019).

Geological modelling software used at Mponeng Mine

The Mponeng Mine facilitates communication between the production team and the MRM department. It is then the daily responsibility of the mine overseer to communicate guidance from the geology department back to the miners. Geological mapping reports are available to the production team

on a central system, Syncromine. Geological instructions are uploaded on Syncromine, and mining teams must acknowledge when they have read the instructions. This way, the geologist can keep track of the information flow between the Geology and Mining departments.

Mponeng Mine uses two software packages from Datamine to create two-dimensional block models, namely Strat3D and Fusion. The Strat3D software automatically builds a structural model from drillhole and seam description data (Datamine, 2019).

A geostatistical method interpolates data points taken at different locations. Sample points are measurements from correlating attributes, for example, reef type, elevation and rock type. The main interpolation techniques are deterministic and geostatistical. “Deterministic techniques use mathematical functions for interpolation. On the other hand, geostatistics relies on both statistical and mathematical methods, which can be used to create surfaces and assess the uncertainty of the predictions” (Esri, 2021).

The Fusion software stores all the geological information that informs Strat3D, including the following geological aspects: “completely configurable templates that capture all geological, geotechnical, geophysical, geochemical, downhole survey, mapping, quality assurance and quality control (QA/QC) and sample data” (Datamine, 2021b).

1.10 Section Summary

From the literature review above, it is clear that accurate 3D modelling plays a critical role in determining resource estimations and mining costs. The current geological mapping approach (tapes and clinometers) makes it difficult and time-consuming to put geological mapping into a format suitable for the 3D geological model or even to display on the digital plans used during the planning sessions. Accurate 3D geological models increase the precision of mining and, therefore, higher gold grade if mining takes place according to plan. The accuracy and prediction of mining are further improved when these models are provided more frequently, specifically before blasting commences.

THREE-DIMENSIONAL SCANNING

1.11 Section Overview

The first 3D scanners, developed during the 1960s, used lights, cameras and projectors to scan objects for research and design. The first computerised model was created using a contact probe in the 1980s. A probe is a 3D contact scanner at the end of an articulated mechanical arm. “The arm may be robotically or manually manipulated over the part's surface. As the probe contacts the object's surface, the scanner records the X, Y, Z position of the probe by taking positional measurements of the armature” (Ebrahim, 2011, p. 9). As scanners evolved after 1985, they became capable of capturing surfaces using white light, lasers, and shadows. The development of optical technology using light began in the mid-1990s. Compared to prior scanning technologies, this technology was much faster. In 1994, REPLICA, which uses the laser stripe scanning method, was launched. See Figure 0-1.

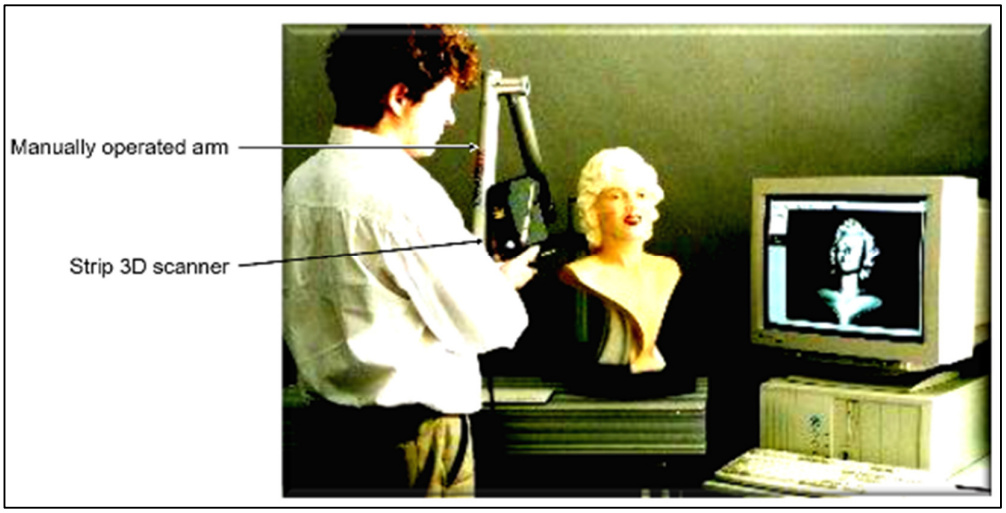


Figure 0-1: Manually operated arm and strip 3D scanner (Ebrahim, 2011).

Introduced in 1996, ModelMaker was able to create 3D models by combining a manual arm with a 3D stripe scanner. ModelMaker was a fast, flexible system that could produce complex models with colour and texture (Ebrahim, 2011).

It is possible to classify 3D non-contact active laser scanning into three main categories. These categories are the time of flight, triangulation and structured light (Ebrahim, 2011). Time-of-flight 3D laser scanning uses laser light to detect an object with laser rangefinder technology and measures accurately within millimetres. A laser emits a light pulse, and the rangefinder determines the distance to a surface by the amount of time taken ('round-trip time') before the detector receives the reflected light (Ebrahim, 2011). The total round-trip distance, *d*, from the scanner to an object is given by Equation 1.

$$d = (c \times t) \div 2 \qquad \text{Equation 1}$$

Where *c* is the speed of light and t is the time of flight

(Moberg, 2017).

The Leica Geosystems time-of-flight 3D laser scanner, ScanStation 2, can scan at a maximum instantaneous scan speed of 50,000 points/second (Diversified Communications, 2022).

3D laser scanners that use the triangulation method use laser light to probe the environment. 3D laser scanner technology shines a laser on an object that uses a camera to look for the location of the laser dot. The laser dot, camera and emitter form a triangle, hence the term 'triangulation' (Ebrahim, 2011). The diagram in Figure 0-2 illustrates the concept of triangulation.

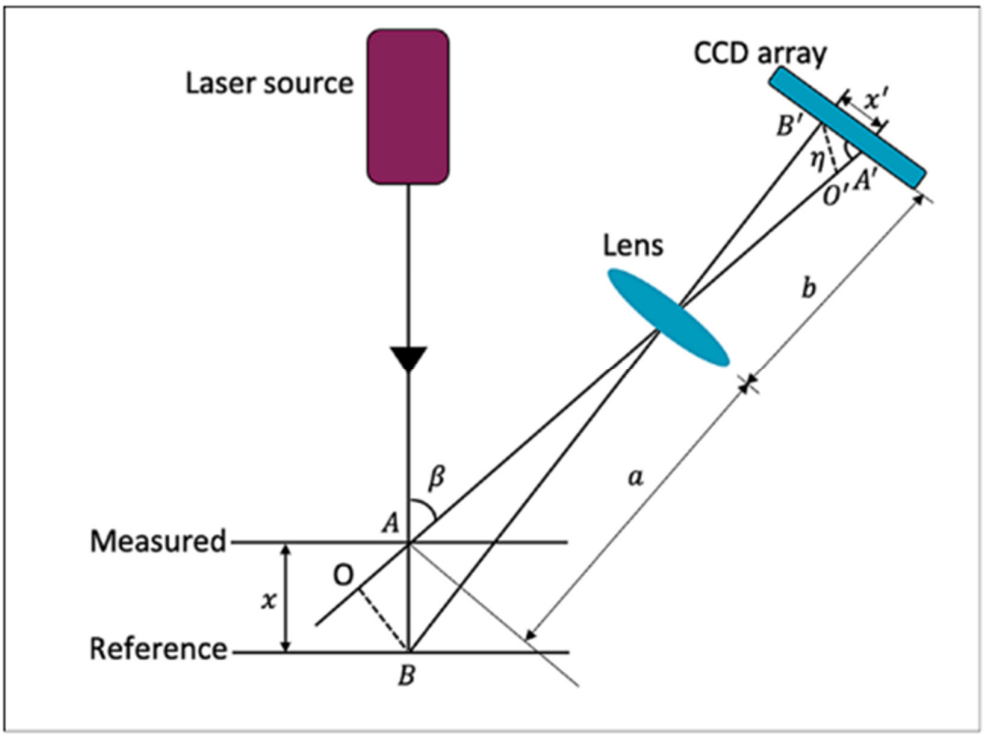


Figure 0-2: Typical laser triangulation system comprises a laser source (Academic library, 2022).

High-resolution scans take more points per second in comparison to low-resolution scans. A disadvantage of this is some motion distortion. However, some laser scanners have level compensators built to counteract scanner movement during scanning (Ebrahim, 2011). The following explains standard active non-contact 3D Structured-light scanners. This includes laser scanners, structured optical light scanners, modulated light scanners, computer tomography (CT) scanners and magnetic resonance imaging (MRI) scanners (Ebrahim, 2011).

1.11.1 Laser scanners

3D laser scanning produces detailed and accurate measurements for 2D drawings and 3D models of land, buildings, and objects (E-Architect, 2020).



Figure 0-3: 3D laser scanning of land, buildings and objects (E-Architect, 2020).

1.11.2 Structured optical light scanners

Structured-light 3D scanners project a pattern of light onto a subject. A liquid crystal displays (LCD) projector or a multi-laser projects the line onto the subject. “An LCD projector is a type of projector based on liquid crystal displays which can display images, data or video” (Techopedia Inc., 2022). A camera placed slightly away from the pattern projector observes the shape of the line, using the triangulation technique to calculate the distance from each point on the line. Structured-light 3D scanners scan multiple points simultaneously, thus reducing distortions caused by motion. Figure 0-4 is an example of a structured optical light scanner.



Figure 0-4: Structured optical light scanners (Taubin, et al., 2014).

1.11.3 Modulated light scanners

Modulated light 3D scanners convert digitised data into visual information by shining a continually changing light on a subject in a sine wave pattern. “A camera detects the reflected light, and the amount the pattern is shifted by determines the distance the light travelled. Modulated light also allows the scanner to ignore light from sources other than a laser, so there is no interference” (Pethe, 2008). Figure 0-5 shows a cross-sectional view of a spatial light modulator (SLM) scanner.

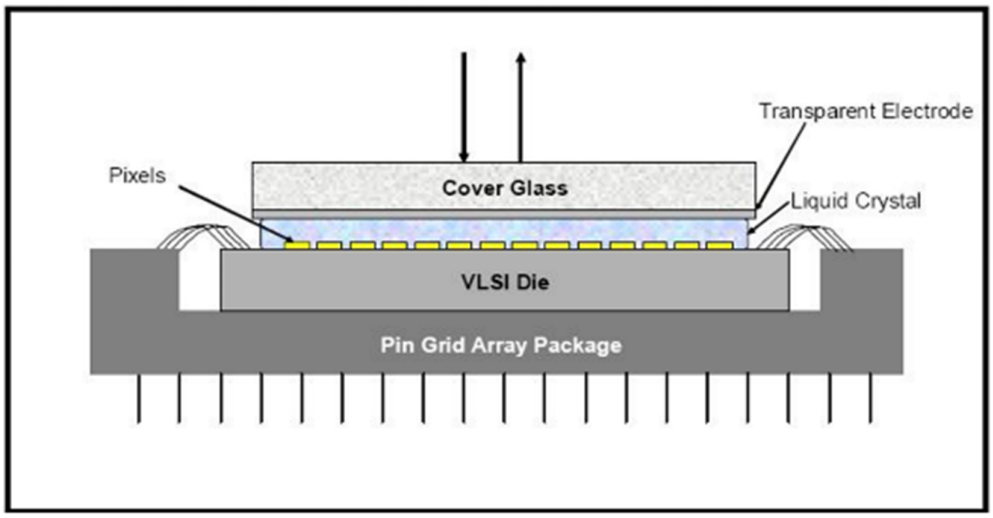


Figure 0-5: Cross-sectional view of a 12K SLM modulated light scanner (Pethe, 2008).

Figure 0-6 shows a Silicon scanner's 1x12288 Linear Array Liquid Crystal. It is possible to electronically control the speed at which the light of the SLM moves to operate at very high speeds, on the order of a few hundred frames per second (Pethe, 2008).

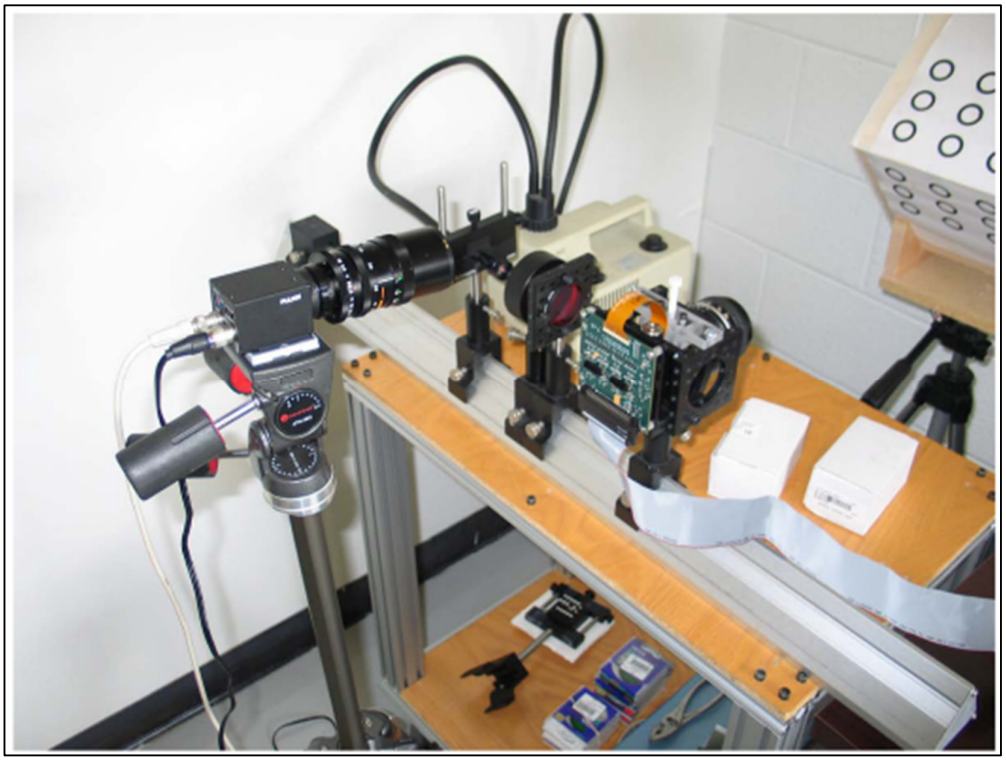


Figure 0-6: Modulated light scanner - 1x12288 Linear Array Liquid Crystal on Silicon scanner (Pethe, 2008).

1.11.4 Computer tomography scanners

"A computerised tomography (CT) scan combines a series of X-ray images taken from different angles around your body and uses computer processing to create cross-sectional images (slices) of the bones, blood vessels and soft tissues inside your body" (Mayo Foundation for Medical Education and Research (MFMER), 2022). X-rays are high-energy electromagnetic radiation that can pass through any object, including the body, to produce images of the shadows of objects (National Institutes of Health, n.d.). CT scans provide doctors with more detailed and accurate images than X-rays, allowing them to diagnose diseases and injuries and

plan medical, surgical, and radiation treatments. Figure 0-7 shows a CT scanner.



Figure 0-7: Computerized tomography (CT) scan (Canon medical systems USA, inc., n.d.).

1.11.5 Magnetic resonance imaging scanners

Magnetic resonance imaging (MRI) scanners produce 3D detailed anatomical images. Living tissues contain water that contains protons whose rotational axis constantly changes. Sophisticated technology measures this change (Medical Device Network, 2022).

Powerful magnets produce a strong magnetic field that forces protons in the body to align with the magnetic field. A radiofrequency current stimulates

protons, causing them to spin out of equilibrium, straining against the magnetic field. The MRI sensors detect the energy released as the protons realign with the magnetic field once the radiofrequency field is turned off. “The time it takes for the protons to realign with the magnetic field, as well as the amount of energy released, changes depending on the environment and the chemical nature of the molecules” (Medical Device Network, 2022). This allows physicians to detect and diagnose illness. Figure 0-8 is an MRI scanner developed for neurological and musculoskeletal imaging functions (Medical Device Network, 2022).



Figure 0-8: SIGNA 7.0T, a magnetic resonance imaging (MRI) scanner (Medical Device Network, 2022).

1.12 Scanning methods

Figure 0-9 summarises the different scanning methods.

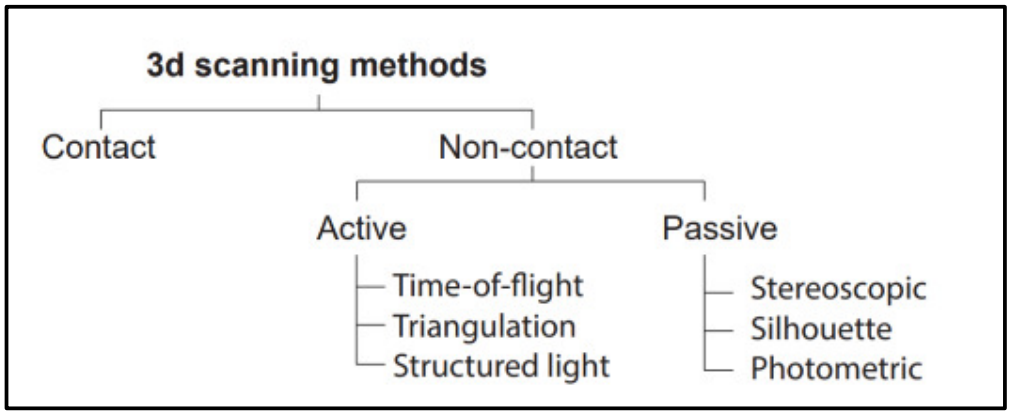


Figure 0-9: Summary of the different scanning methods (Moberg, 2017).

During the process of photometric scanning, a single hand-held camera can capture several overlapping images of an object to analyse the shadows and the "surface normal" determined. With surfaces normal, computer software can recreate objects in three dimensions and with surface textures of high quality (Moberg, 2017). Photometric scanning requires four different software steps:

- Micro-controller code written in C for 3d scanning;
- Raspberry Pi code is written in Python or 3d scanning;
- Raspberry Pi code is written in Python for mapping image pixels to sample points; and
- Merging and meshing clouds in open-source software (Moberg, 2017, p. 22). For example, CloudCompare computer software can recreate the object in three dimensions and with surface textures of high quality (Moberg, 2017).

Images are distributed according to the camera's angle of view to synchronise LiDAR samples with photographed pixels. Figure 0-10 shows images captured with some overlap due to the camera's viewing angles, 62.2° horizontal and 48.8° vertical.

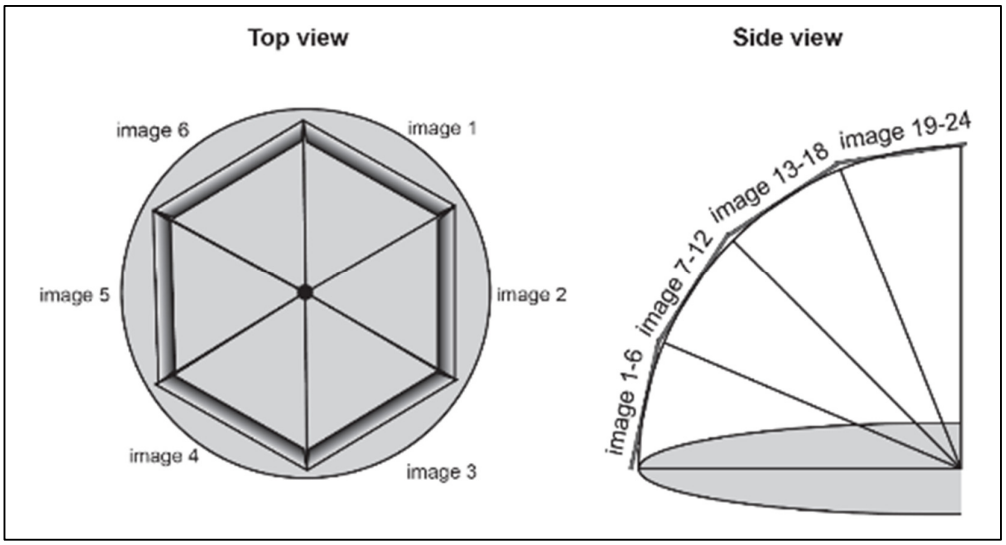


Figure 0-10: Concept of image sectioning (Moberg, 2017).

Raspberry Pi calculates pixels from the images depending on angles phi (φ) (φ) and theta (θ). When the correct image is found, the pixels are organised in columns and rows. The correct pixel is mapped according to the offset between the LiDAR and the camera (Moberg, 2017). Figure 0-11 illustrates the relationship between the camera, LiDAR and the image.

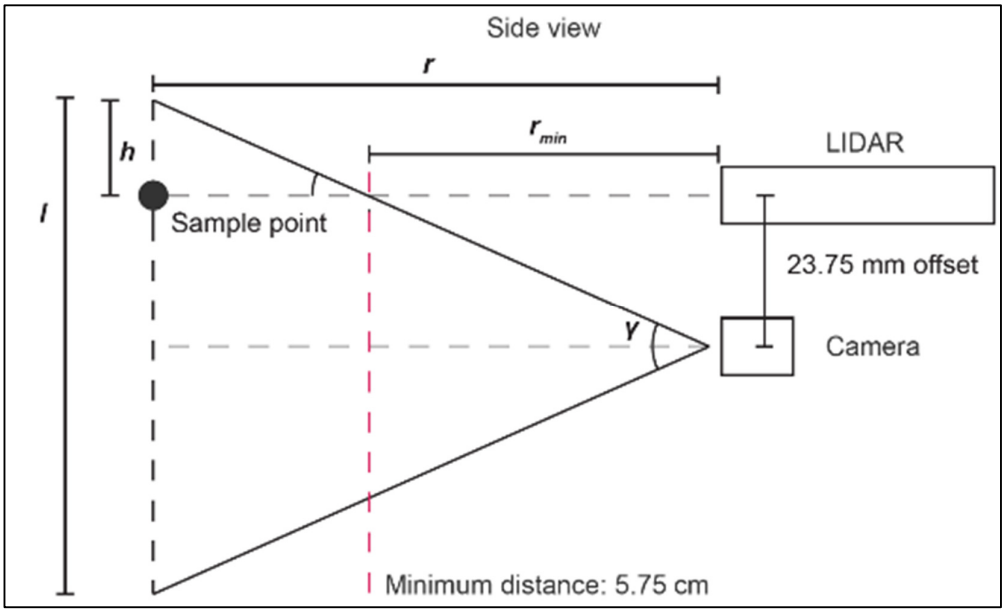


Figure 0-11: Camera offset geometry (Moberg, 2017).

The system's range is limited by how much diffused light is reflected and absorbed by the sensor (Moberg, 2017). Therefore, fewer samples result in a less detailed point cloud but a correct mesh. "While a dense point cloud captures the object shape very well, the inaccuracy of the LiDAR sensor reduces the final mesh quality" (Moberg, 2017, p. 35). Mathematically speaking, the word 'normal' refers to being at right angles or meeting at 90 degrees (Math Open Reference, 2011). Figure 0-12 shows line JK as perpendicular to AB.

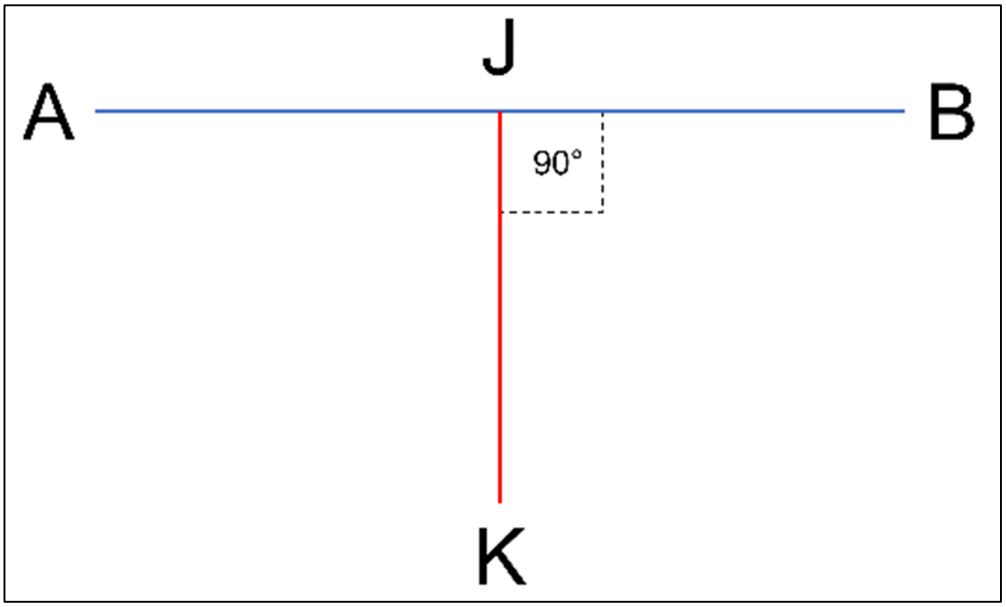


Figure 0-12: Line JK is normal to AB (Math Open Reference, 2011).

The LiDAR sensor calculates normals between a set of points resulting in small planes between points (Moberg, 2017). The calculated normals determine the normal to a point on a surface to estimate the normal of a plane tangent to the surface resulting in a least squares plane fitting estimation problem (Sphinx, n.d.). Least Squares Fitting is “a mathematical procedure for finding the best-fitting curve to a given set of points by minimising the sum of the squares of the offsets ("the residuals") of the points from the curve” (Wolfram Research, Inc., 2022).

The LiDAR sensor captured points on a wall with a minimal gap. With a smaller spacing between points, the tiniest opening in the wall causes a jagged shape instead of a flat wall; see Figure 0-13.

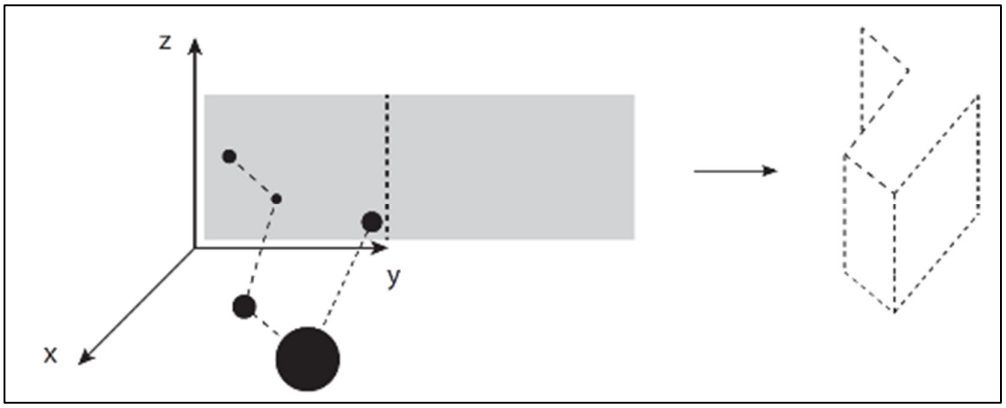


Figure 0-13: Illustration of a very dense point cloud with errors and resulting mesh (Moberg, 2017).

Figure 0-14 shows the result of a scan with fewer sample points resulting in a less detailed point cloud but a correct mesh. The algorithm (Poisson surface reconstruction) averages points to create the most suitable plane (Moberg, 2017).

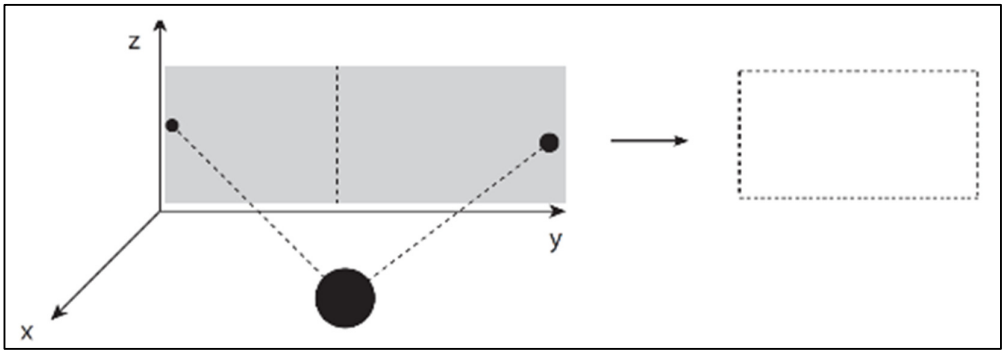


Figure 0-14: Illustration of less dense point cloud with errors and resulting mesh (Moberg, 2017).

“The ‘Poisson surface reconstruction algorithm’ uses point cloud normals to build a 3D surface. The algorithm considers all the points at once and is therefore highly resilient to the noise” (IGI Global, 2022). It is crucial to scan

objects from a straight linear perspective (Moberg, 2017). Moberg (2017) found that a faster and less detailed scan produces the best result.

Hand-held scanners use triangulation range finders which typically range between 25-30 m. Examples of hand-held scanners that use triangulation range finders of are the Leica BLK2GO and the ZEB REVO RT. Leica BLK2GO handheld scanner with a range of 25 m at an accuracy of 6-15 mm, designed for indoor and outdoor use (Leica Geosystems, 2019). Figure 0-15 shows an example of the Leica BLK2GO Imaging laser scanner.



Figure 0-15: Leica BLK2GO Imaging laser scanner (iF Design, 2022).

The ZEB REVO RT with a scanning range of 30m and an accuracy of 1-3cm for indoor and outdoor use (Optron group, 2018). See Figure 0-16 for an example of the ZEB Revo RT scanner.



Figure 0-16: ZEB Revo RT - Real-Time handheld scanner (Optron Group, 2018).

As a result of high-resolution scanning, it is possible that the beam will strike an edge of an object, causing data to appear noisy just behind the edge. Although scanners with a smaller beam width help to solve this problem, they are limited by range as the beam width will increase over distance (Trebuňa, et al., 2018). “Some laser scanners have level compensators built into them to counteract any movement of the scanner during the scan process” (Trebuňa, et al., 2018, p. 3).

An Inertial Measurement Unit (IMU) “is an electronic device that measures and reports a body's specific force, angular rate, and sometimes the

magnetic field surrounding the body, using a combination of accelerometers and gyroscopes, sometimes also magnetometers" (IoT ONE, 2022). determines the position between the handheld scanner and the object being scanned. The IMU allows it to decide where data is collected with the GNSS (Trebuňa, et al., 2018). One should typically use computer software to correlate geo-referenced markers on the scanned image (Figure 0-17) to the pre-defined coordinates of the scanned markers (Trebuňa, et al., 2018).



Figure 0-17: Marker on a scanned image.

Tacheometric measurements combine measured distances and angles (Staiger, 2003). For example, tachymetric Laser Scanners measure one oblique distance (s') to each point of an object, and two orthogonal angles (W1 and W2) see Figure 0-18.

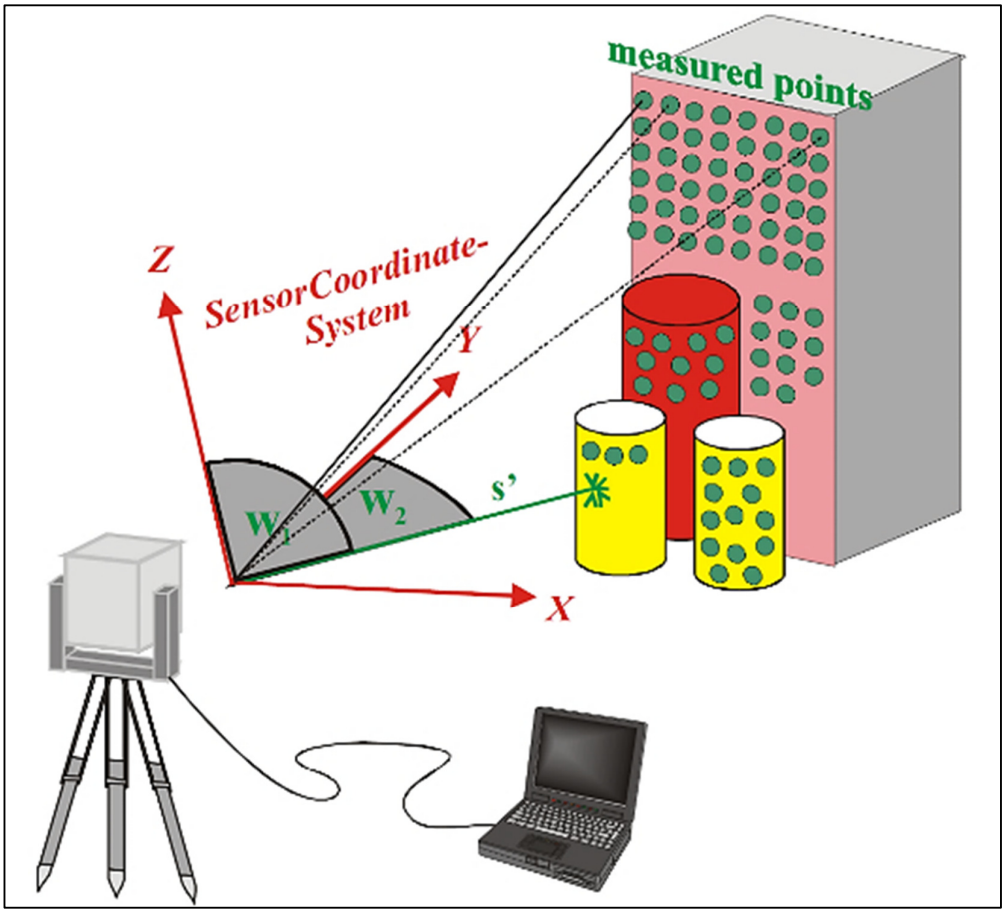


Figure 0-18: The principle of tacheometric Laser Scanning (Staiger, 2003).

Tacheometric Laser Scanners can be divided into three groups (Figure 0-19):

- Panorama-Scanner;
- Hybrid Scanner; and
- Camera Scanner (Staiger, 2003).

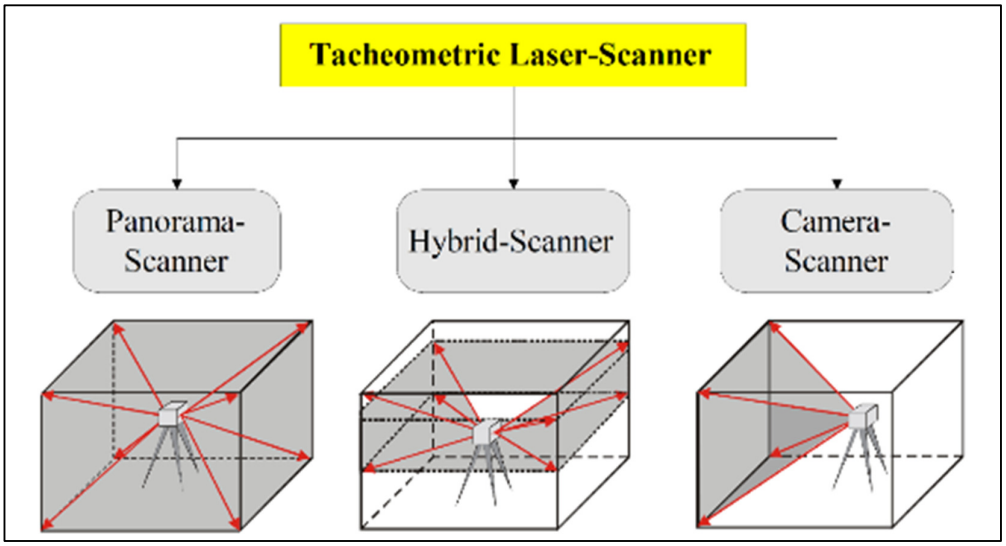


Figure 0-19: The different types of tacheometric scanners (Staiger, 2003).

With Panorama-Scanners, the instrument's base limits the FOW, including its tripod (Staiger, 2003). In addition, panoramic images taken with a 3D scanner “contain depth information. That makes it possible to take measurements within the images, inspect coordinates and add markups, and even include 3D models as augmented reality objects within the imagery” (Arrival 3D, Inc., 2022). An example of a Panorama-Scanner is the Leica RTC360 Laser Scanner with a range between 0.5 - 130 m (SCCS Survey, 2022).



Figure 0-20: Leica RTC360 Laser Scanner (SCCS Survey, 2022).

With a Hybrid Scanner, one rotation axis is without restrictions (often the horizontal movement); the second rotation axis is limited to, for example, 60° due to the use of mirrors (Staiger, 2003). An example of this scanner includes the RIEGL VZ-6000 with a scanning range of 6km that can operate in poor visibility caused by dust, haze, rain and snow, see **Error! Reference source not found.** (RIEGL Laser measurement systems, 2020).

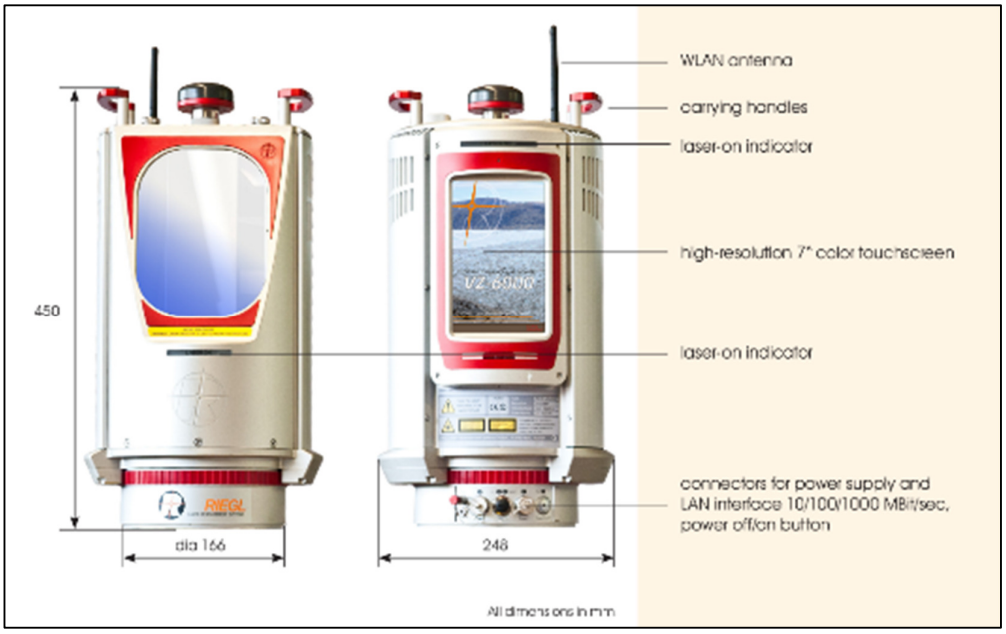


Figure 0-21: RIEGL VZ-6000 laser scanner (RIEGL Laser measurement systems, 2020).

Camera Scanner works on the photogrammetry principle, which "is a 3-dimensional coordinate measuring technique that uses photographs as the fundamental medium for metrology (or measurement)" (Geodetic Systems, Inc., 2020). The Camera Scanner has a limited Field of View (FOW); see Figure 0-22. In addition, this type of scanner captures a view from outside of the object(s) (Staiger, 2003).

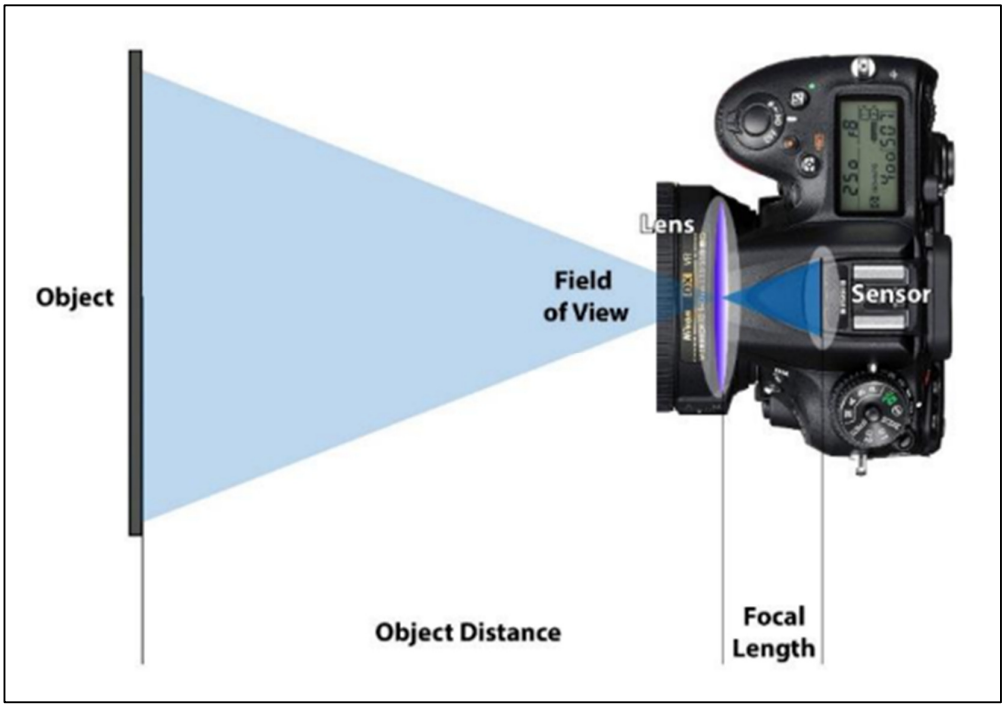


Figure 0-22: Camera field of view relationship (Geodetic Systems, Inc., 2020).

The range of acceptable sharpness determines the optimal distance that a camera should be used from an object refers to the depth of focus (Geodetic Systems, Inc., 2020). Figure 0-23 demonstrates the focus depth relationship.

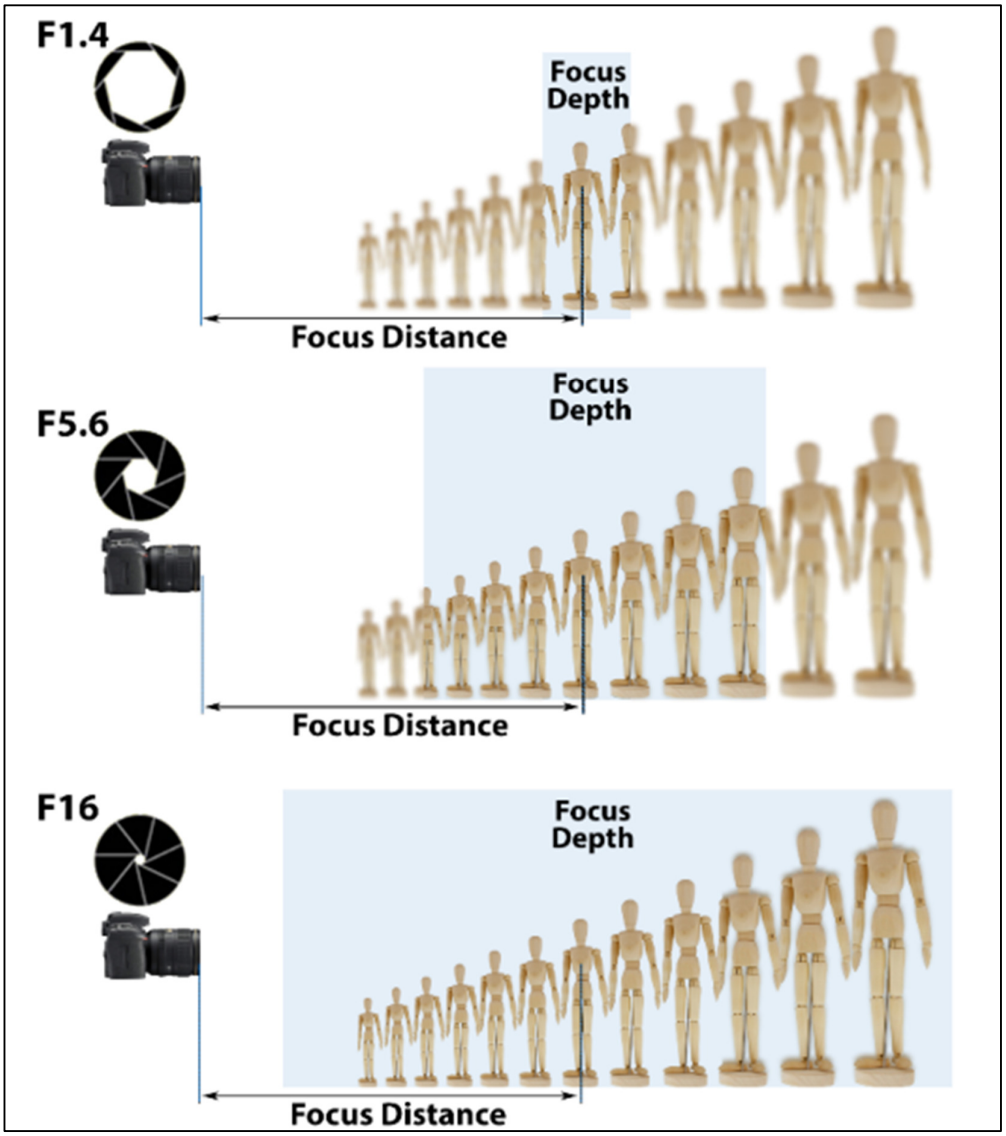


Figure 0-23: F-number to focus depth relationship (Geodetic Systems, Inc., 2020).

With a Hybrid Scanner, one rotation axis is without restrictions (often the horizontal movement); the second rotation axis is limited to, for example, 60° due to the use of mirrors (Staiger, 2003). An example of this scanner includes the RIEGL VZ-6000 with a scanning range of 6km that can operate

in poor visibility caused by dust, haze, rain and snow, see **Error! Reference source not found.** (RIEGL Laser measurement systems, 2020).

1.12.1 Point clouds

Point clouds create 3D surfaces from scanned objects. “Point clouds are often converted to polygon mesh or triangle mesh models or CAD models through a process commonly referred to as surface reconstruction” (Trebuňa, et al., 2018, p. 5). Figure 0-24 is an example of point clouds of a scanned building.



Figure 0-24: Point cloud of a scanned building (Trebuňa, et al., 2018).

The point set registration process allows the alignment between point clouds and 3D models (Trebuňa, et al., 2018). “CloudCompare is a free & open-source software package that allows the 3D registration of point clouds based on (at least) 3 known points” (Rock Mapper Helpdesk, 2022). Align point cloud based on known points using the [FaceID]_pointcloud CSV file from a 3D scan. “CloudCompare automatically detects the correct columns for X/Y/Z and RGB (colour)” (Rock Mapper Helpdesk, 2022). Once the [FaceID]_pointcloud CSV file is opened in CloudCompare, a window appears that allows picking a minimum of three known points for

georeferencing on the point cloud; this is referred to as “to align entities”. The picked points will be shown as A0, A1 and A2 in 3D and in a table; see Figure 0-25.

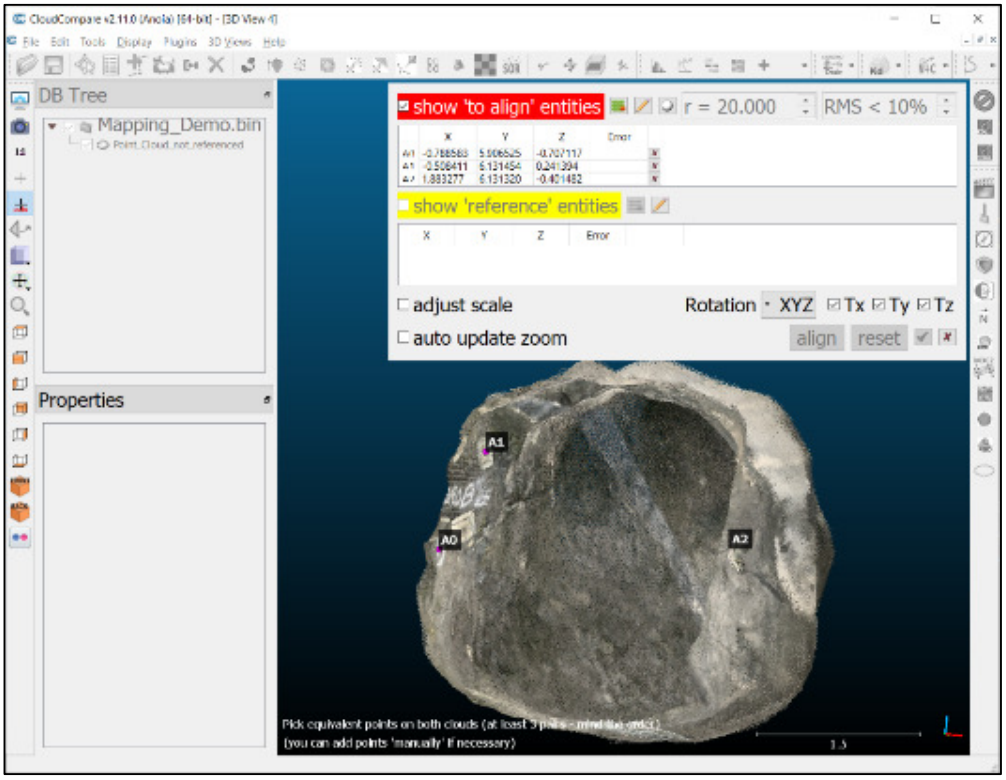


Figure 0-25: Picked points are shown as A0, A1 and A2 in 3D and in a table CloudCompare software (Rock Mapper Helpdesk, 2022).

The next step is to enter surveyed reference coordinates of points A0, A1 and A2 in the table with the heading “show reference entities” reference point coordinates are numbered R0, R1 and R2, see Figure 0-26 (Rock Mapper Helpdesk, 2022).

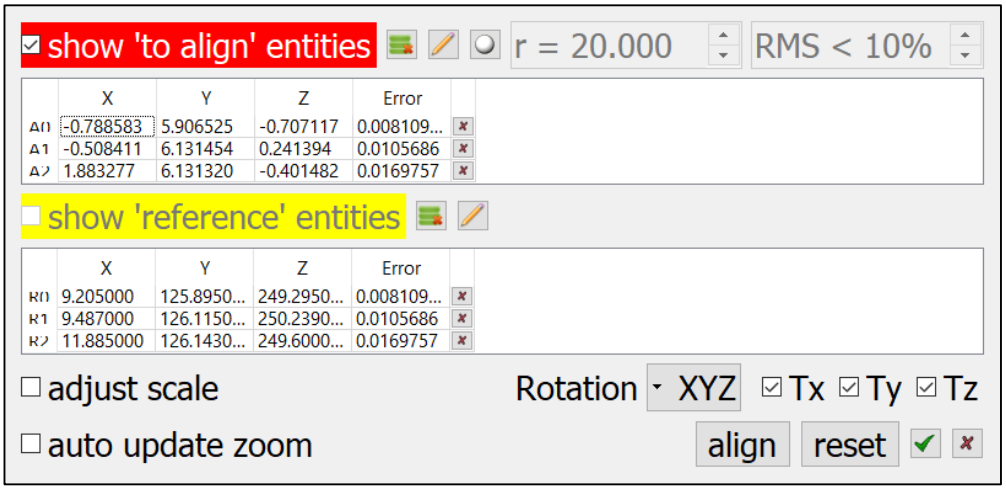


Figure 0-26: Reference point coordinates (Rock Mapper Helpdesk, 2022).

Once the align button is pressed, the point cloud will be aligned to match the reference point coordinates (Rock Mapper Helpdesk, 2022). Both publications by Morris and Langari (2012) and Yashchuk (2009) note that all the calibrations and specifications of an instrument are only valid under specific, controlled environmental conditions – dependent on variables such as temperature, pressure and humidity. Environmental changes affect instruments: zero drift and sensitivity drift (Morris & Langari, 2012). Zero drift can be corrected by recalibration of the scanning instrument. Manufacturers usually calibrate laser scanners and recommend that users re-calibrate them regularly (Mijic, 2015). Sensitivity drift measures the error per each environmental constraint to which the instrument characteristics are sensitive (Morris & Langari, 2012). It is possible to reduce drift error by ensuring that scanning occurs within the range of the scanning instrument (Wang, et al., 2021).

Simultaneous localisation and mapping (SLAM) are an algorithm that uses data from the mapping system's onboard sensors – 3D LiDAR, RGB camera, and IMU to determine the trajectory as the scanner moves through an area (Higgins, 2020). The most popular process for correcting errors is finishing back where one started (Higgins, 2020); see Figure 0-27.

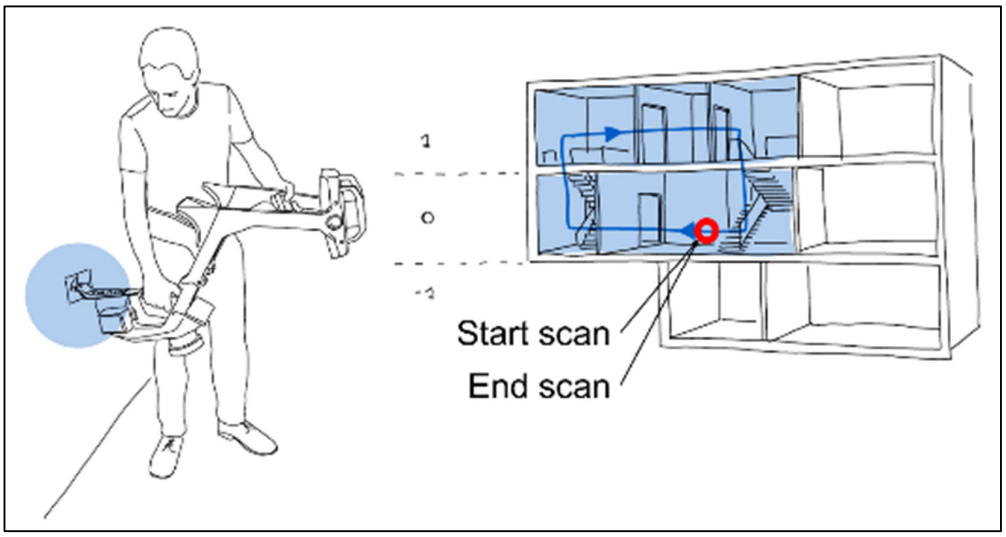


Figure 0-27: End scan at the scan start point (Higgins, 2020).

Coordinated control points can be used when the scanned environment does not allow for a closed loop. For example, when the scan is geo-referenced, the control points are used to snap the scanned image to corresponding coordinate points. This method should be used where survey-grade accuracy is of the utmost importance (Higgins, 2020).

1.13 Case Studies

1.13.1 3D Scanning in an open pit coal mine in Indonesia

3D LiDAR technology was used in a study in the East Kalimantan Province of Indonesia for more effective mine mapping as an alternative to traditional mine mapping methods. Mining in the East Kalimantan Province consists of open pit coal mining (Septarini, et al., 2013).

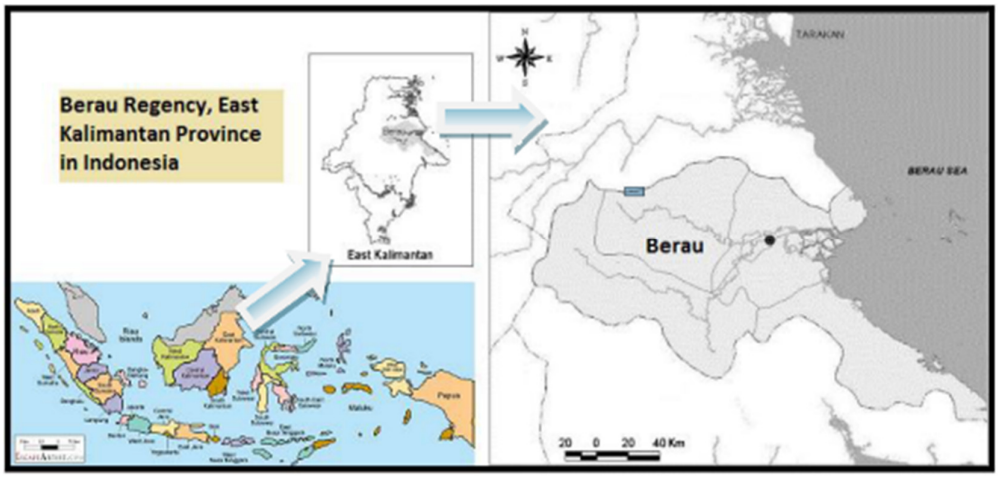


Figure 0-28: East Kalimantan Province (Septarini, et al., 2013).

3D LiDAR data was obtained in point clouds, which were then filtered and grouped according to the needs of getting a digital terrain model (DTM). A DTM is a 3D “digital file of a detailed representation of the topographical variations in the surface of the Earth. A DTM does provide a 3D image of the land surface” (Septarini, et al., 2013, p. 4). The DTMs of 2010 and 2012 were used to calculate the volume difference between the two DTMs (Septarini, et al., 2013). The DTMs were stacked so that the volume difference could be calculated. The DTMs were obtained by generating the

ground points (after the classification process) using Global Mapper software (Septarini, et al., 2013). The “Unsigned Subtraction” method (positive numbers) (O’Reilly Media, Inc., 2022), was used to compare the volume difference between the DTMs between 2010 and 2012. Global Mapper and Surfer software were used to compare the result from the volume of the mine excavation in 2010 and 2012. Point cloud cleaning was done to eliminate spikes in the DTM (Septarini, et al., 2013) to ensure an accurate volume calculation. The point data was classified into two main groups: ground and non-ground. “The orange points mean ground points, and the white points mean non-ground points” (Septarini, et al., 2013, p. 5). In this instance, non-ground classified points may represent vegetation and the black points unclassified data in the data set (Prerna & Singh, 2015). Figure 0-29 display data from 2010 and 2012.

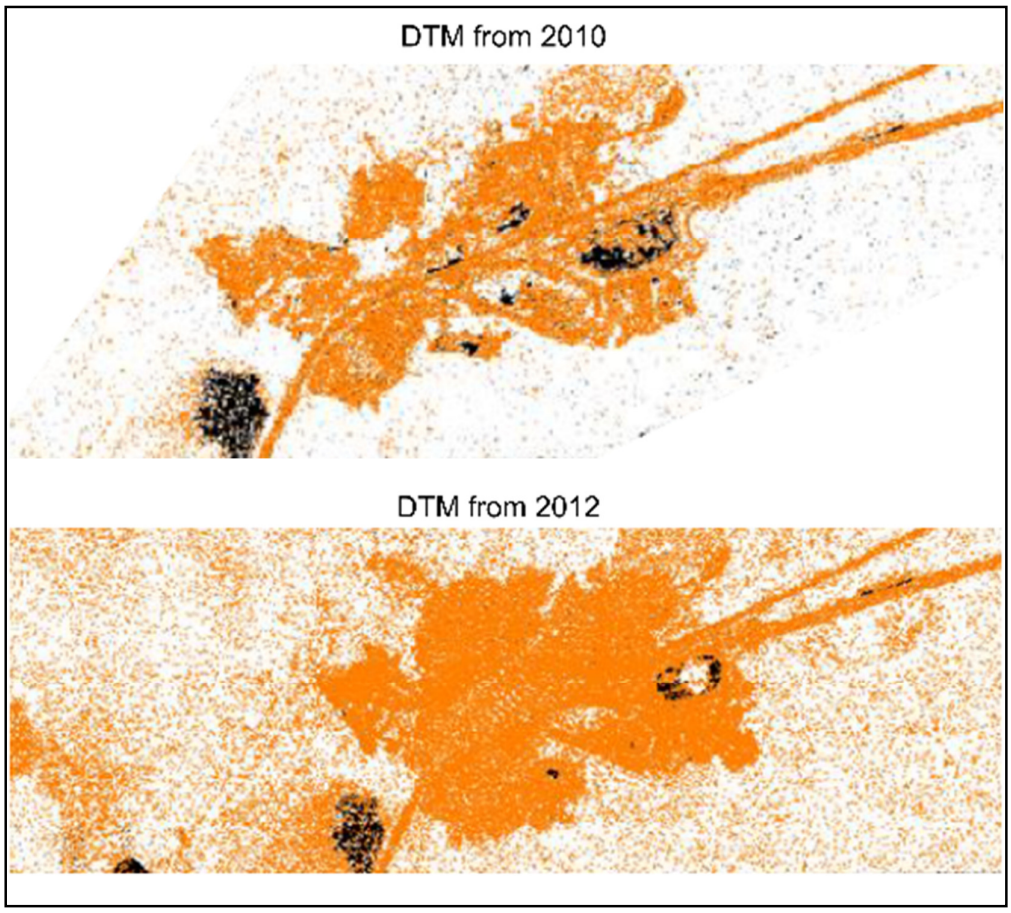


Figure 0-29: Compared point cloud difference between DTMs (Septarini, et al., 2013).

Table 0-1 shows the difference in volume by using two different software programs, Global Mapper v14 and Surfer v10, with an applied cut factor and fill factor. “The cut factor is used to adjust the volume of excavated material to account for the expected amount of the material to swell when it is excavated. The fill factor is used to account for the additional volume of material that would be required due to the compaction of the soil when it is placed” (Septarini, et al., 2013, p. 6).

Table 0-1: Volume calculation using Global Mapper and Surfer (Septarini, et al., 2013).

	Software		
	Global Mapper v14 (m^3)	**Surfer v10 (m^3)**	**Volume Difference (m^3)**
Cut Volume	101,931	101,938	6.3
Fill Volume	0.2	0	0.2

The result of the scan is primarily used to report the volume of blasted rock. Scans are captured before and after blasts to calculate the volume of blasted rock, and therefore, the advance of excavations can be determined once the blasted material has been removed (Ahamad & Ojha, 2015). In addition to the advantage of calculating volume from excavations, geological and geotechnical mapping are also available from the scans.

Because scans do not take long to capture in the workplace, this has an added safety aspect as mine personnel can spend less time on the face and thus reduce the probability of accidents and injuries. This is possible as technology has enabled remote scanning of workplaces (Ahamad & Ojha, 2015).

1.13.2 3D Scanning in an underground room-and-pillar limestone mine in South Korea

Daesung MDI Donghae Limestone Mine is in Donghae-si, Gangwon-do, South Korea. Daesung MDI Donghae Limestone Mine is an underground operation that uses a hybrid room-and-pillar mining method. The case study aims to determine if it is possible to maximise ore recovery while ensuring the stability of stopes by using horizontal and vertical safety pillars. This limestone mine used 3D LiDAR scanning technology to analyse the orientation of a joint in a vertical safety pillar (Lee & Choi, 2019).

The 3D point cloud data obtained from the 3D LiDAR scan made it possible to measure the dip directions of joint sets. The study collected data on 79 joints with distinctive orientations from the entire stope area under investigation (Lee & Choi, 2019).

1.13.3 Using laser scanner face mapping to improve geotechnical data confidence at Sishen Mine, an iron ore open-pit mining operation

Sishen Mine is a large open-pit mining operation in South Africa that requires reliable geotechnical data to design and evaluate pit wall stability. The primary data sources to achieve this are “geotechnical borehole data, face mapping data, geotechnical laboratory testing data and implicit structural models” (Russell & Stacey, 2019, p. 11). Face mapping has traditionally been done via direct contact with the face through a technique

referred to as line mapping (Russell & Stacey, 2019). Line mapping measures the spacing between structural discontinuities, see Figure 0-30.

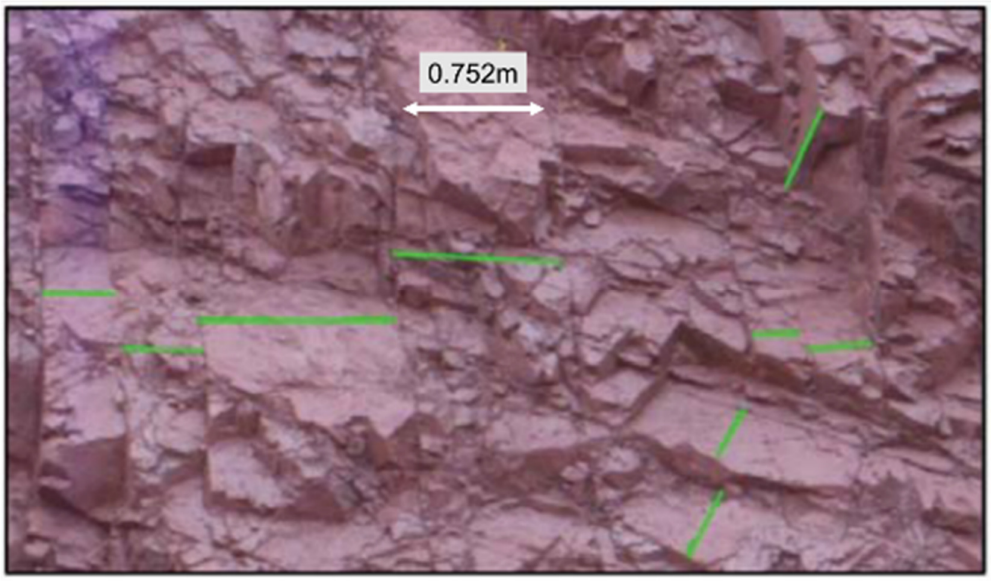
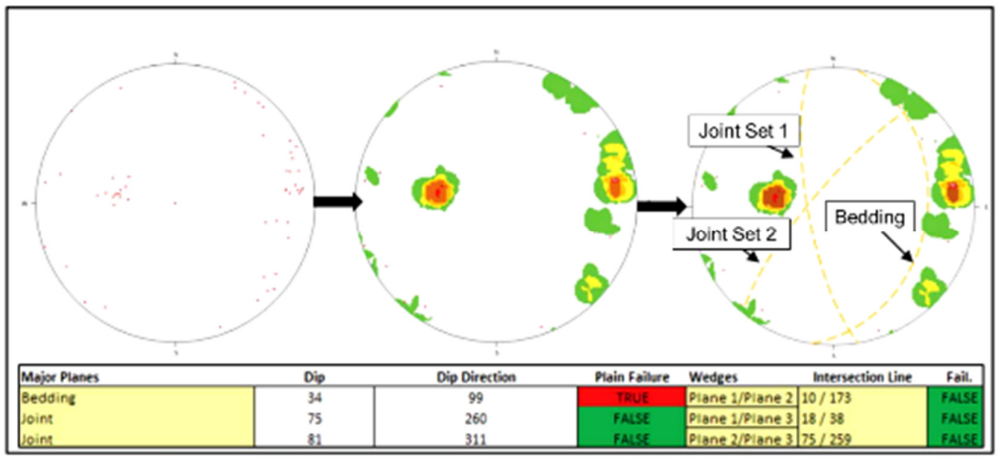


Figure 0-30: Measurement of discontinuity spacing (Russell & Stacey, 2019).

Digital mapping of faces to capture geological discontinuity and structural orientation has become more prevalent in recent years. In 2013, Sishen Mine acquired a terrestrial laser scanner with the resolution, photographic capabilities and software capable of carrying out geotechnical face mapping (Russell & Stacey, 2019). During the study by Russell and Stacey, a mapping procedure was set up based on accepted face mapping methods, the data requirements of the mine and the capabilities of the laser scanner system. Mapping data from the scans was integrated into the Acquire geological data management system. Acquire is a purpose-designed structured query language (SQL) database system that stores the mine's

geotechnical data (Russell & Stacey, 2019). This method integrates scanner software, Microsoft Excel, and the Acquire geological database system. The scanner software makes information available in text or CSV format. Sishen uses an Excel template to analyse and delineate dominant discontinuities and rock mass grading before entering data into the mine's Acquire geotechnical database. Figure 0-31 shows the delineation of significant discontinuity planes ready for export and capture in the Acquire database.



Major Planes	Dip	Dip Direction	Plain Failure	Wedges	Intersection Line	Fail.
Bedding	34	99	TRUE	Plane 1/Plane 2	10 / 173	FALSE
Joint	75	260	FALSE	Plane 1/Plane 3	18 / 38	FALSE
Joint	81	311	FALSE	Plane 2/Plane 3	75 / 259	FALSE

Figure 0-31: Delineation of significant discontinuity planes for export and capture in the Acquire geotechnical database (Russell & Stacey, 2019).

Acquire, a geotechnical database, allows for data to be queried based on various parameters and for statistical analysis to be carried out. “Rock mass parameters from either face mapping or borehole logging datasets can be queried with the required lithological and spatial constraints applied. This feeds into the geotechnical design process by providing up-to-date rock mass parameters” (Russell & Stacey, 2019, p. 18). Likewise, the mapping

report sheet feeds into the geotechnical design process by providing up-to-date rock mass parameters (Russell & Stacey, 2019). Figure 0-32 is an example of the output Excel face mapping report.

BIF (BIF, LY, LYT) | All | All | North | Middle | South | RMR | GSI

MAPPING / LOGGING PARAMETER REPORT

Material Type BIF (BIF, LY, LYT)

Joint Spacing - Mapping

Count	2953
Min	0.02
Max	12.78
Average (Normal)	0.844
Std. Dev (Normal)	0.892
Average (Log Normal)	0.570
Std. Dev (Log Normal)	2.472
CV	105.64%

Joint Persistency - Mapping

Count	836
Min	0.14
Max	37.5
Average (Normal)	4.689
Std. Dev (Normal)	5.062
Average (Log Normal)	1.754
Std. Dev (Log Normal)	2.472
CV	107.95%

Fracture Frequency - Mapping

Count	2953
Min	0.0782
Max	50
Average (Normal)	2.705
Std. Dev (Normal)	3.343
Average (Log Normal)	2.837
Std. Dev (Log Normal)	2.904
CV	123.58%

Joint Spacing - Logging

Count	1746
Min	0.005
Max	70.85
Average (Normal)	0.926
Std. Dev (Normal)	2.459
Average (Log Normal)	0.389
Std. Dev (Log Normal)	3.512
CV	265.63%

Fracture Frequency - Logging

Count	584
Min	0.141
Max	122.22
Average (Normal)	9.115
Std. Dev (Normal)	8.412
Average (Log Normal)	0.000
Std. Dev (Log Normal)	0.000
CV	92.30%

Mapping RMR

Count	57
Min	51
Max	71
Average (Normal)	61.456
Std. Dev (Normal)	4.145
Average (Log Normal)	61.314
Std. Dev (Log Normal)	1.072
CV	6.74%

Figure 0-32: Excel face mapping report sheet from Acquire geotechnical database (Russell & Stacey, 2019).

Figure 0-33 is a schematic data flow for geotechnical face mapping data at Sishen Mine.

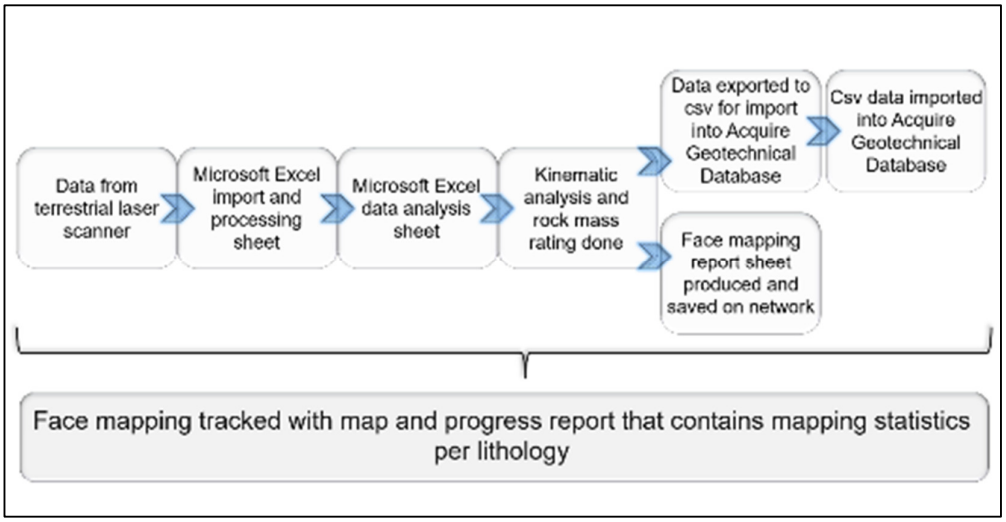


Figure 0-33: Schematic data flow for geotechnical face mapping data at Sishen Mine (Russell & Stacey, 2019).

The system integrates the scanner software, Microsoft Excel, and the Acquire geological database system. The scanner software allows for exporting the various individual parameters in text or CSV format. For data management at Sishen, an Excel template was set up to carry out kinematic analysis, delineation of predominant discontinuities and rock mass rating before importing the relevant data into the mine's Acquire geotechnical database.

A terrestrial laser scanner can create a high-resolution point cloud covering several hundred square metres in a couple of minutes. These scanned point clouds produce fast and efficient digital face mapping (Russell & Stacey, 2019). Figure 0-34 shows a high-resolution point cloud for face mapping (Russell & Stacey, 2019).



Figure 0-34: Terrestrial laser scanner using a vehicle-mounted set-up (left) and a high-resolution point cloud for use in face mapping (right) (Russell & Stacey, 2019).

A surveyed reference point needs to be positioned on the face and two camera tripod positions need to be accurately surveyed (Russell & Stacey, 2019). This is important if the scanned image needs to be geo-referenced to feed into Sishen Mine's geological model. Sishen Mine realised the following advantages of laser scanning:

- The laser scanner provided faster and more accessible data collection;
- The laser scanner provided faster data processing and was less demanding on software systems;
- More accurate discontinuity orientation measurements were obtained using the laser scanner (up to 15° difference in dip measurements between the two techniques was observed); and
- Planes oblique to the exposed face were more readily observable with the laser scanner (Russell & Stacey, 2019).

(Russell & Stacey) determined that the laser scanner would give reliable roughness measurements for discontinuity traces greater than 2 m in length for typical scan ranges between 50 m and 200 m. The research showed that scanner inaccuracy would prevent the reliable measurement of discontinuity roughness for shorter traces in instances where the height of the surface irregularities is less pronounced (Russell & Stacey, 2019). At Sishen, the Micromine 3D modelling software package has been adopted to analyse designs and incorporate spatial geotechnical data into the design and analysis process (Russell & Stacey, 2019).

The literature from Sishen Iron Ore Mine showed that the terrestrial laser scanner provides a practical, faster and safer way to collect face mapping data. The results obtained from the terrestrial laser scanner were compared to manual techniques and a stereo photosystem such as Sirovision (Russell & Stacey, 2019). The system is safer and allows inaccessible rock faces to be mapped because no contact with the face is needed. The photographic overlay of the 3D mapping face was an accurate means of interpreting structural and rock mass features on the underlying scan surface (Russell & Stacey, 2019).

The terrestrial laser scanner system at Sishen Mine has proved invaluable for geotechnical data capture, geotechnical hazard assessment and structural mapping. The laser scanner also makes the rapid collection of data possible when surface support such as wire mesh or shotcrete is to be applied to the rock face soon after excavation. Russell and Stacey were

confident that the additional data the laser scanning made available would enhance the quality of designs and reduce risk accordingly. They, therefore, regard the scanner as “a tool of strategic importance” (Russell & Stacey, 2019, p. 20).

1.14 Section Summary

3D laser scanning offers more advantages to the mining industry, which, as discussed, will improve the overall accuracy and efficiency of mining. This is primarily due to the reduced time taken to capture large surface areas and the geological mapping process not being dependent on traditional, less accurate mapping methods. Geospatial data are also stored on a digital system whereby the data is always readily available to all production team members. Monitoring the flow of blasted ore becomes a traceable process with higher accuracy, increasing ore grade estimations and affecting profit calculations. The frequency of scanning and surface mapping is increased when utilising 3D scanners. This means that the entire pre-blasting planning and preparation process could be accelerated. As per the case studies, 3D scanning systems commonly used on open pit mines are suitable for the narrow, tabular stopes found on Mponeng.

RESEARCH METHODOLOGY

1.15 Section Overview

The quantitative and qualitative research methodology aimed to investigate using a cost-effective 3D LiDAR scanner for underground use. The primary purpose of this scanner will be to capture underground geological mapping information without interrupting production. Furthermore, the data captured underground should be distributable among relevant stakeholders; the data is processed as soon as an employee returns to the surface. Therefore, finding a fast and easy mechanism to share the scanned underground geological mapping information with the production team was essential. The reason for this is to guide the production team on SW control.

The priorities used to guide the weighting between device suitability and appraisal of performance in the testing phase are introduced in this chapter. The initial approach was developed during the research to short-list eligible hardware and software. A literature survey process supports evaluating the short-listed laser scanner hardware and software.

The research describes applied data collection methodologies and then discusses how the collected information is analysed. Finally, the results illustrate obstacles encountered during the research.

1.15.1 Priorities of the Research Criteria

The following criteria were applied in the short-listing and the identifying of the choice of a laser scanner for the practical underground conditions of narrow tabular mining:

- **Ease of use.** The scanner must be used daily to acquire and share information productively. The buy-in and willingness of underground personnel to use the device optimally was an additional and important consideration;
- **Accuracy and quality of laser scanners.** It is vital to build the 3D block model from accurate information. Therefore, the manufacturer's accuracy specifications had to be considered; and
- **Cost of 3D scanners and software.** The evaluation included the financial outlay of purchasing and maintaining the laser scanning system, which would consist of software and the cost of software upgrades.

Cost played an important factor since the project was in the test phase. It was essential to keep all costs as low as possible to ensure that underground use of the proposed 3D LiDAR scanner was accepted upon presentation of the research results. Therefore, the availability of tools and devices dictated research feasibility, the research intended to find technology that could be advantageous to both the production and geology disciplines.

The production department may benefit from the use of non-georeferenced scans. Non-geo-referenced scans and the reef widths can be compared to each other to identify grade dilution. The scanning will enable the production team to scan the workplace during the underground shift, plot daily advances, plan equipment and complete legal documents such as safety reports while underground. This may help reduce extra surface time, which is additionally desirable as computers are limited for the use of shift boss. The scans may also indicate substandard cleaning of stope panels and include a record of roof support for safety standard reporting.

However, the primary goal is for the geology department to use geo-referenced scans to digitise the underground stope mapping directly onto Deswik CAD. This mapping will then update the 3D geological block model. This will ease the workflow and help proactive action towards better controlling the SW and grade dilution.

1.16 Deliberation of Devices and Methods

Before conducting a literature review to compile a short list of 3D scanner technologies, the current devices used for 3D mapping underground on the Mponeng Mine were reviewed. The following total stations and electronic distance measurement (EDM) capabilities are the primary items of equipment investigated in this project:

- South Total Station - N7, a product from V.I. Instruments; and

- TS07 3 R500 Total Station, produced by Leica Geosystems

Additionally, information on traditional measuring (using tapes), map processing and software requirements (including file formats) currently used for integration with the 3D block model were compiled. Finally, it was necessary to determine if the proposed research methods and shortlist of alternative scanners would benefit Mponeng Mine. It was also essential to ensure that shortlisted alternative scanners would yield a smooth integration of the workflows discussed in Chapter 6.

Three devices were short-listed according to the prerequisite criteria for the practical use of a 3D scanner underground. The prerequisite criteria consider range, accuracy, weight, ease of use, safety, durability and cost-effectiveness. The devices are listed as follows:

- Structure Sensor Mark II, built by Occipital, a spatial computing company, see Figure 0-1;
- The non-cellular Apple iPad Pro is 11-inch with Wi-Fi and 256 GB storage capability, see Figure 0-2; and
- Apple iPhone 13 Pro Max with Wi-Fi 128 GB storage capability; see Figure 0-3.



Figure 0-1: The Occipital Structure Sensor (Mark II)) (3D Printing Systems South Africa, 2021).



Figure 0-2: Apple iPad Pro 11-inch (iStore, 2021).



Figure 0-3: iPhone 12 Pro (Apple Inc., 2022).

All these devices have hardware specifications and compatible software to which the data is downloaded and presented with limitations. These limitations are discussed in more detail in the research. The shortlist of devices additionally has system requirements and particular applications (apps) considered in selecting the most optimal choice(s). Discussion in this section will highlight all information necessary for comparison of the relevant 3D scanning technologies and to justify the decisions on those submitted to the testing phase of the study.

Photogrammetry 3D scanning technology is the process whereby photos of a 3D object are stitched together with software to produce a 3D model that represents the colour and texture of the scanned object (Aniwaa Pte. Ltd., 2021). Another significant influence in the decision-making process was the total cost of the applications. Therefore, they were purchasing these applications. The costs that apply when exporting 3D scans, as well as the cost of additional software requirements (that is, other apps necessary for data manipulation, display and conversion. Furthermore, the file formats in which exportable data becomes available must be compatible with Mponeng's established software. Finally, data storage and scan-capturing mechanisms were noted, as some applications may require an internet connection.

1.16.1 Current technologies used at Mponeng Mine

Total Stations

Mponeng Mine currently uses two types of Total Station. They are the South Total Station - N7 from V.I. Instruments and the Leica TS07 3" R500 Total Station from Leica Geosystems to survey underground workings for depletion calculations of the reserve block model. Mine surveyors go underground daily to survey development ends that have been blasted. Mine surveyors also survey stope panels during the month, and a final measurement is reported for payment purposes. Both the development and stope advances are plotted on Syncromine software. The mine surveyors' scans are exported in the form of points. Once the mine surveyor has

downloaded the scanned points, they connect them manually to determine the outlines of excavations.

The South Total Station - N7 device measures an ultra-fast speed of under three seconds in fine mode over 600 metres. It works with a rechargeable lithium battery that lasts six hours in temperatures ranging from -20° Celsius to 50° Celsius. The dimension of the Total Station is 196 mm x 192 mm x 360 mm, and it weighs 6.2 kg. The accuracy of scans is ± (3 + 2 ppm x Distance) mm (South VI Instruments, n.d.). Figure 0-4 is an image of the South Total Station - N7. The cost of a new Total Station is currently R 145k (V. I. Instruments, 2022).



Figure 0-4: Total Station N7 (South VI Instruments, n.d.).

The Leica TS07 3” R500 Total Station typically measures at the speed of 2,4 seconds in precise mode over a range of 3,5km. It works with an exchangeable lithium battery. The GEB361 model battery for the TS07 has an operating time of up to 30 hours. The GEB331 model battery has a working time of up to 15 hours. It can withstand temperatures between -20° Celsius and 50° Celsius. The Total Station weighs between 4,3kg and 4,5kg. The accuracy of scans is 1,5 ppm (SCCS Survey, 2015). Figure 0-5 is an image of the TS07 3” R500 Total Station. The cost of a new Total Station is currently R 200k (Leica-geosystems, 2022).



Figure 0-5: TS07 3" R500 Total Station (SCCS Survey, 2015).

As a scanner alone weighs 4,5 – 6,2 Kg (SCCS Survey, 2015), these instruments quickly become an arduous and heavy load to carry. At Mponeng Mine, underground transportation by rail-bound man-carriage is

not always available. As a result, survey equipment must be carried to and from worksite locations. Travelling distances are often more than 4 km one-way, and accessing workplaces usually involves climbing through steep areas or through confined spaces. Large, heavy equipment can therefore be cumbersome to carry into workplaces. Choosing the most suitable instrument also requires consideration of the vertical angle measurement capability of the instrument, which makes observations over certain angles/degrees impossible and complicates checking backsight pegs. This poses a problem in confined excavations, for example, box holes/ore passes, steep raises and stope panels.

Deswik CAD software used at Mponeng Mine

Mponeng Mine uses Deswik CAD to capture and export geological mapping information. Deswik CAD supports a wide variety of file formats. The file formats of interest to the research were OBJ, DXF and DWG.

“Deswik Mapping is a Microsoft Windows tablet application that allows geologists to create geological maps and photography in their underground workplace” (Anderson & Gall, 2020, p. 4). Figure 0-6 shows a face section scanned and mapped on a tablet using the Deswik Mapping application.



Figure 0-6: Face section from Deswik Mapping application (Anderson & Gall, 2020).

Although Mponeng Mine uses Deswik software, Mponeng Mine did not purchase the Deswik Mapping application, which potentially could streamline the mapping process. Therefore, Mponeng Mine is unable to use the Deswik Mapping application. Deswik Mapping uses survey pegs to align scanned images with corresponding survey pegs when georeferencing scanned images. For example, Figure 0-7 shows a mine surveyor measuring from a roof peg (spad with numbered copper disc).

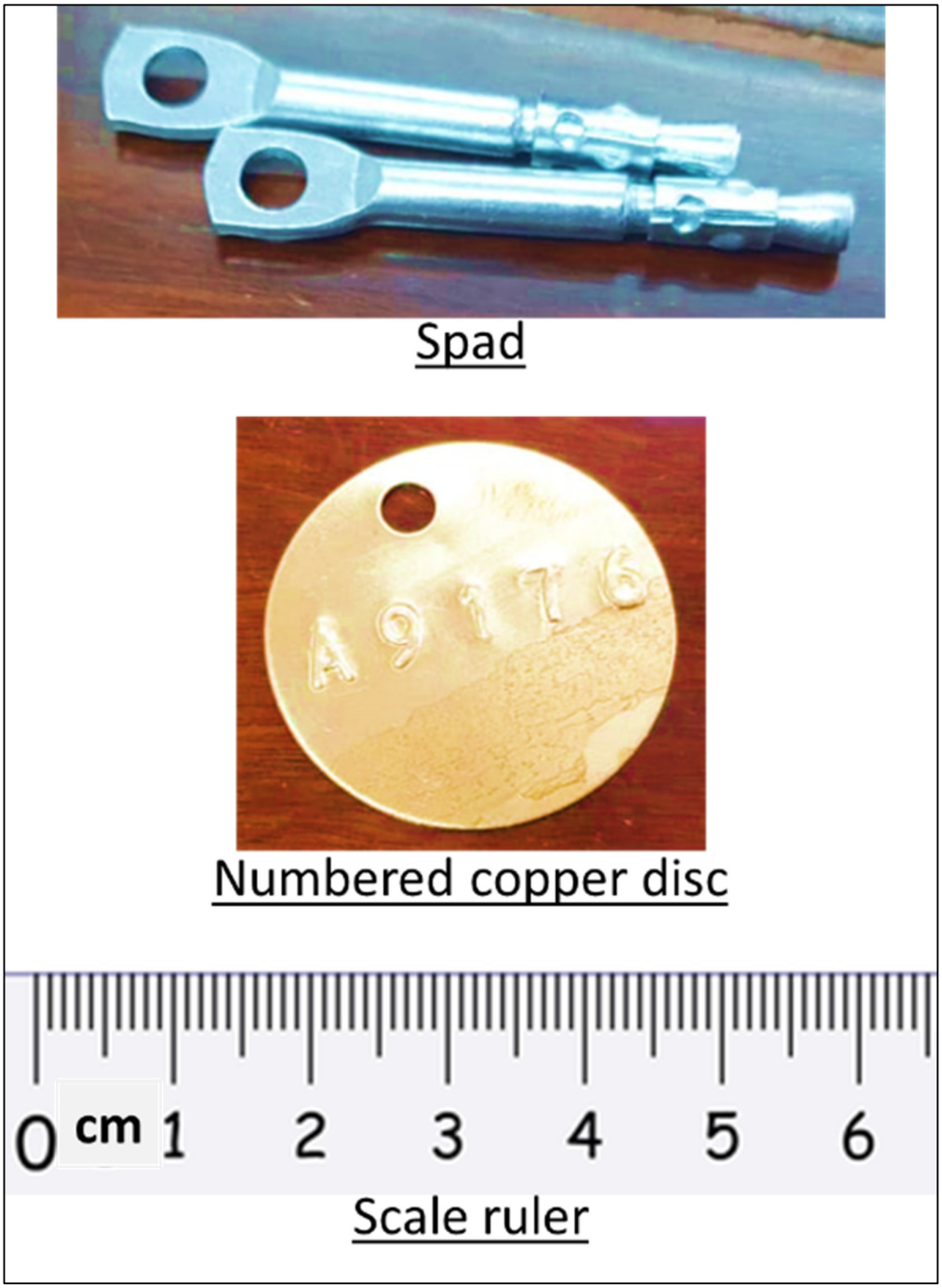


Figure 0-7: Brass spad with numbered copper disc(Nagel, 2022).

Mponeng Mine does not use Deswik's mapping tools. Instead, the geologist uses a clinometer, tape, and photographs to capture underground

measurements in notebooks. Once the geologist is on the surface, they plot the measurements in Deswik CAD on a flat surface at the correct elevation (Z). This information is fed into the 3D geological model. The geologist's photographs of the stope face underground are used in the mapping report to explain and show the position of the CW with the hanging wall and footwall of the stope panel; the norm is to use two to four photographs. Unfortunately, photographs are not an accurate representation of the complete stope panel. In addition, the next blast may result in the loss of valuable geological data of the stope panel in 3D space.

1.16.2 Technologies investigated in the research

Occipital Structure Sensor (Mark II)

The Occipital Structure Sensor (Mark II) is an upgrade of the original Structure Sensor (TC Join TechCrunch, 2021). The Occipital Structure Sensor (Mark II) scanner in the medical field captures 3D models of any body part for custom-fit prosthetics. (Occipital, Inc., 2021f)The Canvas application, which uses Apple LiDAR devices, can capture small and medium-sized residential rooms but not extensive industrial facilities. (Occipital, Inc., 2020c). Therefore, Occipital Inc. recommends using 3D LiDAR-based scanners when scanning extensive industrial facilities is required (Occipital, Inc., 2020c).

In Figure 0-8, this scanner is a hardware fitting for an iPad and is powered by the fitted mobile device's iPhone Operating System (iOS).



Figure 0-8: Occipital Structure Sensor (Mark II) (Birch, 2021).

The scanner sensor projects an infrared (IR) speckle pattern to the scanned object(s). Once it reaches dark and reflective objects, the pattern distorts, this technology application is called structured light (Occipital, Inc., 2020c).

Black objects absorb the IR laser emissions and as a result, lasers emitted by this device reflect randomly, causing objects or features to disappear. Some users have solved this problem by applying paint or powder to the scanned objects to help the sensor capture depth information (Occipital, Inc., 2020c).

The Occipital Structure Sensor (Mark II) scanner is a lightweight, portable wireless device that can accurately scan within +/- 4 mm at 40 cm (Rodin4D, 2021). An accelerometer and gyroscope are built-in to track 3D scans more effectively (3D Scan Expert, 2019). This scanner's infrared technology (Class 1 laser) is widely recognised in the industry for its safety, ease of use and outstanding performance (Rodin4D, 2021). For either indoor or outdoor scans, it is recommended that the scanner be used within a range of 0.3 m to 5 m (Occipital, Inc., 2020d).

The Occipital Structure Sensor (Mark II) price is approximately R10,800 as of November 2021 (3D Printing Systems South Africa, 2021). As per the above review, obstacles in obtaining accurate quantitative results were foreseeable. Therefore, this option was flagged for a preliminary qualitative test to measure the feasibility of using this hardware. Occipital, Inc. manufactures Room Scanner, Occipital Canvas, and Room Capture. All these applications were investigated before DigiMine simulations were performed. However, in underground use, the Occipital Structure Sensor (Mark II) is more difficult to protect because it is attached to the iPad. As a result, the scanner would be more likely to be damaged.

For the Occipital Structure Sensor (Mark II) to be usable, the 'Structure Sensor Calibrator application from Occipital Inc. needs to be downloaded (Art.Illinois.edu, 2021). Occipital, Inc. developed the first 'Scanner' application for the Occipital Structure Sensor (Mark II) to capture objects in 3D with an application size of 18.9 MB.

The application is compatible with iPhone, iPad and iPod touch. An iPad would require iOS 10.0 or a later operating system version for this application to be operable. Scanned objects can be shared via email in 'Object File format' or 'Polygon Model File' (Apple Inc., 2021b).

Object files provide parallel views of a file's contents from program linking and execution. An executable and linking format (ELF) "header resides at the beginning of an object file and holds a road map describing the file's

organisation” (Oracle Corporation, 2010). The layout of an 'Object File Format' (Table 0-1) consists of 'Program Linking View' data and corresponding 'Program Execution View' data. Table 4 shows how the data between the 'Program Linking View' data and 'Program Execution View' data compare for linking purposes. As a result of this linking process, an OBJ image file can be viewed in 3D software, such as Microsoft 3D Builder.

Table 0-1: Object File Format (Oracle Corporation, 2010).

<table>
<tr><th>Program linking view</th><th>Program execution view</th></tr>
<tr><td>ELF header</td><td>ELF header</td></tr>
<tr><td>Program header table (optional)</td><td>Program header table</td></tr>
<tr><td>Section 1</td><td rowspan="2">Segment 1</td></tr>
<tr><td>…</td></tr>
<tr><td>Section n</td><td rowspan="2">Segment 2</td></tr>
<tr><td>…</td></tr>
<tr><td>…</td><td>…</td></tr>
<tr><td>Section header table</td><td>Section header table (optional)</td></tr>
</table>

Figure 0-9 illustrates the result of an OBJ file open in Microsoft 3D Builder.

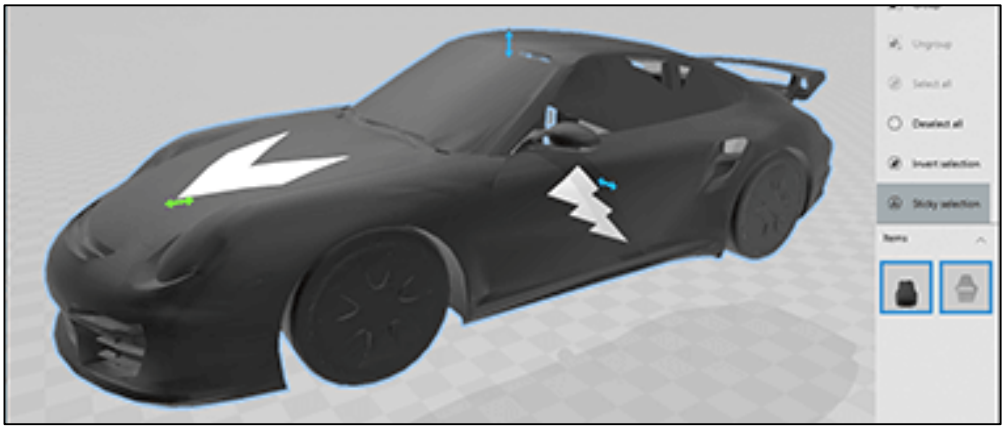


Figure 0-9: OBJ file open in Microsoft 3D Builder (Sharpened Productions, 2021h).

Polygon Model File Format (PLY), also known as Stanford Triangle Format, originated at the Stanford Computer Graphics Laboratory in the 1990s. Due to the origin of the PLY file format, the PLY format is sometimes referred to as the Stanford Triangle Format or Stanford PLY. A polygonal model was initially created using 3D laser triangulation. PLY files describe only a single object in a format that is general enough to be usable by a wide range of software (Digital Preservation Home, 2020). Table 0-2 shows the list of 3D software that supports the PLY file format.

Table 0-2: 3D software that supports PLY file format (CGI Furniture, 2022).

	3D file format
STL	Stereolithography File
3MF	3D Manufacturing Format
3DS	3D Studio is the native file format used by 3ds Max
MAX	3ds Max format
OBJ	Object File
COLLADA	COLLAborative Design Activity
VRML	Virtual Reality Modelling Language
X3D	X3D supports geolocation and multi-texture rendering
STEP	Standard for Exchange of Product model data
FBX	Filmbox

PLY file format is a 3D file format that stores graphic objects in ASCII and Binary format to allow compact storage and faster saving and loading times. Vertices and faces represent the core of a PLY file with coordinates in three dimensions with x, y and z properties. In addition, PLY files describe properties, for example, colour and image of surface materials. Furthermore, the PLY format can store a point cloud, a collection of vertex elements without the specification of faces connecting them (Digital Preservation Home, 2020).

Figure 0-10 is an example of the file structure of a PLY file format.

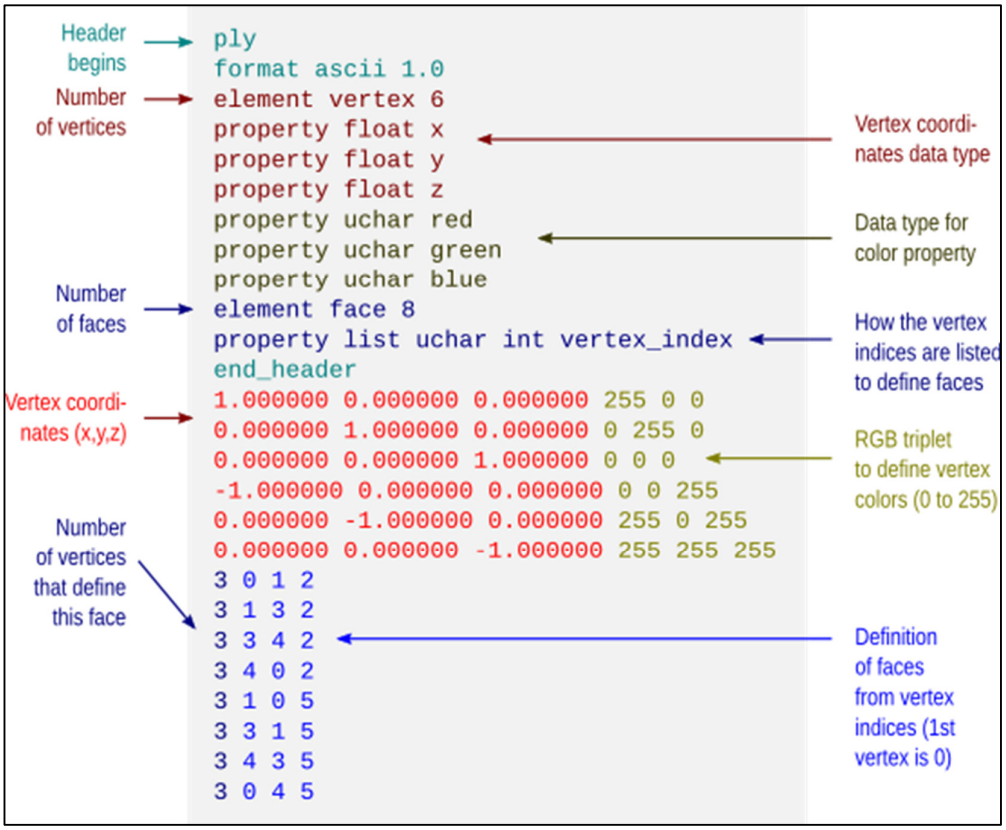


Figure 0-10: File structure of a PLY file format (WordPress.com., 2011).

Figure 0-11 shows an object in PLY format with colour attributes assigned to each vertex.

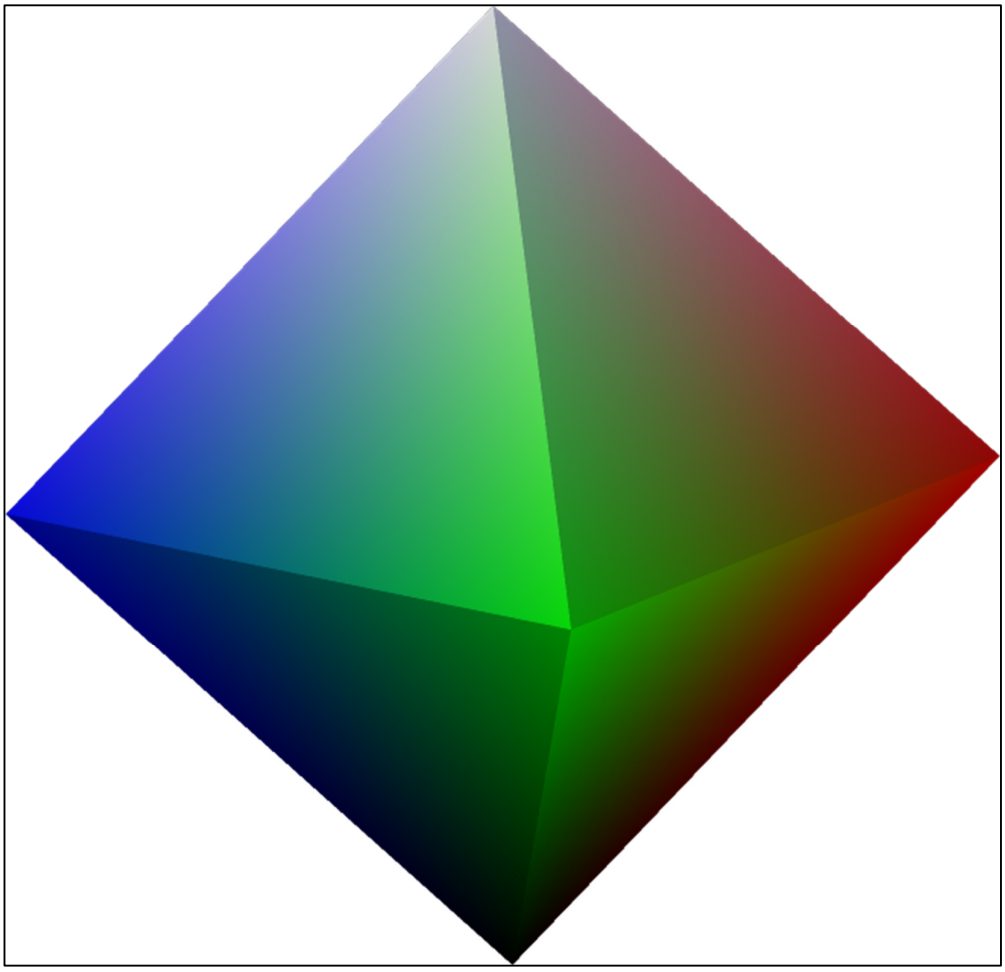


Figure 0-11: An object in a PLY file format with colour attributes assigned to each vertex format (WordPress.com., 2011).

The cost of downloading and using Occipital Structure Sensor (Mark II) application is free (Apple Inc., 2021b). However, the following three applications were found preferable to use for the qualitative research method, they are:

- Room Scanner application;
- Occipital Canvas; and
- Room Capture application.

The ‘Room Scanner application’, ‘Occipital Canvas’ and ‘Room Capture applications were downloaded for use in the qualitative research method are described in detail below.

‘Room Scanner’ application

Structure SDK, 1.2 for iOS, was released on 13 July 2021 with a "Dark Object Pre-set that enhances depth in scenes containing dark, shiny objects (Occipital, Inc., 2020a). With this application, it is possible to retrieve textured 3D scans of objects and rooms - see Figure 0-12 (Occipital, Inc., 2020a).



Figure 0-12: Scanned object and room by the ‘Scanner’ application (Occipital, Inc., 2021e).

It is also possible to calculate volumes of scanned objects (Occipital, Inc., 2021e). The ‘Room Scanner’ application is user-friendly because no formal training is required to use the scanning application. However, this application is not suited for large areas and only scans accurately at less than 5 m. Scans within a 5 m range are reportedly between 97% and 99%

accurate (BeLight Software Ltd., 2021). The accuracy of the 'Room Scanner application is tested by exporting scanned data to a 3D file format and comparing measurements from scans with measurements of scanned objects (Reality Capture Review, 2018).

'Occipital Canvas'

This free software creates photogrammetric scans of objects and rooms. In 2017 Occipital Canvas released iOS operating system requirement for Occipital Canvas. With 'Occipital Canvas', it is possible to get real-time measurements from 3D room scans. The 'Scan to Cad' service makes it possible to convert 3D scans to CAD files (Aniwaa Pte. Ltd., 2021b). With the 'Scan to Cad' service, 2D floor plans can be available in approximately two business days at the cost of less than $0.01 per square metre in the following file formats:

- AutoCAD (.DWG) (Occipital, Inc., 2021d);
- Revit (.RVT) (Occipital, Inc., 2021c); and
- Portable Document Format (.PDF) (Aspose Pty Ltd., 2021b) (Occipital, Inc., 2021a).

The main features of Occipital Canvas include:

- The application automatically creates floor plans of scanned rooms based on measurements collected during 3D scanning;
- The cost of converting 3D scans to CAD files is $29 per model;

- User-friendly interface for a more effortless user experience; and
- Email Sharing Service: The 3D scanning app allows users to send their 3D scans via email (Aniwaa Pte. Ltd., 2021b).

The Occipital Canvas application produces accurate measurements of scans within 1-2% of manually verified dimensions (Occipital, Inc., 2021b).

'Room Capture' application

Occipital, Inc. developed the 'Room Capture' application for the Occipital Structure Sensor (Mark II) to capture a 3D model of an entire room. It requires an iPad 11.0 or later operating system and is 18.3MB. The cost of downloading and using the application is free of charge. Scans measure accurately per the metric system (Apple Inc., 2021a). Figure 0-13 is an example of a scanned room from the 'Room Capture' application.



Figure 0-13: Scanned room by 'Room capture' application (Sketchfab, 2021a).

'Room Capture' is used mainly to scan and edit environments in other applications. Scans can be shared, for example, by email in the following file formats:

- Object File (.OBJ) (Sharpened Productions, 2021h) (mesh, containing 3D information and mapping points);
- Joint Photographic Experts Group (.JPG) (Sharpened Productions, 2021e) containing texture information; and
- OBJ Material Template Library File (.MTL) (Sharpened Productions, 2021g) maps the texture to the mesh (Occipital, Inc., 2020b).

The Structure Sensor II is an add-on to the iPad, which makes it vulnerable to damage. The Structure Sensor II was tested but found to be unsuitable for the intended underground scanning application due to the unavailability of a suitable application.

1.16.3 Apple products with 3D scanner function

Apple iPad Pro 11 inch

With the iPad Pro 11-inch released in May 2021, it is possible to perform 3D LiDAR scanning without acquiring additional hardware (GSMArena.com, 2021a). In addition to the iPhone 12 Pro, the iPhone 12 Pro Max also has the scanning capability of up to five metres away. Furthermore, the iPad Pro-11-inch also reduces constraints, reducing the possibility of hidden overlapping objects (Wilson, 2020).

The Apple iPad Pro 11-inch (GSMArena.com, 2021a) is 247.6 mm x 178.5 mm x 5.9 mm and weighs 466 grams. The system runs on the latest iPadOS and comes with the following choice of memory: 128GB 8GB RAM, 256GB 8GB RAM, 512GB 8GB RAM, 1TB 16GB RAM, 2TB 16GB RAM. The Apple iPad Pro 11-inch can communicate information via hotspot using Wi-Fi without a SIM card (GSMArena.com, 2021a). The Apple iPad Pro 11-inch with Wi-Fi and memory of 256GB sells for R18 000 (Pepkor Trading Ltd. Pty., 2022). Before the testing phase of the project, a device belonging to the University of the Witwatersrand was readily available for research purposes. A limitation of the Apple iPad Pro is that the 11-inch size specification may seem cumbersome for underground use. In addition, the

Apple iPad Pro 11-inch is yet to be proven as either dust-proof or water-resistant (GSMArena.com, 2021a).

Apple iPhone 12 Pro Max

The Apple iPhone 12 Pro Max was launched in October 2020, released, and made available for public use in November 2020. The system is dust and water-resistant for up to 6 m depth for 30 minutes. The cost of the Apple iPhone 12 Pro Max with 256GB memory is R24 999 (iStore, 2022).

The research focuses on using the Apple iPhone 12 Pro Max's time of flight (TOF) 3D LiDAR scanner for 3D depth technology. In addition, it is possible to send and receive data with ease via Wi-Fi or hotspot with the Apple iPhone 12 Pro Max. When considering the layout of narrow tabular mining, there are space limitations, which decrease the practicality of Wi-Fi for underground use and furthermore, Wi-Fi works on the "line-of-sight" principle. Therefore, it becomes increasingly difficult to use advanced technology dependent with Wi-Fi. A drone-based photogrammetry program would be an example of this. This technology would not be feasible to implement at the Mponeng Mine because of the extensive excavations and the use of advanced technology requiring Wi-Fi (Datamine, 2021a).

Some phone features worth mentioning are the accelerometer, gyroscope and barometer (GSMArena.com, 2021b). The accelerometer measures directional movement on three axes. First, it detects the phone's orientation

while it measures the linear acceleration of movement (GSMArena.com, 2021c). Figure 0-14 illustrates the axes of the iPhone accelerometer.

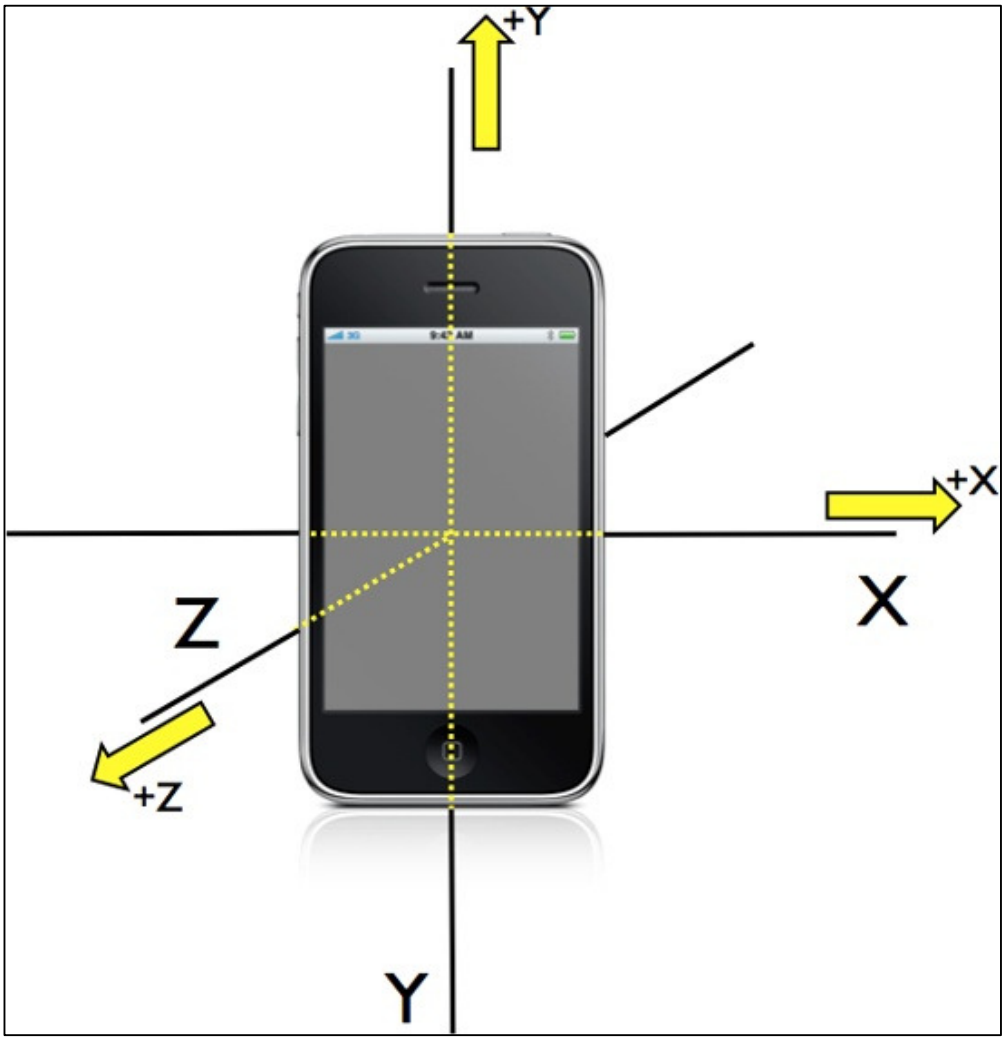


Figure 0-14: The iPhone accelerometer axes (Allan, 2022).

The gyroscope also measures information on three axes by tracking the rotation or twist of the phone while scanning (GSMArena.com, 2021c). As a result, the accelerometer and the gyroscope's combined function produce scans with fewer distortions. “In practice, that means that an accelerometer will measure the directional movement of a device but will not be able to

accurately resolve its lateral orientation or tilt during that movement unless a gyro is there to fill in that info" (GSMArena.com, 2021c).

Accuracy testing for specific usage is required; therefore, manual geology mapping will be compared with geology mapping captured from 3D scans. A benefit that separates the iPhone from the iPad is that it has a measuring application called "Measure". With this application, it is possible to measure objects that would typically be inaccessible. In other words, this application helps one get close enough to an object to measure its length and height (Gallagher, 2021).

Apple iPad Pro and Apple iPhone Pro Max applications

The iPad Pro and Apple iPhone Pro were used to analyse scans quantitatively and qualitatively in the research.

Regulations to be observed

An employer must comply with the Chief Inspector of Mines' instructions when he or she directs the employer to prepare a Code of Practice (COP) regarding employee and other health and safety matters (Mine Health and Safety Council, 2018). The Mine Health and Safety Act require formal written permission from underground mines to use any electronic photographic equipment underground (Department of Mineral Resources and Energy, 2021). The safety implications involved with a phone were considered a possible disadvantage. For this reason, it is essential to

establish if it would be safe to use a mobile phone in an underground hazardous environment. Underground use of electronic photographic equipment requires under MHSA regulations noting and recording the results of flammable gas tests in the workplace. “Only double protected or intrinsically safe type explosion protected (Ex) Identification Application (ia) (Auret, 2010) explosion protected apparatus remains energised where flammable gas is more than 1.4% by volume in the air. All other explosion-protected apparatus must be de-energized at flammable gas concentrations above 1.4% by volume in the air” (Mine Health and Safety Council, 2018).

“The casing for iPhone 12, 13 and 12/13 pro allows you to bring the world’s most popular smartphones into hazardous area Ex Zone 1” (ExNor AS, n.d.). Consequently, Mponeng Mine will be required to cover the iPhone with a protective casing if flammable gas concentrations exceed 1.4% by volume.

Scaniverse an application for a LiDAR 3D Scanner

The Scaniverse - LiDAR 3D Scanner application is available from the Scaniverse - Toolbox AI, Inc. and, according to Apple (2021), can only work on the following devices with a LiDAR sensor:

- iPhone 13 Pro;
- iPhone 13 Pro Max;
- iPhone 12 Pro;
- iPhone 12 Pro Max; and

- iPad Pro devices from 2020 onwards (Apple Inc., 2021c).

The Scaniverse - LiDAR 3D Scanner application can create scans of objects, interiors and exteriors within a 5 m radius (Thess, 2022). The size of the application is 30.9MB and the cost of downloading and using the application is free of charge. Scanned objects can be shared via iMessage, where they can be viewed in either 3D or Augmented Reality applications. For this application to operate, the device requires iPad OS 14.0 and an A12 Bionic chip - or later versions, respectively (Apple Inc., 2021c). Scanned models can be exported to a variety of 3D file formats, as shown in Table 0-3.

Table 0-3: Scanned models exported to 3D file formats.

	File Format
OBJ	Object File
FBX	Filmbox
LAS	Laser File or LiDAR Data Exchange File

Figure 0-15 is a scanned image of a building produced by Scaniverse - LiDAR 3D Scanner application.



Figure 0-15: Scanned object by the Scaniverse application (Sketchfab, 2021b).

3D Scanner App™

The 3D Scanner App™ application is compatible with iPhones, iPad, iPod Touch and Mac. Each of these devices needs LiDAR-equipped Pro models to operate with the following or with later versions of the following respective operating systems:

- iPhone requires iOS 14.0;
- iPad requires iPadOS 14.0;
- The iPod touch requires iOS 14.0; and
- Mac requires macOS 12.0 (Apple Inc., 2021d).

The size of the application is 6.6 MB, and the cost of downloading and using the application is free of charge (Apple Inc., 2021d). Scanned objects can be shared via iMessage, Augmented Reality and Quicklook by using the Universal Scene Description Zipped format (USDZ) (Sharpened Productions, 2021m) (iPhoneTricks.org, 2021). Scanned models can be exported to the following 3D file formats:

- Object File (.OBJ) (Sharpened Productions, 2021h);
- GL Transmission Format (.glTF) (Sharpened Productions, 2021d);
- Binary GL Transmission Format File (.GLB) Developed by The Khronos Group (Sharpened Productions, 2021c);
- Digital Asset Exchange (.DAE) (Sharpened Productions, 2021a); and
- Stereolithography File (.STL) (Sharpened Productions, 2021l).

The LiDAR function results in dimensionally accurate 3D scans compared to manual measurements. It can create 3D scans of objects and interior and exterior areas that can be imported into 3D modelling programs, including Blender, 3Ds Max, SketchUp, and Maya. Some features of the 3D Scanner application include editing and measuring (iPhoneTricks.org, 2021).

Polycam application for a LiDAR 3D Scanner

The Polycam - LiDAR & 3D Scanner application was developed by Polycam Inc. and is designed for iPad to capture, edit and share 3D scans. The size of the application is 52MB and is compatible with iPhone, iPad (from 2015 or later), iPod touch and Mac. To operate on these devices, the iPhone and iPad would minimally require iOS 14.0 or later. In contrast, the Mac would require either macOS 11.0 or a later version, as well as an Apple M1 chip (Apple Inc., 2021e).

The cost of downloading and using the basic Polycam – LiDAR & 3D Scanner application is free. On the other hand, the price of the Polycam Pro application is R4 600. The Polycam – LiDAR & 3D Scanner application, in conjunction with the LiDAR sensor of the device, provides a photo and LiDAR mode. With photo mode, 3D models can be created from the images. The LiDAR mode makes 3D scans of large objects, for example, buildings (see Figure 0-16) and dimensionally accurate spaces without an internet connection.



Figure 0-16: Polycam 3D scanned model with measurements (Apple Inc., 2021e).

Scans can be captured and their processing can be continued later making this application efficient. No time is wasted on processing one scan before continuing with the following scan. In addition, captured 3D scans can be shared on the Polycam community with Polycam Web (Apple Inc., 2021e).

The Polycam Pro application is required to export 3D models. 3D mesh data models can be exported in the following file formats: OBJ, FBX, DAE, GITF and STL.

3D colour point cloud data models can be exported in the following file formats:

- Drawing Exchange Format File (.DXF) (Sharpened Productions, 2021b);
- Polygon Model File (.PLY) (Sharpened Productions, 2021i);
- LiDAR Data Exchange File (.LAS) (Sharpened Productions, 2021f);
- Celestia Sampled Trajectory Data File (.XYZ) (Sharpened Productions, 2021n); and
- PTGui Project File (.PTS) (Sharpened Productions, 2021k).

Blueprints of models can be exported in either Portable Network Graphic (.PNG) or Digital Asset Exchange (.DAE) file formats. (Sharpened Productions, 2021j) and (Sharpened Productions, 2021a).

The Polycam Pro application measures accurately within 25.4 mm and has manual and automatic measurement tools (Apple Inc., 2021e). Miller, et al. (2022) studied the accuracy of LiDAR-captured scans from the Apple iPhone 13 Pro and the FARO Focus 3D ground-based scanner. According to Miller, et al. (2022) the FARO Focus 3D, ground-based scanners have been shown to record accident scenes accurately using LiDAR technology.

The FARO Focus 3D ground-based scanner requires a tripod and alignment sphere (Miller, et al., 2022). Figure 0-17 is an example of the Focus3D X 330 laser scanner on a tripod.



Figure 0-17: Focus3D X 330 laser scanner (FARO, 2014).

With the iPhone 13 Pro Max LiDAR data can be captured in a less than two minutes using the Polycam Pro application. To evaluate the LiDAR scan accuracy, some real-life vehicles were scanned with both Apple's iPhone 13 Pro Max and the FARO Focus 3D ground-based scanner. CloudCompare software was used to compare the accuracy differences between the LiDAR scans collected by Apple's iPhone 13 Pro Max and the FARO Focus 3D ground-based scanner. A traditional ground-based scanner like the FARO Focus 350 costs tens of thousands of dollars, while the iPhone 13 Pro Max costs $1399.00 (USD). The Polycam Pro application used for point cloud export can be downloaded free of charge (Miller, et al., 2022). “With such a

low cost and speed of data capture, mobile phone LiDAR is a promising technology; however, there was a wide range of accuracies in the data sets. Depending on the data acquired, this range may not be acceptable. More research is needed to understand this range and if more accurate results could be obtained from differing methodologies, subject matter, and application selection" (Miller, et al., 2022).

The differences between Polycam's LiDAR Mode and Photo Mode are accuracy and time. LiDAR Mode produces 3D scans in seconds, with Photo Mode, where it is required to take multiple photo sets and stitch the objects together manually (Funkner, 2021). Figure 0-18 demonstrates a stone pillar scanned using the Polycam LiDAR Mode and Photo Mode.

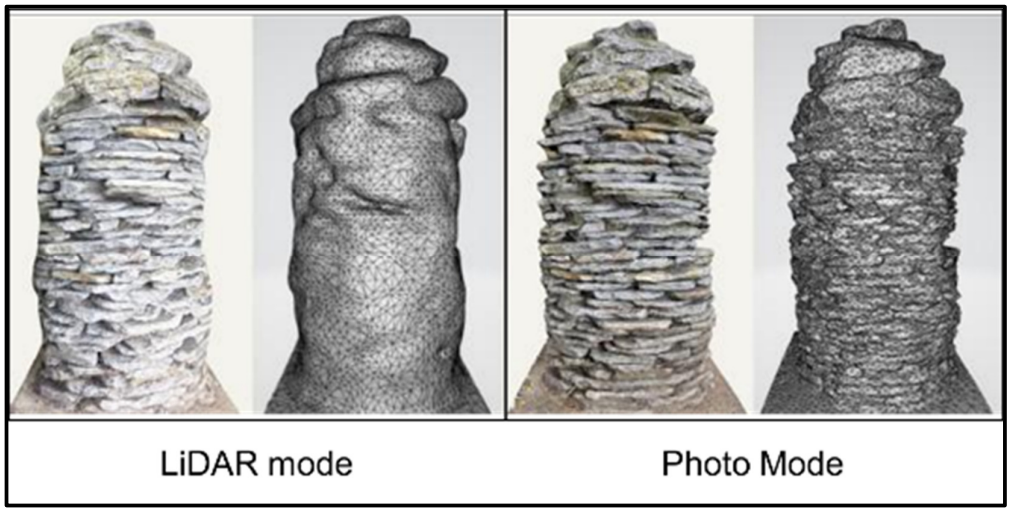


Figure 0-18: Stone pillar that was created with LiDAR Mode and Photo Model (Funkner, 2021), (3DWithUs, 2021).

Note that the image of stones in Figure 0-18 captured in Photo Mode shows the stones in more detail than the image of the stones in Figure 0-18

captured with LiDAR Mode. Since the Photo Mode example shows more detail than the LiDAR Mode, this may be a positive contribution to the research since the geological mapping scans may offer more information on geological features, enabling more detailed geological mapping reports.

SiteScape is an application for LiDAR 3D Scanner.

The 'SiteScape - LiDAR 3D Scanner' application can only work on devices with a LiDAR sensor, available on the iPhone 12 Pro, iPhone 12 Pro Max and 2020/2021 iPad Pro (Apple Inc., 2021f) The application is ideal for scanning 3D models where accuracy within 2.54 cm is necessary, for use in engineering, construction and architecture. The application size is 8.7MB, and the app's download and use are free. Scanned models can be exported to "CAD programs including Autodesk Revit, AutoCAD, ArchiCAD, Navisworks, Plangrid, BIM 360 and many more" (Apple Inc., 2021f)In addition, scanned objects can be shared with a secure link where 3D scans can be viewed in any web browser on any device (Apple Inc., 2021f).

For the SiteScape application to operate on the iPhone, it requires iOS 14.5 or later and a device with the A12 Bionic chip or later (Apple Inc., 2021f). Likewise, the application to operate on the iPad requires iPadOS 14.5 or later and a device with the A12 Bionic chip or later (Apple Inc., 2021f). SiteScape is a popular LiDAR 3D scanning application for architecture, engineering, and construction that are accurate within 2.54 cm. With SiteScape, it is possible to export scans seamlessly to CAD programs such

as Revit, AutoCAD, ArchiCAD, Sketchup, Navisworks, and Revizto (Apple Inc., 2021f).

Most mesh-based 3D model formats are captured as cloud point data, and scans can only be exported in the following file types:

- Polygon Model File (.PLY);
- The E57 file format specified in ASTM E2807 standard (.E57); and
- Rich Chart Builder Project format (.RCP).

1.16.4 Software short-listed for scan analysis

The software considered to be used to analyse scan results for the research were:

- Meshlab;
- Deswik CAD; and
- CloudCompare.

Several of the hardware applications indicated compatibility with Deswik CAD. As Mponeng Mine uses Deswik CAD as its main CAD package, scanners and apps that allow easy data integration with this software was considered most desirable. The file formats Deswik CAD supports for viewing scans are shown in Table 0-4.

Table 0-4: Supporting file formats - Deswik CAD for viewing scans

	File Format
LAS	Laser File or LiDAR Data Exchange File
OBJ	Object File
PLY	Polygon Model File
STL	Stereolithography File

Finally, CloudCompare software was considered with the most potential and suitable for analysing scan results.

CloudCompare software

CloudCompare is free software that can be used for educational or commercial use. “CloudCompare is a 3D point cloud (and triangular mesh) processing software” (CloudCompare, 2020). For the research, CloudCompare was initially used to geo-reference scans to fit onto survey pegs and measure distances from different file formats to test the iPhone Pro Max accurately. It was then realised that Deswik CAD could perform the same functionality. Additionally, scans opened in CloudCompare after the iPad tests in the DigiMine produced a lesser quality than those opened and viewed in Deswik CAD. Therefore, this software option was eliminated from the research before underground testing. Deswik CAD was the preferred approach to geo-reference scans by fitting them onto survey pegs.

Table 0-5 shows some of the file formats that CloudCompare supports.

Table 0-5: CloudCompare supported file formats (CloudCompare, 2020).

Open point cloud formats	Manufacturer's formats	Triangular meshes
ASCII	DP	OBJ
LAS	Riegl	PLY
E57	FARO	STL
		FBX

Polylines or polygon formats	Supported file formats
SHP	Bundler
DXF	Photoscan PSZ

The Bundler Import Tool and associated methods generate orthophotos as images or clouds and coloured DTM generation. Bundler Import Tool is used for the geometric correction of aerial images and orthophotos from multiple images. This software automatically calibrates intrinsic and extrinsic cameras from various aerial images (CloudCompare, 2015).

The PSZ extension is a compressed PostScript format and the PSZ file format is compatible with the software and can be installed on the Mac OS Windows system platform (File-Extension.info, 2022).

1.17 Data Collection and Analysis

1.17.1 Initial research design

The research started with a literature review to consider resources and methods and a review exercise of what scanners were available. At the time of the review, the readily available scanners were the ‘Occipital Structure Sensor (Mark II)’ and the Apple iPad Pro, released in 2020. The second step was to decide where to test these scanners, in which environment and under what conditions. The aim was to try the output of the different scanning applications and what influence light may have on the quality of scans tested underground at Mponeng Mine. Hence, the intention was to try these scanners at the DigiMine at the University of the Witwatersrand. The DigiMine is a simulated environment of an underground gold mine. The third step was deciding what scanning applications would best suit the research going forward. Figure 0-19 shows an illustration of this initial research design workflow.

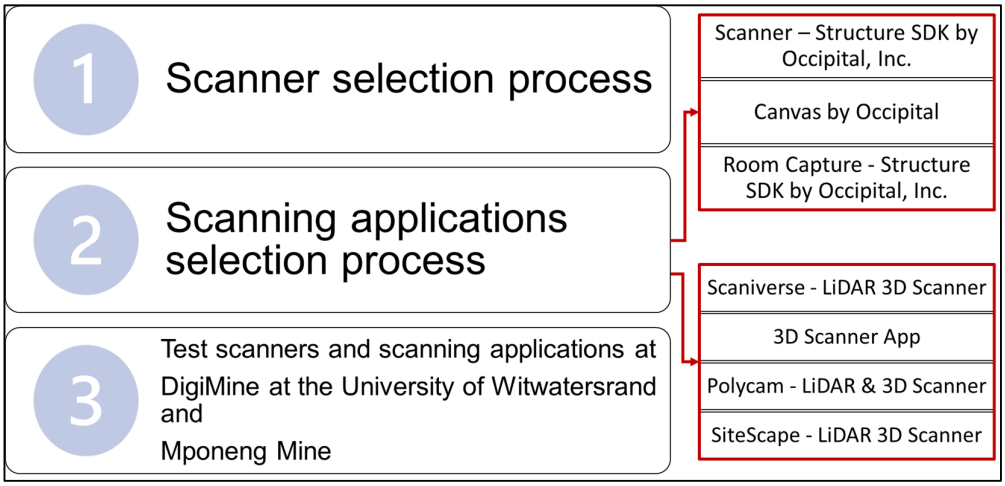


Figure 0-19: Selection of the most suitable scanners and applications for the research.

Scans were to be captured with the Occipital Structure Sensor (Mark II) with the following applications from Occipital:

- Room Scanner;
- Occipital Canvas; and
- Room Capture.

Scan capturing with the Apple iPad Pro 11-inch was with the following applications:

- Scaniverse;
- 3D Scanner app;
- Polycam; and
- Sitescape.

The quality and accuracy of the scans, along with considerations of cost and ease of use, were to be reviewed, and assessments made as to the value-add each 3D scanner offered. After comparing and analysing the quality of the scans captured with the CloudCompare and Deswik CAD software, the best quality scanner and sensor were chosen as the recommended software and scanner to obtain the best results. The time taken to capture scans at the DigiMine and at Mponeng Mine, along with the maximum area to be captured and saved was used to categorise further the value of time, cost, accuracy and presentation that specific scanner software offers. Finally, the scanner, suitable application, file format and software processing were selected and utilised in the last phase of the research. The goal was to use the selected scanner to scan stope panels underground at Mponeng Mine and then gather scanned information of stope panels after the consecutive blasting of these panels.

The volume of the ore blasted was determined using the selected scanner and applications. The output of the scanner's data and subsequent volume calculation were to be compared with the volume measured and calculated by the traditional mine survey method of measuring with tapes.

1.17.2 Actual research workflow

Several adaptations in the research methodology had to be made to overcome obstacles and accommodate unforeseen circumstances. First, the Structure Sensor Mark II was tested on surfaces in an office environment using all apps listed in Section 4.4.1. This was done to test the

scanner and scanning applications' capability in terms of accuracy and quality. The software could accommodate the research objectives.

The scan quality from the Structure Sensor is excellent. There is, however, no app currently available that allows scanning areas greater than 10 m². Canvas is capable, but the files have to be sent to Canvas for processing (at a cost). The raw files could not be downloaded directly from the iPad, so this was not explored further. The Structure Sensor Mark II was eliminated before the next research phase in the underground simulation at DigiMine.

The Apple iPad Pro 11-inch was available for initial testing in the DigiMine on 28th May 2021. The resultant scans were dark, and an additional light source was bought and introduced for the research in response to this observation. Therefore, it was necessary to attach the light source to the Apple iPad Pro 11-inch. This was a practical decision for transporting, protecting and using the scanner effectively during the research in the DigiMine and underground. The problem was overcome by 3D printing a holder to fit onto the iPad Pro. The 3D printed holder made the carrying and utilisation of the scanner much better as the operator had better control of the scanner. The problem was overcome by 3D printing a holder to fit onto the iPad Pro. Scanning was done using the Sitescape and 3D Scanner apps, and the processing was done in CloudCompare and Deswik CAD. The scanning exercise yielded excellent results, and the device progressed to the next research stage.

Underground stope scanning was scheduled so scanning and measurements via the traditional measuring could occur simultaneously. Scanning with the Apple iPad Pro 11-inch was done on the 5th of July 2021 and 7th of July 2021 during visits to the 113-68-East 5 and East 2 panels of the VCR reef, respectively.

At this stage, Mponeng Mine had realised the value added by scanning stope panels. Furthermore, Mponeng Mine purchased an Apple iPhone 12, Pro Max, in September 2021, enabling further research to prove the value of the Apple LiDAR 3D scanner.

A scanning exercise was done in three rooms of the Mponeng Mine Survey Office to compare dimensions with distometer measurements. This accuracy test was performed using the same applications used in the DigiMine research exercise with the iPad Pro, with the addition of Scaniverse. The outcome of these results is discussed in section 1.20.1.

Another intention was to compare scans with the Polycam – LiDAR scanning app. Unfortunately, Mponeng Mine does not have an account with Polycam that could export scans from the iPhone to an outside source (such as OneDrive). For this reason, Polycam results could not form part of the research. Files were exported to CloudCompare for qualitative examination of scans. The results warranted underground testing and are discussed under section 1.20.1. This is done to prove accuracy in areas that are difficult to access for traditional geological mapping, as well as the durability

of the Apple iPhone 12 Pro Max in challenging underground conditions such as heat.

In September 2021, the iPhone Pro Max was tested underground at the CLR's 120-80 E1A panel. This scan was repeated less than a month later, in October 2022, to determine whether second scans with the same technology could provide helpful feedback for the goal of dilution control. The outcome of these results is discussed in section 1.22. Finally, the research presents workflows for Geological and Production, respectively. The Geological Scanning Workflow is the process the geologist will follow to capture and report geological information in the scanning process. The Production Scanning Workflow is where the production team captures and reports production-related information during the scanning process.

1.18 Section Summary

The research methodology had to be streamlined to accommodate quantitative and qualitative data. During the first phase of the research, various specifications of scanners short-listed were considered for use in the experimental part of the research. During the next research phase, the scanners were tested in a controlled environment (Wits DigiMine) before further testing was continued underground at Mponeng Mine. 3D LiDAR scans were captured in underground working stopes in real-life conditions to test the durability and practicality of the scanner. These scans were downloaded to a computer from the scanners and then saved on a central

server for all relevant departments to access. With free software (CloudCompare), the scans were geo-referenced and pulled into Deswik CAD for further use.

RESULTS AND OBSERVATIONS

1.19 Section Overview

The results and observation chapter discusses the results obtained from the different scanners and scanning applications conducted in the quantitative and qualitative research exercises. The research exercises with the iPad Pro were conducted at DigiMine and underground at Mponeng Mine. The aim was to compare the capabilities of the selected scanners and determine the best-suited scanning application for Mponeng Mine.

1.20 Apple iPad Pro 11-inch in the DigiMine at Wits

In May 2021, the iPad Pro was subjected to testing at DigiMine. The DigiMine represents an underground stope panel of a narrow tabular mining method. It also has a crosscut tunnel that displays geological features, see Figure 0-1.

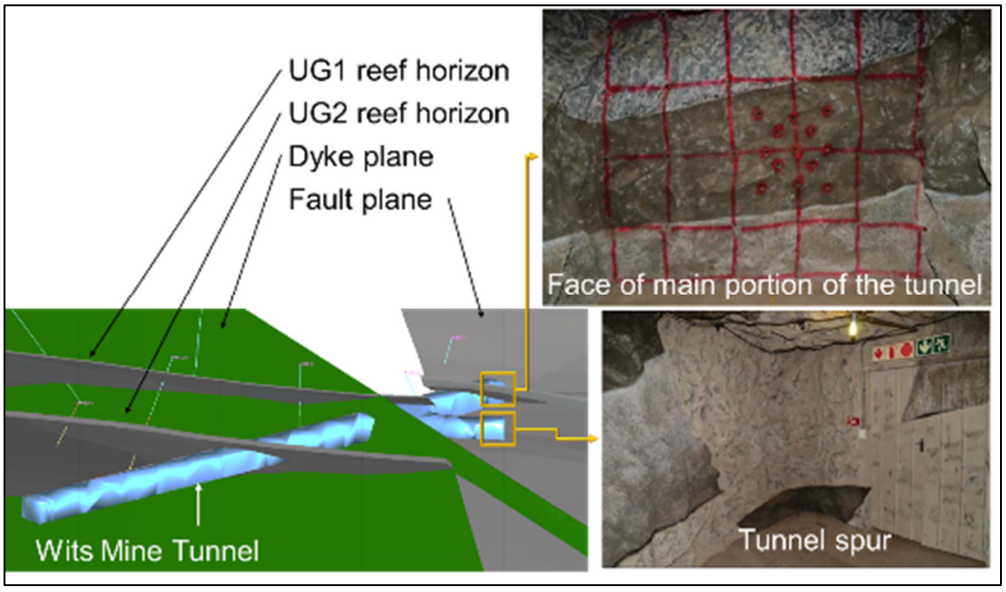


Figure 0-1: Leapfrog Geo Model of the Wits Mine Tunnel showing UG1 and UG2 stratigraphy as well as the fault and dyke relationship (Birch, 2018).

Figure 0-2 shows the Wits DigiMine control room and life-size mining stope.

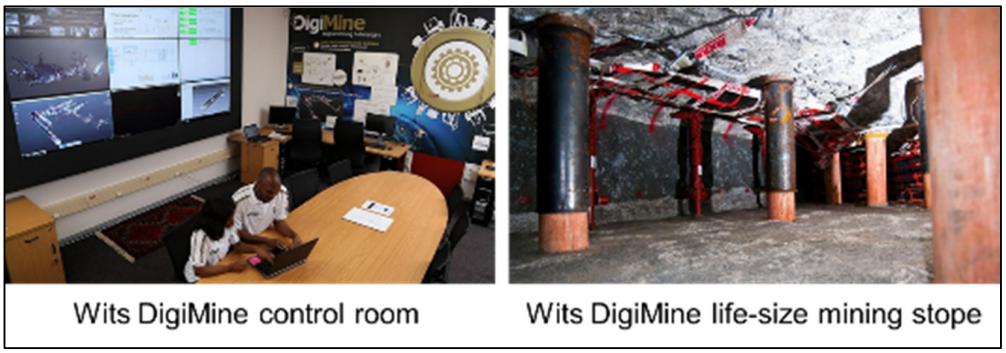


Figure 0-2: The Wits DigiMine control room and life-size mining stope (Moyo, 2018).

Qualitative research is intended to evaluate scans of stope panels in this simulated environment to decide on equipment suitability and application for underground scanning. Firstly, observations indicated a shortcoming in the

quality of scans due to a lack of illumination of the surfaces to be scanned. The observations and solutions designed to overcome this obstacle are documented in Section 1.20.1. Secondly, the quality of exported scans was used to compare shortlisted software.

1.20.1 Insufficient light-source illumination

First, the SiteScape application was attempted in DigiMine at the University of the Witwatersrand in 'Polygon Model File' format. Unfortunately, as demonstrated in Figure 0-3, the first scans of the stope panel were not very useful. Therefore, they could not be used to evaluate the app objectively.

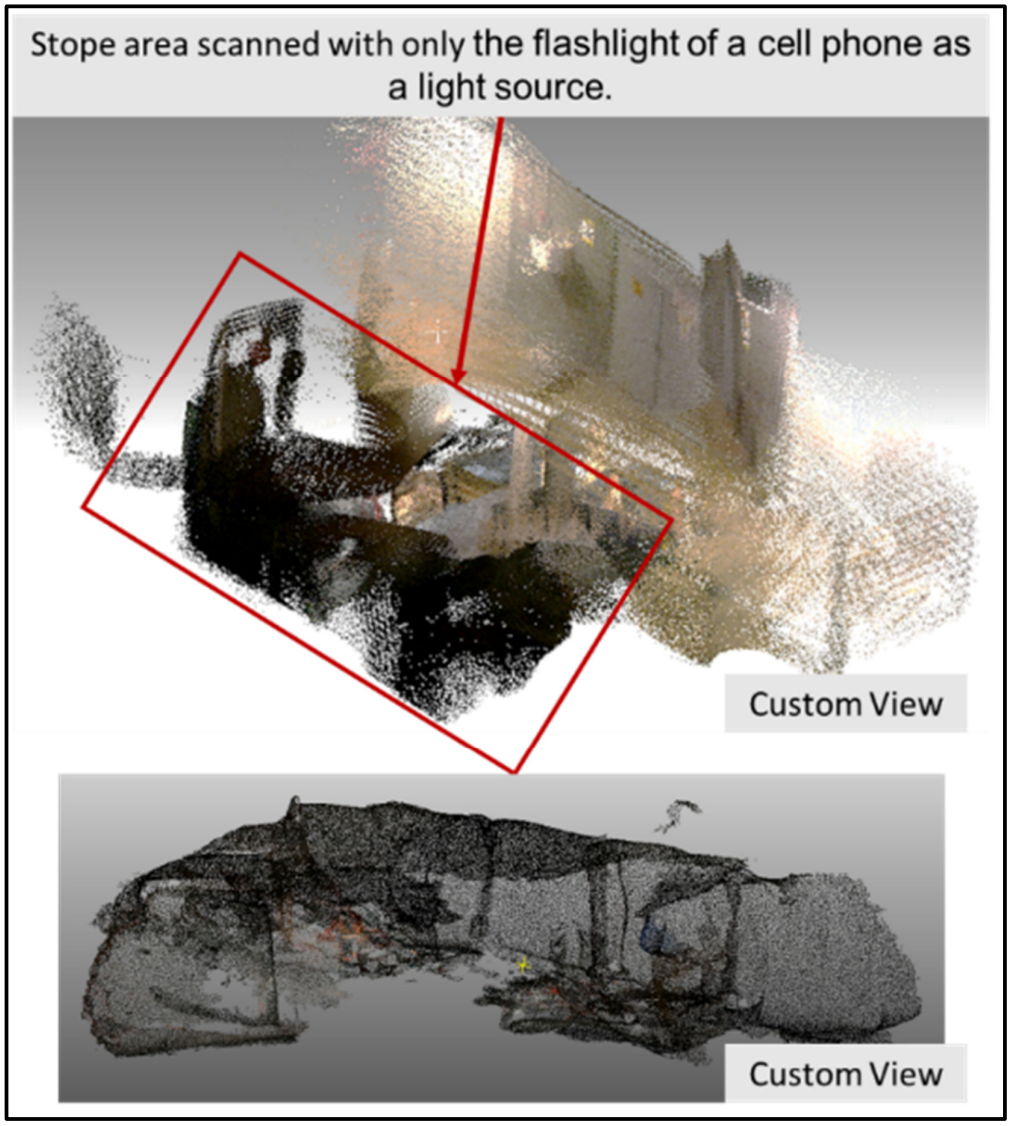


Figure 0-3: Initial scan of stope panel at DigiMine before light-fitting modification; iPad using SiteScape to export Polygon Model File at University of the Witwatersrand in May 2021.

It is clear from the result that a light source with insufficient illumination capability was used. As a result, the scan quality was not improved by using only a cell phone flashlight, and it became evident that more intensive problem-solving was required.

Solution: Mobile LED video light

Due to the ineffective scan result shown in Figure 0-3, an alternative light source for subsequent scanning was investigated. The decision was made to purchase a 'Mobile LED Video Light with Smartphone Bracket' to get a better result from scans when scanning in the dark. Figure 0-4 shows the light source attached to the iPad during scanning.



Figure 0-4: Image of 'Mobile LED Video Light with Smartphone Bracket' (CameraStuff, 2006).

Figure 0-4 also illustrates the 'Mobile LED Video Light' that can be mounted onto the iPad with a protective 3D-printed cover to protect the iPad from underground conditions. Hence, this problem was used to better prepare

the hardware against the harsh conditions for underground testing. The mounting mechanism for the chosen light source on the iPad Pro 11-inch had to be 3D printed. Figure 0-5 is an image of the Ultimaker S5 printer used to 3D print the iPad Pro 11-inch holder.

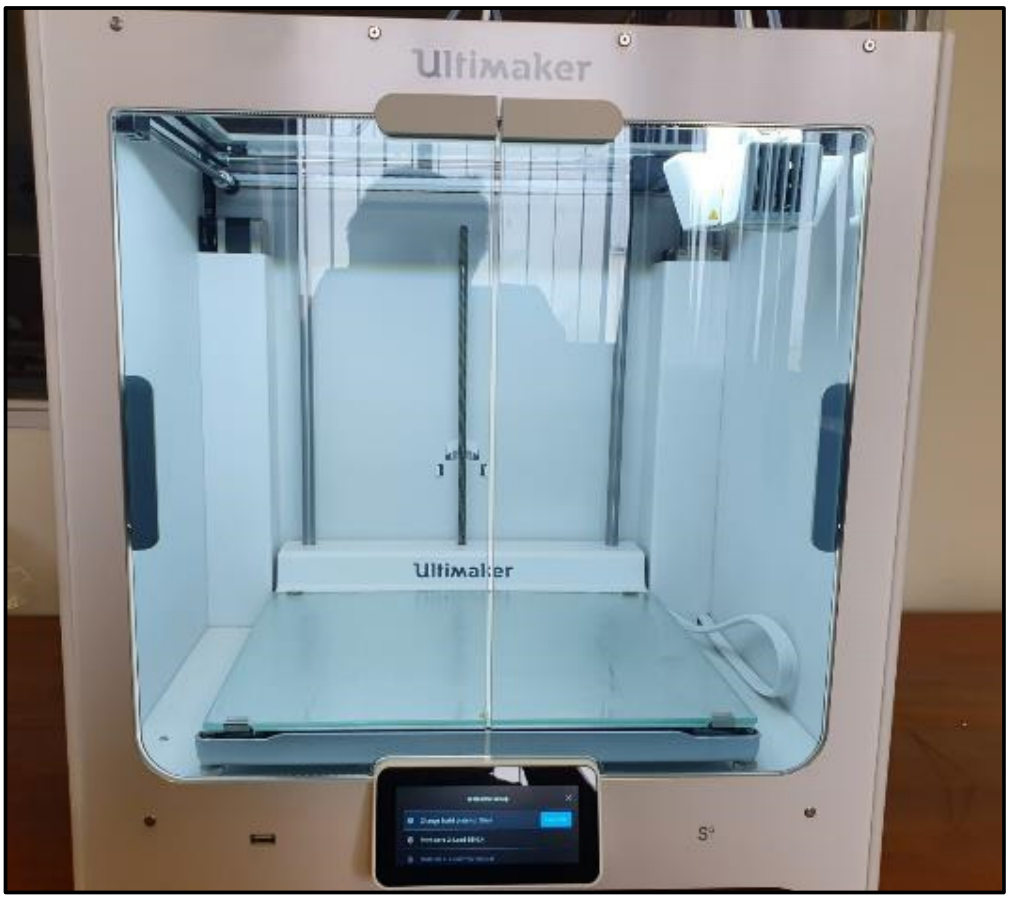


Figure 0-5: Ultimaker S5 printer (Birch, 2021).

Figure 0-6 is a diagram showing the back view of the iPad Pro 11-inch holder, designed using Shapr3D software, and Figure 0-7 shows a front view of the resultant 3D printed holder for the iPad Pro 11. Note the portion allocated for the Mobile LED Video Light protection at the bottom middle of the design in Figure 0-6.

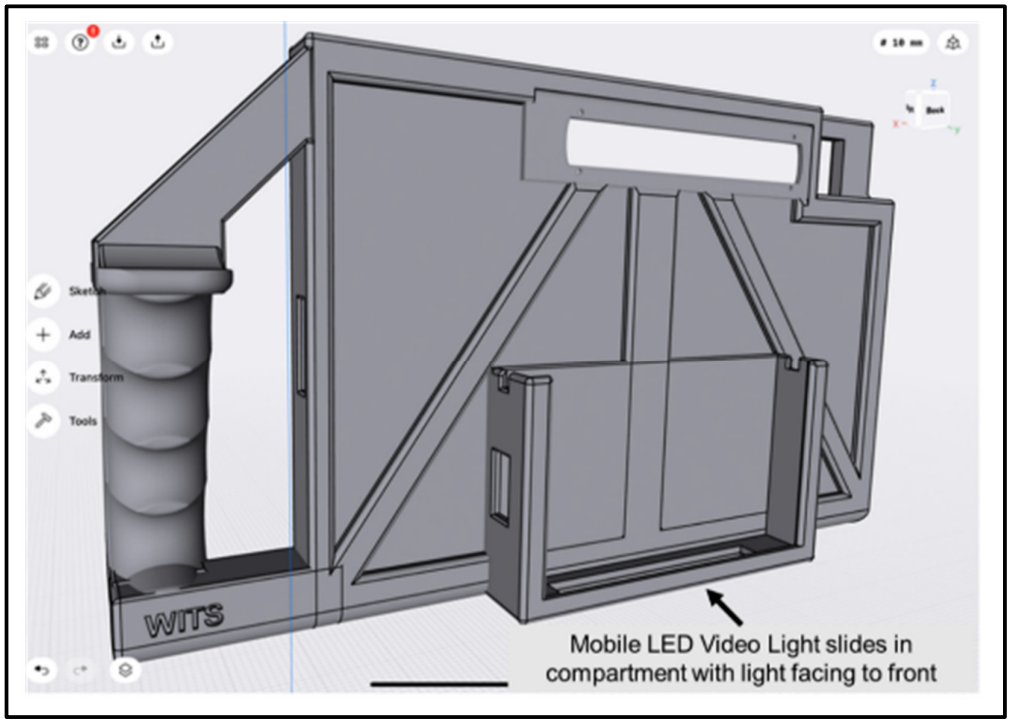


Figure 0-6: The back view of the iPad Pro 11-inch holder was designed using Shapr3D software.

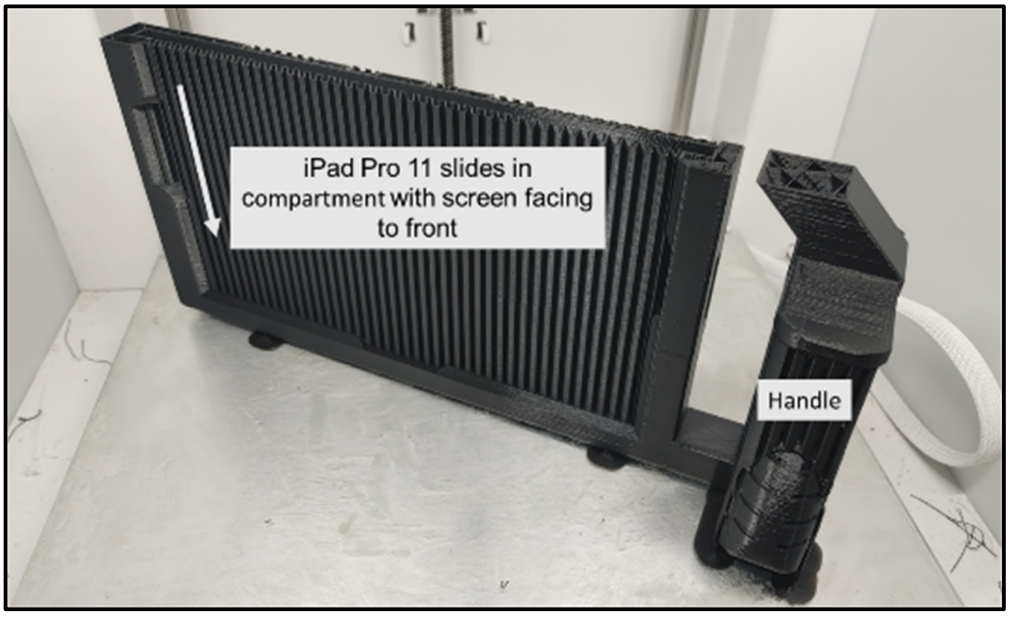


Figure 0-7: Front view photograph of iPad Pro 11-inch holder during printing.

Outcome - Insufficient light-source illumination

Under normal conditions, the stope panel of the DigiMine is very dark. However, the clarity of the cross-sectional scan through the stope panel shown in Figure 0-8 indicates that an added light source sufficiently complimented the quality of the scanning exercise.

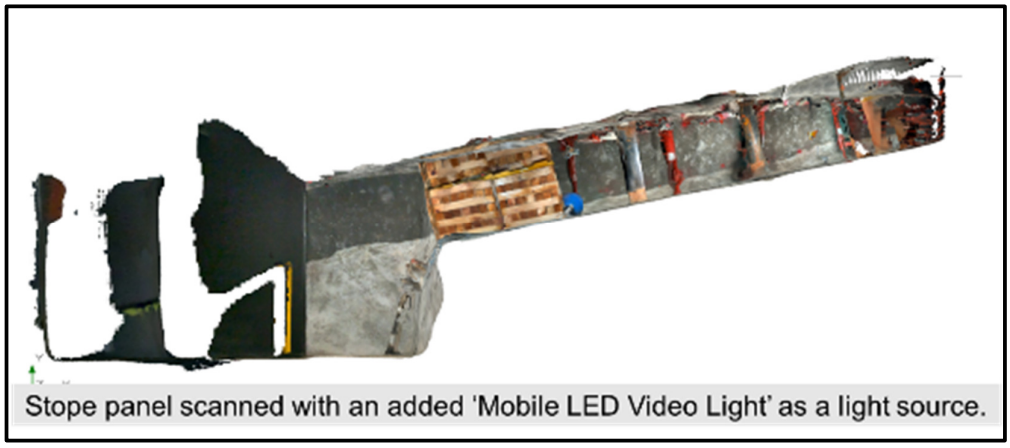


Figure 0-8: Cross-section through the stope panel of DigiMine scanned after light-source insufficiency was mitigated; with iPad at the University of the Witwatersrand in May 2021.

1.20.2 Quality of scans: Application trade-off

The initial phase of the research resulted in the 'SiteScape - LiDAR 3D', 'Scaniverse- LiDAR 3D' and '3D Scanner App' applications.

SiteScape - LiDAR 3D application

The SiteScape - LiDAR 3D Scanner application only exported point cloud data and scans which were all exported in the 'Polygon Model File' format. Figure 0-9 is an image of the scanned stope panel after the file was sent and opened using CloudCompare. It is clear from Figure 0-9 that the scan consists only of points, with a minimal rendering of textures of the scanned DigiMine stope.

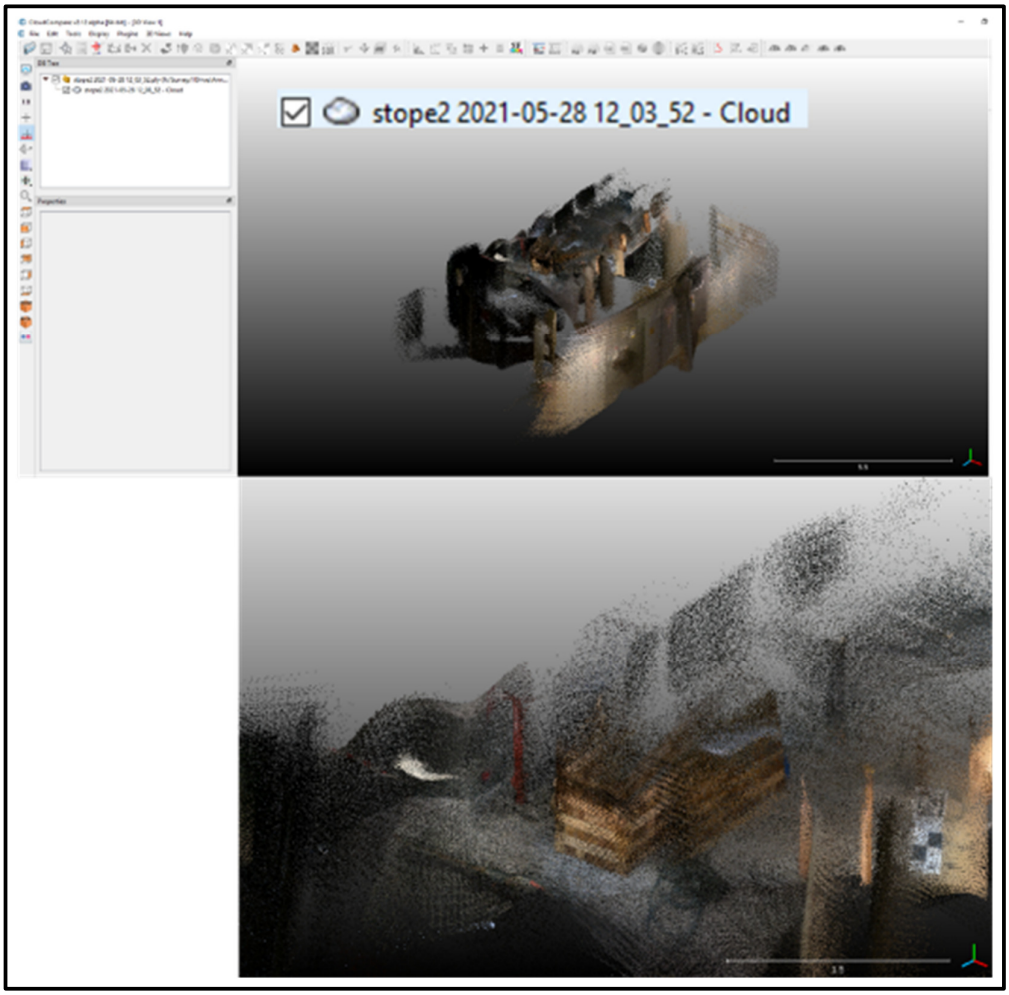


Figure 0-9: 'Polygon Model File' of stope area in the DigiMine exported to CloudCompare to assess iPad scanning using the SiteScape application during May 2021.

Figure 0-10 illustrates a portion of a crosscut scan of the DigiMine using the SiteScape - LiDAR 3D Scanner application.

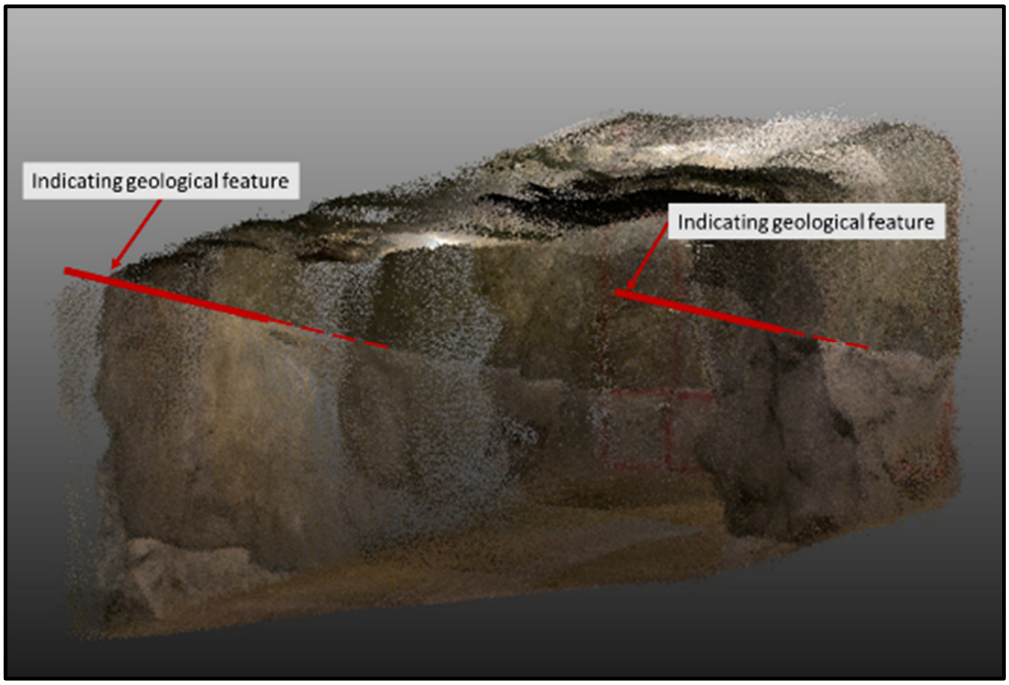


Figure 0-10: 'Polygon Model File' format of a portion of crosscut at the DigiMine to assess iPad scanning using the SiteScape application during May 2021, illustrating geological features.

The image's geological features are very clear and indicate that this application can produce scans of good quality once exported in a PLY format. However, since the minimum recommended SW at Mponeng mine is 1.2 m, this does not allow much room for movement in a stope panel. The aim is to produce one scan of the entire stope panel. The person who captures the scan will therefore have to move around in the stope panel to capture the stope as the whole panel in one scan. For this reason, it would be helpful if a pause function was available on the scanning application to pause the scan when moving in the panel. Unfortunately, the SiteScape application does not have a 'pause' function during scanning, and SiteScape only exports Point Cloud Data in the compatible PLY file format.

In other words, it is not capable of producing 3D Mesh Models. For these two reasons, the SiteScape application was considered a non-priority on the short-list of applications and did not warrant additional inquiry.

Scaniverse - LiDAR 3D application

It was found that only a limited of points could be exported as point cloud data and that the application created three different scans of one scanned area. This will require combining the three scans to get one scanned model. Therefore, the Scaniverse application was considered a non-priority on the short-list of applications and did not warrant additional inquiry.

3D Scanner App

Figure 0-11 is an example of a scan from the 3D Scanner App exported in an 'Object File' format of the crosscut at the DigiMine. Note the clear visibility of the geological feature on the excavation sidewalls; this file format shows the texture of objects.

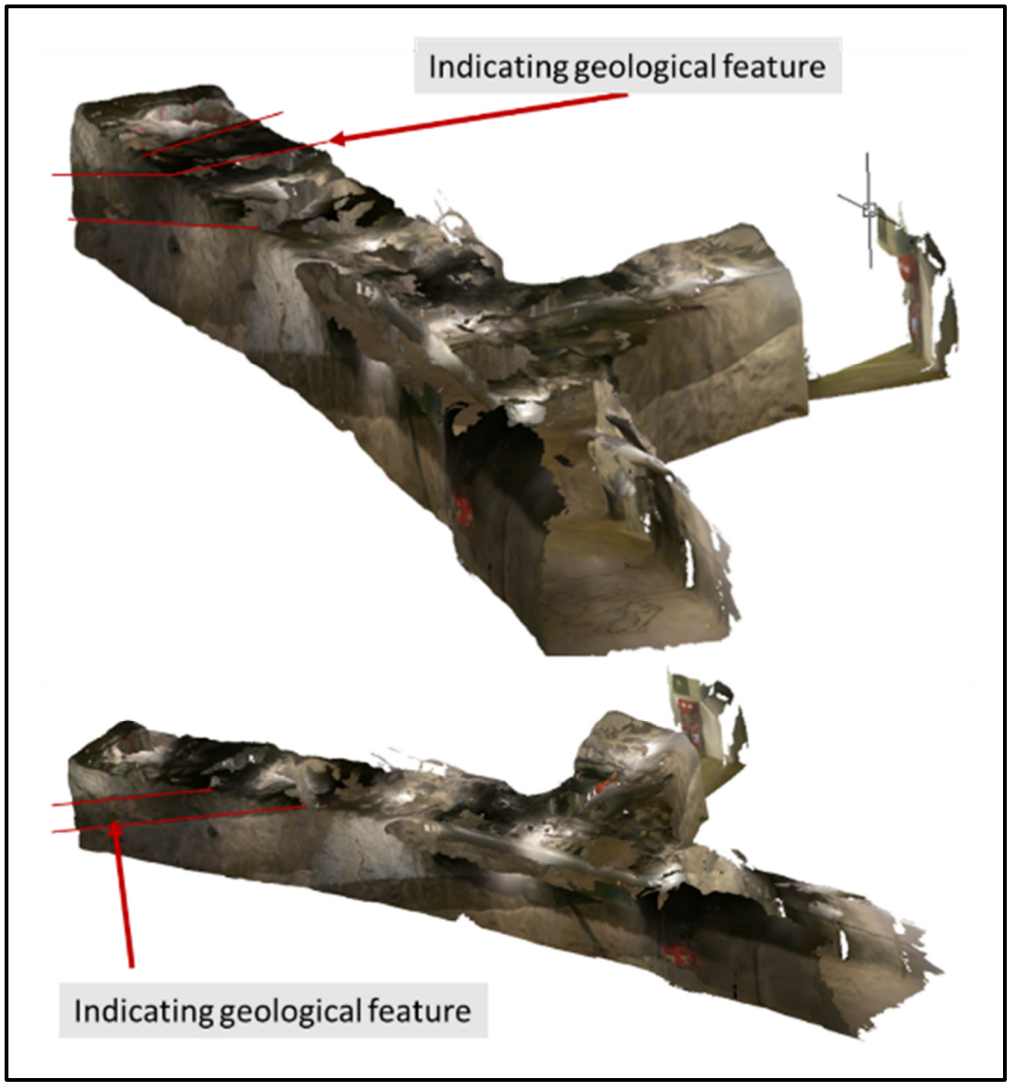


Figure 0-11: 'Object File' format of the crosscut at the DigiMine exported to Deswik CAD to assess iPad scanning using the '3D Scanner' application during May 2021, illustrating geological features.

The black lines indicated in the image in Figure 0-12 are multi-slice lines (otherwise known as contour lines) created on the crosscut tunnel of the DigiMine; this exercise was done with Deswik CAD software. This feature helps create an outline of the excavation instead of redrawing or tracing the outline of an excavation.



Figure 0-12: 'Object File' format processed in Deswik CAD showing Multislice lines of the crosscut at the DigiMine (as black lines) in Deswik CAD to assess iPad Pro scans using the '3D Scanner' application in May 2021.

Outcome - Quality of scans: Application trade-off

The Apple iPad Pro performed very well under the simulated conditions of DigiMine and was deemed suitable for entering the next phase of underground testing at Mponeng Mine. Observation of scans indicated that the 3D Scanner app should be used to export scans directly to Deswik CAD

to produce the best results. The result in this section supports favouring an Object File format over a Polygon File format.

1.21 Apple iPhone Pro Max in On-Surface Conditions

In September 2021, the Apple iPhone Pro Max was purchased, and dimensional accuracy was tested by scanning three adjacent office rooms that had each been measured with a distometer. Firstly, to confirm the added value of the smartphone (since access to the iPad was limited), measurements taken with a distometer were compared with measurements from the scans for quantitative application. Secondly, the quality of scans from the 3D Scanner App was exported as 'Laser File' (LAS) and 'Object File' (OBJ) into CloudCompare and Deswik Cad software.

1.21.1 Accuracy testing: application trade-off – office rooms

For the accuracy of testing, measurements were taken with a HILTI PD-I distometer, see Figure 0-13.



Figure 0-13: HILTI PD-I distometer (Munro, 2022).

The measurements of the distometer are accepted as correct. This is because the distometer was set to measure from the base of the distometer. Table 0-1 shows measurements of the rooms taken with the distometer.

Table 0-1: Distometer measurements

Distometer measurements				
	Length (m)	**Width (m)**	**Height (m)**	**Total m³**
Room 1	3.911	3.901	2.582	39.393
Room 2	7.883	3.904	2.590	79.708
Room 3	3.977	3.912	2.588	40.264

The distometer measurements were then compared to scanned distance measurements reported by the '3D Scanner App'. After that, the manual measurements were used to calculate each room's volume, which was then compared to the 'scanned volumes' of the rooms. This exercise aimed to determine which scanning application produced the most accurate scans compared to the distometer-derived volumes.

Scanned Measurements- Office rooms

Table 0-2 illustrates the different rooms scanned using the 3D Scanner App with measurements obtained from a distometer.

Table 0-2: Distometer versus scan - dimension comparison and variance in rooms measured.

Key:
Distometer
3D Scan App

	Length			**Width**			**Height**			**Volume**		
	(m)	**(m)**	*% Variance*	**(m)**	**(m)**	*% Variance*	**(m)**	**(m)**	*% Variance*	**(m^3)**	**(m^3)**	*% Variance*
Room 1	3.911	3.890	*0.537*	3.901	3.890	*0.282*	2.582	2.550	*1.239*	39.393	38.587	*2.047*
Room 2	7.883	8.280	*5.036*	3.904	3.970	*1.691*	2.590	2.640	*1.931*	79.708	86.781	*8.874*
Room 3	3.977	3.850	*3.193*	3.912	3.880	*0.818*	2.588	2.600	*0.464*	40.264	38.839	*3.540*

Note: Distometer dimensions taken as correct; % variance is ±

View of scans - office rooms

As Deswik was not available at the time of the research, all images of files were exported from separate apps into CloudCompare. Figure 0-14 illustrates scans exported in the (.LAS) file format from the 3D Scanner App.

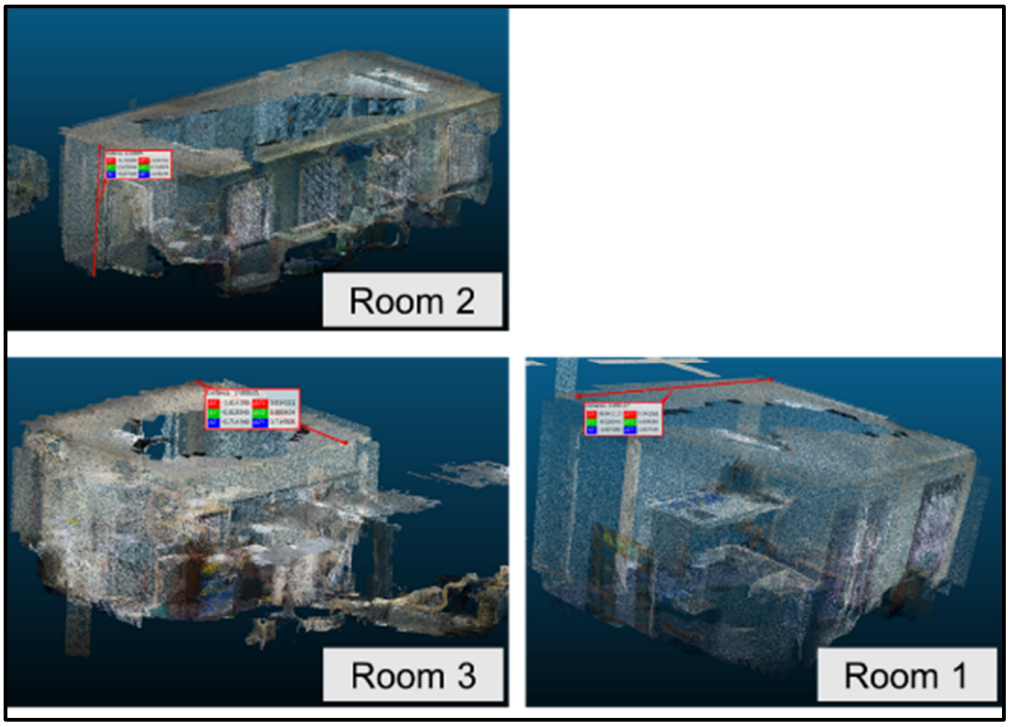


Figure 0-14: Rooms scanned with the 3D Scanner App on iPhone Pro.

1.21.2 Accuracy testing: Application trade-off at the DigiMine

The following distances were measured with a distometer: 1 m, 5 m and 10 m. A marker represented the measured distance at the 1 m, 5 m and 10 m positions. Figure 0-15 shows an enlargement of the 1 m mark on the floor of the tunnel placed at 1 m from the face of the tunnel. To show that data

can be collected from the tunnel's exterior, the image was captured from the bottom.

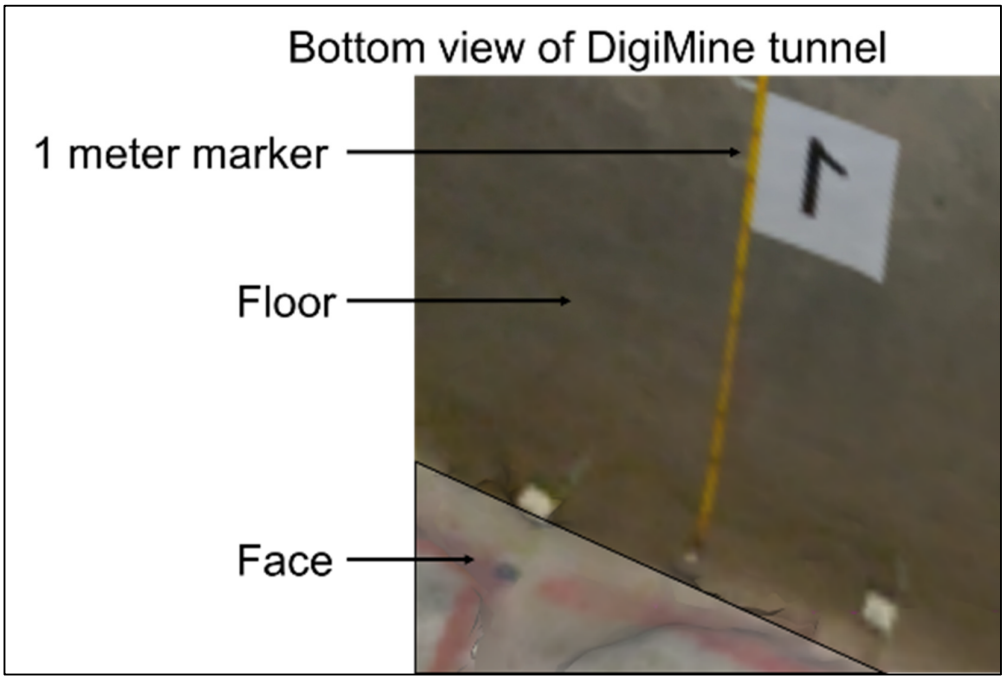


Figure 0-15: Enlargement of 1m mark measured from the face of the DigiMine tunnel.

The distometer measurements captured in the DigiMine tunnel were compared to measurements from the scanned image reported by the '3D Scanner App'. Figure 0-16 shows a bottom view of the '3D Scanner App' scan captured in the DigiMine tunnel.

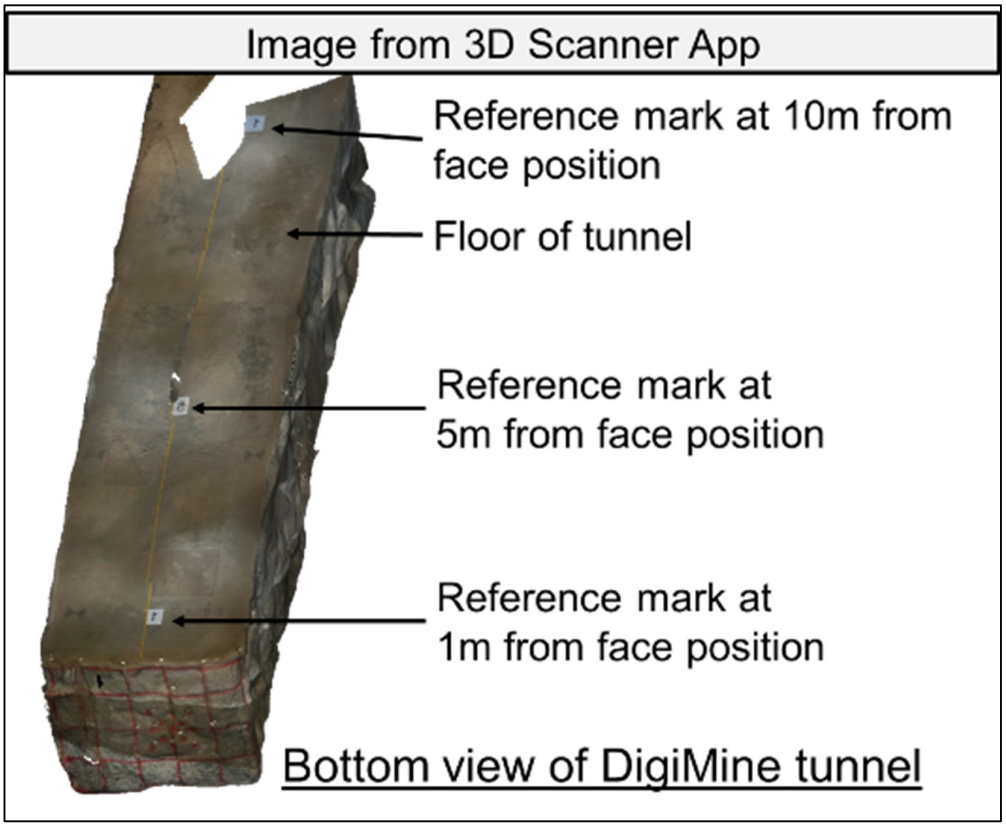


Figure 0-16: Bottom view of the '3D Scanner App' scan captured in the DigiMine tunnel.

Results from the scan were then compared to the measurements captured with the distometer to determine an accuracy reading between the scanned image and the distometer.

Scanned measurements - DigiMine

Table 0-3 shows the measurements from the different positions captured from the 3D Scanner App exported in an OBJ file format and comparisons to the distometer measurements.

Table 0-3: Accuracy test results from the 3D Scanner application (.OBJ). from DigiMine.

Key:
Distometer
3D Scan App

Length			**Width**			**Height**			**Volume**		
(m)	**(m)**	*% Variance*	**(m)**	**(m)**	*% Variance*	**(m)**	**(m)**	*% Variance*	**(m^3)**	**(m^3)**	*% Variance*
1.000	0.952	*4.800*	2.700	2.720	*0.741*	2.400	2.200	*8.333*	6.480	5.697	*12.087*
5.000	4.570	*8.600*	2.700	2.590	*4.074*	2.300	2.360	*2.609*	31.050	27.934	*10.036*
10.000	10.030	*0.300*	2.700	2.660	*1.481*	2.400	2.380	*0.833*	64.800	63.498	*2.009*

Note: Distometer dimensions taken as correct; % variance is ±

Outcome - View of scans

It is apparent that the visual quality of scans taken with the Apple iPhone Pro Max is comparable to Apple iPad Pro and confirms superiority to Occipital Structure Sensor Mark II regarding the research objectives. The correlation between qualitative and quantitative results supports the '3D Scanner App' superiority. When used in conjunction with this app, the laser file format (.LAS) was found acceptable for rendering images with enough detail for making observations. However, Object Files were still considered as most favourable for practical use. This section does not show that the preferable software for processing files is CloudCompare but that it acts as an acceptable substitute for analysis in instances when Deswik CAD is unavailable.

Performance of the Scaniverse and Sitescape applications affirmed it as a non-priority on the short-list of applications and did not warrant additional inquiry. However, as Sitescape only exports Point Cloud Data in the compatible PLY file, Scaniverse may instead be considered as an alternative as exports are possible in files (OBJ and LAS) compatible with 3D Mesh Models. Consideration must also be given if the compatibility or suitability of the '3D Scanner App' should decline soon (for example, updates that institute unacceptable compulsory membership fees).

1.22 Underground Stope Scanning

The next testing phase involved the Apple iPad Pro 11-inch and Apple iPhone Pro Max with photometric LiDAR scanning technology at Mponeng Mine in an underground production stope. The outcomes of initial testing were integrated with the '3D Scanner' Application, and OBJ files (OBJ or LAS being acceptable formats) were exported for processing in Deswik CAD. The naming convention of underground workplaces at Mponeng Mine can be explained in the following form: Mining level, raise line number and then panel number.

Apple iPad Pro 11-inch in an underground production stope

On 5 July 2021, the 113-68-East 5 panel of the VCR was visited for scanning. Figure 0-17 is a cross-section of this panel showing some visible differences in ground formation.

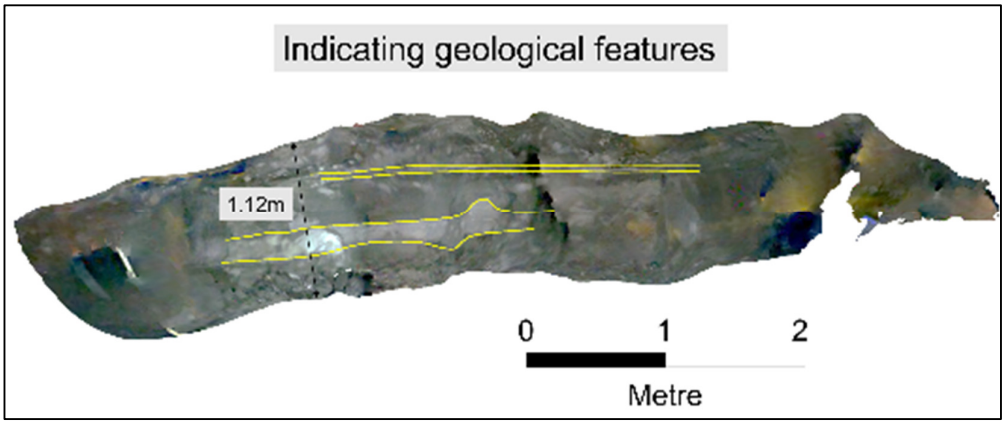


Figure 0-17: Visible ground formation in the 113-68-East 5 stope panel.

Note: there was no advance of the face after the measurements from 5 July 2021.

Table 0-4 shows measurements compared at 5m intervals from the 113-68-East 5 stope panel of the VCR from three different sources, namely:

- Manual measurements underground on 5 July 2021;
- Measurements from Deswik CAD; and
- Measures that were done by the sampling team on 6 July 2021.

Table 0-4: Measurements from 113-68-East 5 stope panel of the VCR.

Method	iPad Pro, 3D Scanner App and Deswik Software		Manual measurements from an underground visit		Sampler Measurements	
Date	5 July 2021		5 July 2021		6 July 2021	
	Range of measure.	Average of stope	Range of measure.	Average of stope	Range of measure.	Average of stope
Stope width (cm)	103-161	138	119-139	130	88-136	120
Hanging wall (cm)	7-41	23	0-75	21	0-32	12
Footwall (cm)	47-74	65	58-85	69	55-108	84
Channel Width (cm)	5-46	23	4-41	20	0-50	24

Note: Measurements are taken at 5m intervals.

Comment on results from Table 0-4: Although measurements were reported at 5 m intervals, the position of the 5 m intervals differs in x and y positions. This exercise aimed to determine an average SW for the total panel. When the geologist reports the SW on the mapping report, they measure the SW at regular intervals over the entire panel. All the measurements are added and divided by the number of measurements captured. For this reason, the minimum and maximum range of measurements in Table 0-4 will vary. The accuracy is considered as a fit for purpose accuracy. In other words, to report the average SW over the total panel, the measurements from the scans are accepted as accurate and reported and accepted by the Mponeng Mine to guide the production team in SW control. Figure 0-18 shows the measurements as reported by the sampling department.

Figure 0-18: Sampling report for 113-68-East 5.

Figure 0-19 shows the 20 cm measured CW of the VCR in the 113-68-East 5 stope panel.

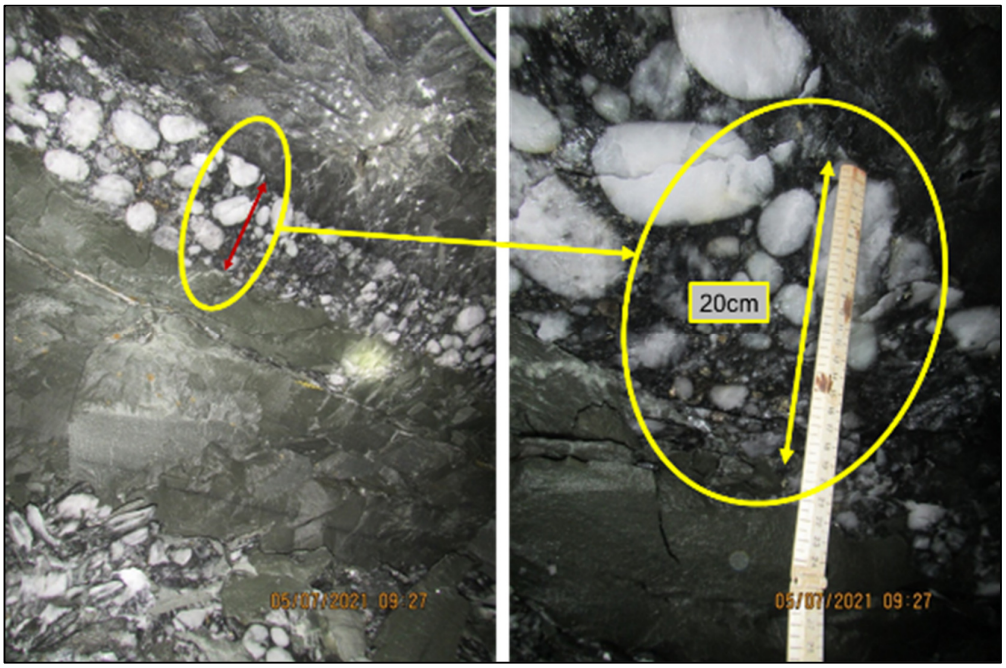


Figure 0-19: 20cm measured CW of the VCR in the 113-68-East 5 stope panel.

The recommended SW for the 113-68-East 5 stope panel of the VCR was 120 cm. It is clear from the underground measuring results that the average SW of panels needs to be reduced by 10 cm. Table 0-5 shows the volume calculation of the 113-68-East 5 stope panel of the VCR. The scan measurements of the total panel show 12.6 m³ more than the manual measurements from the underground visit. When the scan measurements of the entire panel are compared to the sampled measurements, the scan measurements show 28.4 m³ more than the sampling measurements. This

variance demonstrates the significance of the loss that Mponeng Mine experienced due to poor SW control.

Table 0-5: Volume calculation of 113-68-East 5 stope panel of the VCR.

Method	iPad Pro, 3D Scanner App and Deswik Software	Manual measurements from an underground visit	Sampler Measurements
Stope width (m)	1.38	1.30	1.20
Face length (m)	33.60	33.60	33.60
Advance (m)	4.70	4.70	4.70
Volume (m^3)	217.93	205.30	189.50

The calculated volumes reported in Table 0-5 are a concern as the difference in volume calculated from the scanning software differs 28.4 m^3 from that of the samplers' measurement. Although both these measurements get reported on Mponeng Mine, the geologist validates all SW data. For this exercise, the scanned image is deemed acceptable for SW control as it is backed by a clear visual representation of the scanned image. On 7 July 2021, the 113-68 East 2 panel of the VCR was scanned and Figure 0-20 provides a top and side view of the scanned image combined with the measured faces from the survey department.

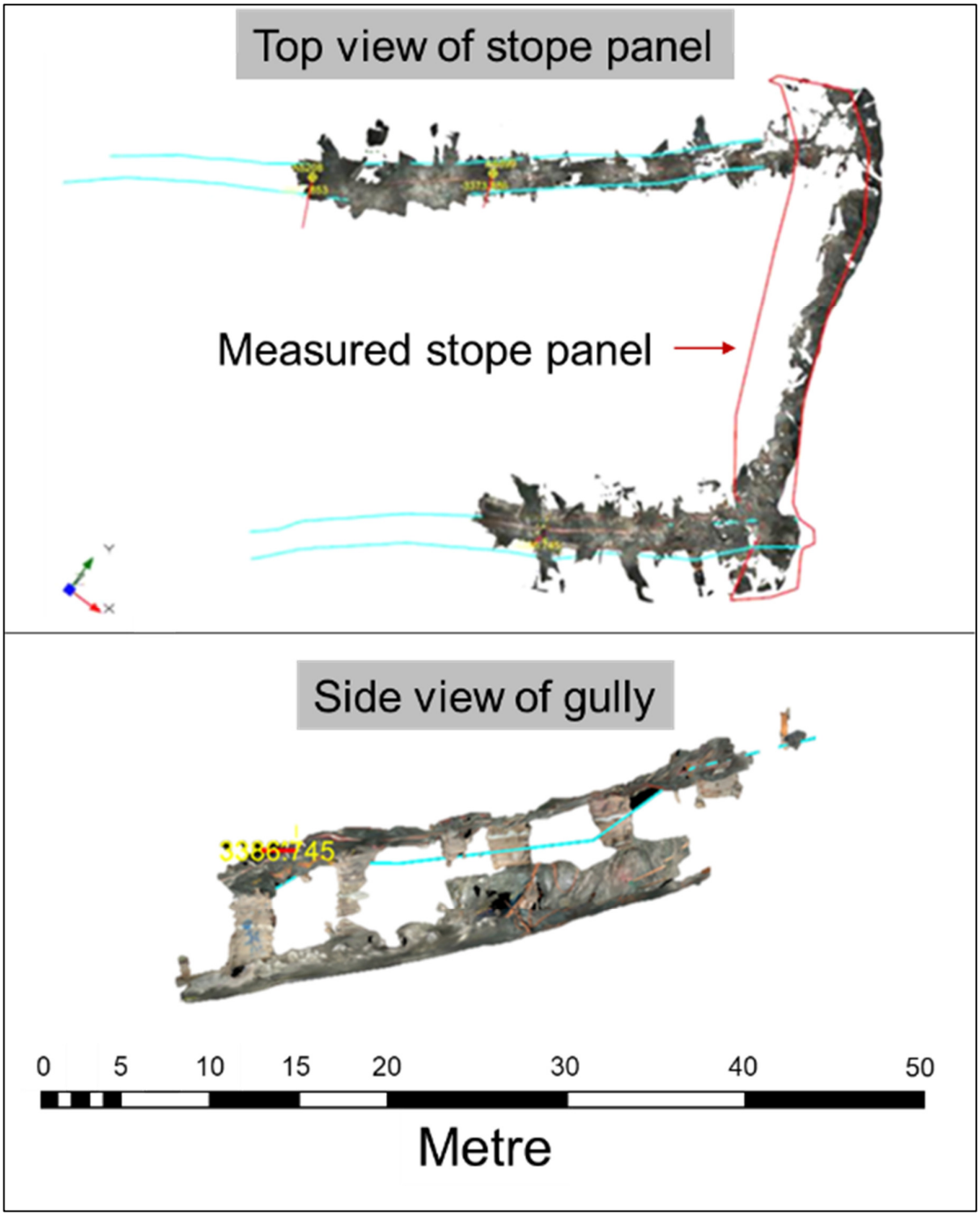


Figure 0-20: 113-68 East 2 panel of the VCR.

Figure 0-21 demonstrates the accuracy of the geo-referenced scan on the survey control point (target). After geo-referencing, the scan was accurate

within 20 cm on the plane and for SW control, this accuracy is accepted by Mponeng Mine.

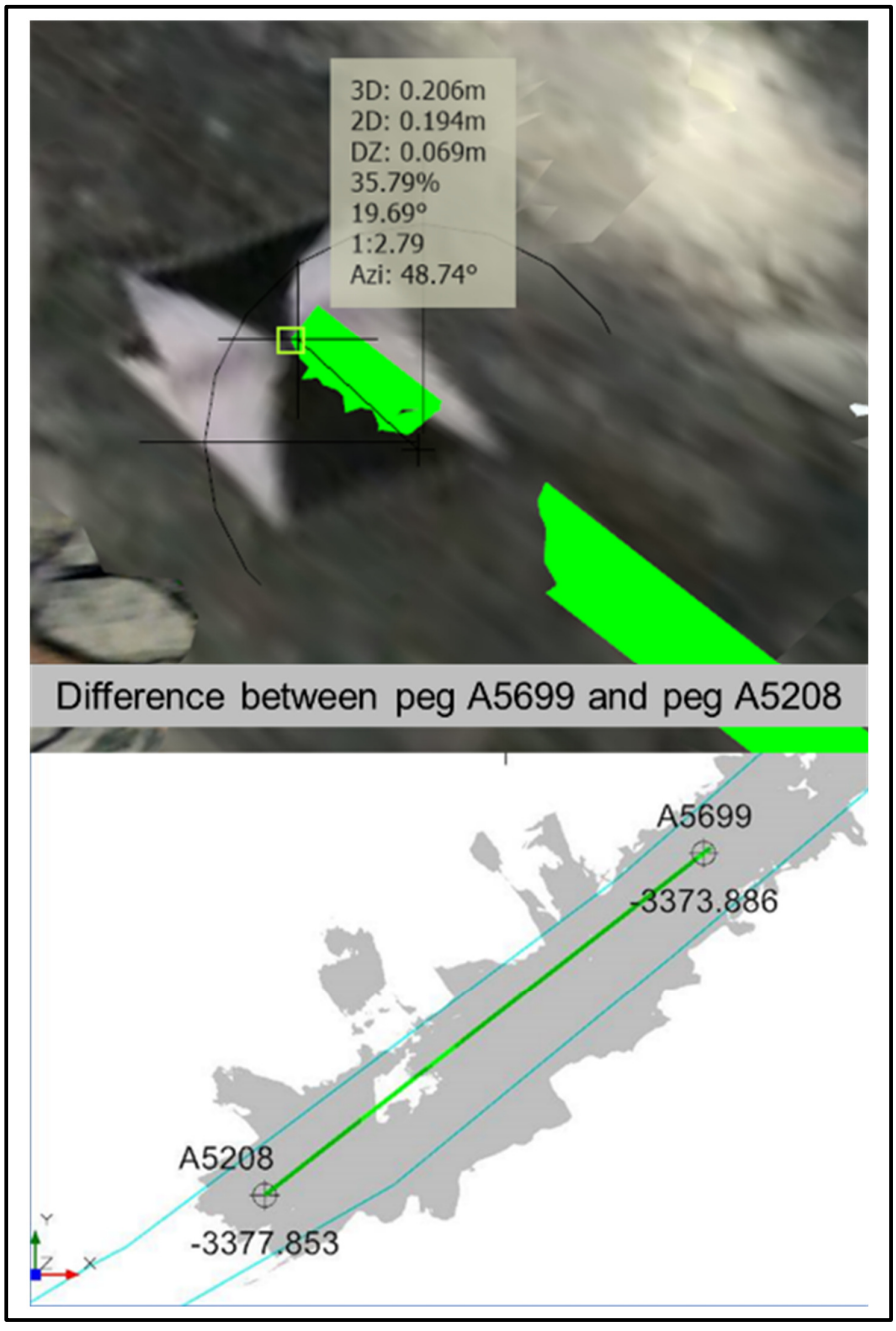


Figure 0-21: Scan accurate to within 20 cm.

Figure 0-22 shows the survey point (target) that was placed below the survey peg. This was done to make identifying the survey peg on the scan easier and to make the geo-referencing easier.

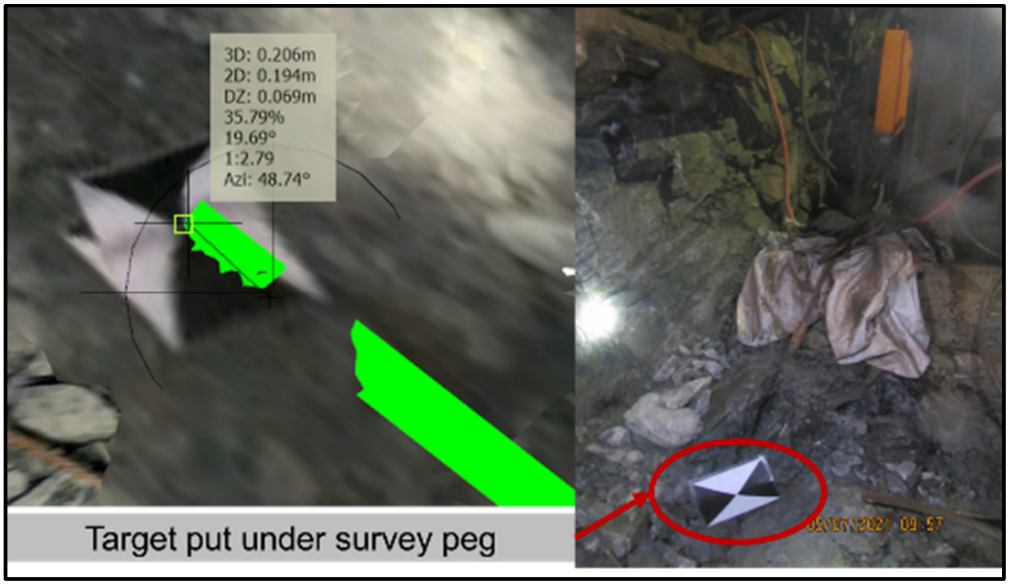


Figure 0-22: Survey point (target) that was placed below the survey peg.

The MHSA Chapter 17(14)(b) defines that the difference "between the measured position and final position of a survey station does not exceed 0,1 (zero comma one) metres" (Mine Health and Safety Council, 1996, p. 15). The accuracy of survey stations, both horizontal and vertical planes, is calculated with the following equation:

$$Class\ A = 0.015 + S/30000 \qquad \textit{Equation 2}$$

"Where S is the distance in metres between the known and the unknown survey station" (Mine Health and Safety Council, 1996). The horizontal displacement between the measured peg and the measured point on the

scan is 0.015. This does not exceed 0,1 m as defined according to MHSA Chapter 17(14)(b).

Figure 0-23 is the mapping report of the 113-68 East 2 panel of the VCR. The mined SW captured for this panel was 122 cm and the recommended SW for this panel was 120 cm. The 2 cm difference is not accepted according to survey standards; however, it would be acceptable to report the average SW of a stope panel because the purpose of the scans is to identify and report excess dilution. Therefore, the scans do not require acceptable survey accuracy to fulfil their intended use, but the survey control must conform to the MHSA regulation on survey accuracy.

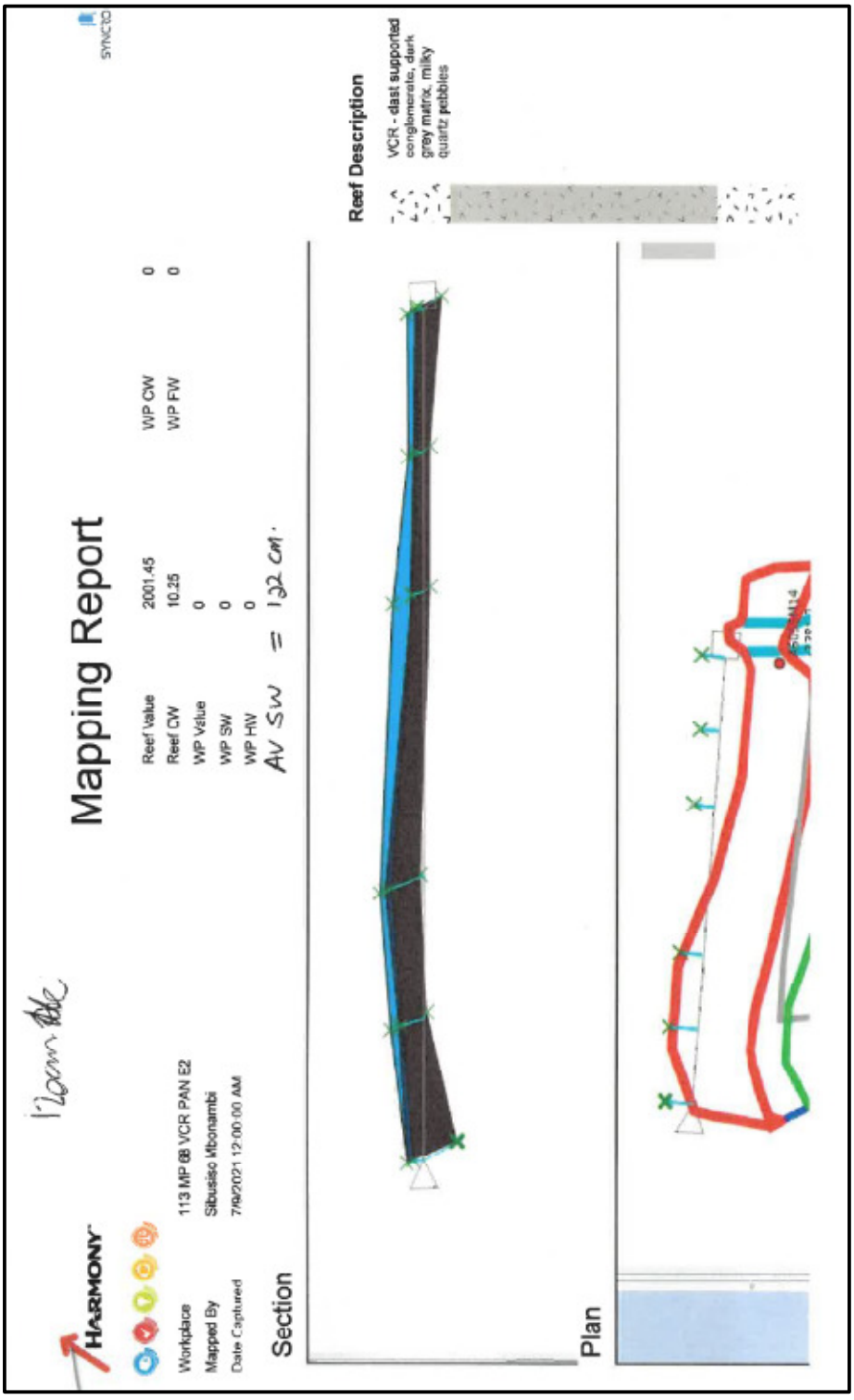


Figure 0-23: Mapping report of the 113-68 East 2 panel of the VCR.

Traditional mapping of the 113-68 East 2 panel took approximately 35 minutes, and the scanning took around 12 minutes. The mapping of the 113-68 East 5 panel took about 44 minutes, and the scanning took about 15 minutes.

Apple iPhone Pro Max underground testing

After Mponeng Mine purchased an Apple iPhone Pro Max, it became easier to conduct consecutive scans on stope panels to investigate SW control. Therefore, on 15 September 2021, the iPhone Pro Max was tested underground at the CLR's 120-80 E1A panel. Figure 0-24resulted from this scanning exercise and showed the advantage of capturing a scan of the stope face without disturbing the production team. Figure 0-24 shows the production team working whilst protected by temporary support.

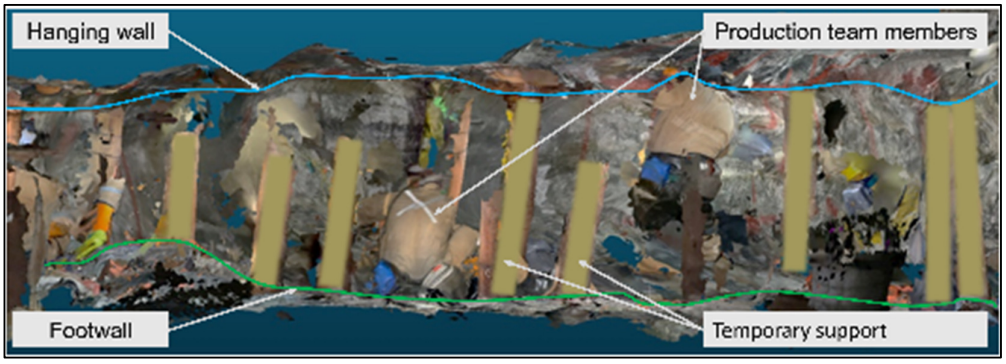


Figure 0-24: The 120-80 E1A panel of the CLR.

The distance from the stope face where the support system shall be installed is an important consideration in support design. The theory of

tributary areas is used to design stope support. “The tributary area is given as a function of the height of potential rock mass instability and support force” (Daehnke, et al., 2001, p. 144). Figure 0-25 illustrates the tributary area requirements for rockfall conditions.

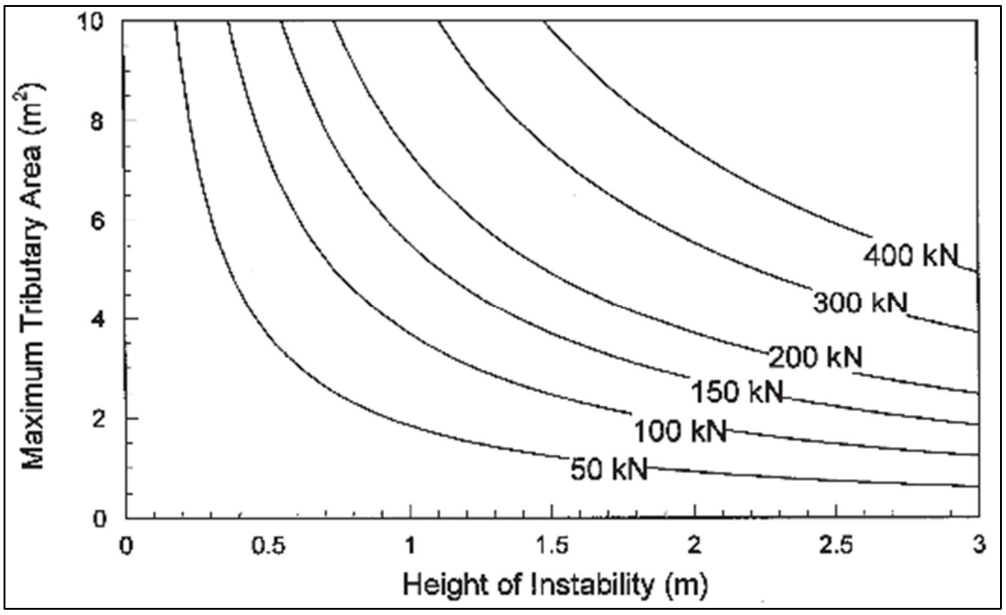


Figure 0-25: Tributary area requirements for rockfall conditions(Daehnke, et al., 2001).

“At 200 mm deformation the support unit carries a load of 180 kN. For the rock mass to be stable over this deformation range (based on the tributary area criterion), the maximum tributary area should not exceed 4.5 m²” (Daehnke, et al., 2001). From Figure 0-25 a 1.5 m height of instability is calculated assuming that the support unit load (N) is 180 kN. In this example the instillation distance of support from the stope face is 1.5 m. Ideally, this distance should extend to the sweeping line (typically 5–6 m from the face) and the stope's back area (Daehnke, et al., 2001); see Figure 0-26.

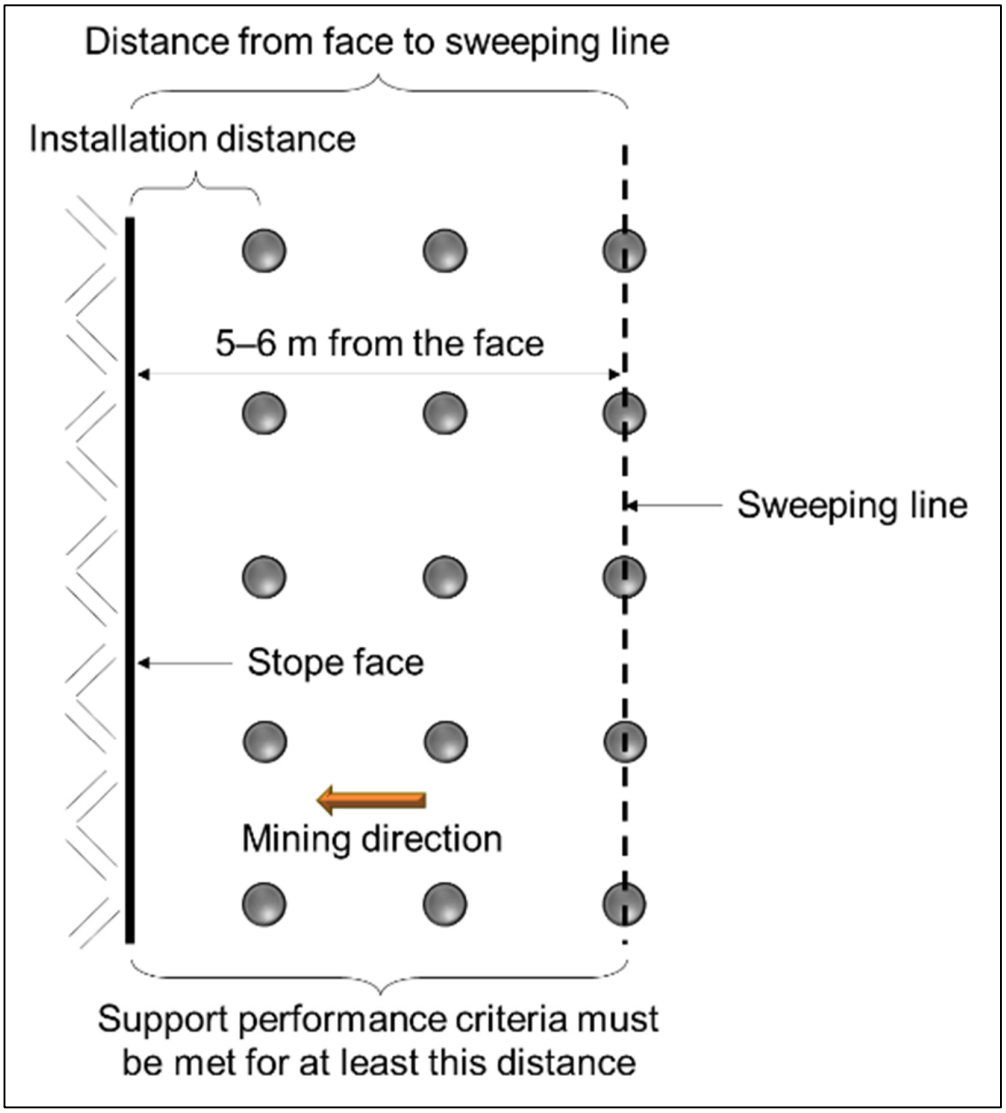


Figure 0-26: Stope plan view indicating minimum distance behind the face (Daehnke, et al., 2001).

“By ensuring the support performance criteria are met for this distance, the rock mass stability is maintained over an area extending at least up to the sweeping line” (Daehnke, et al., 2001). For this reason, the geologist is not allowed to move in between the stope face and stope support. Instead, scans need to be captured within the supported area. Because the scan has

a scanning range of 5 m, it makes it possible to scan from a safe, supported position. The geologist is not permitted to go beyond the installed Stope support to measure SW or the dip direction of faults. This information can now be measured from the scan of the stope face.

Figure 0-27 shows the mapping report of the CLR's 120-80 E1A panel from 15 September 2021. The mapping report indicates a portion of the reef in the hanging wall observed on the scan. This panel measured an SW of 121 cm with a recommended SW of 120 cm. Therefore, the geologist recommended that the production team lift the footwall position but maintain the recommended SW to expose the reef in the hanging wall.

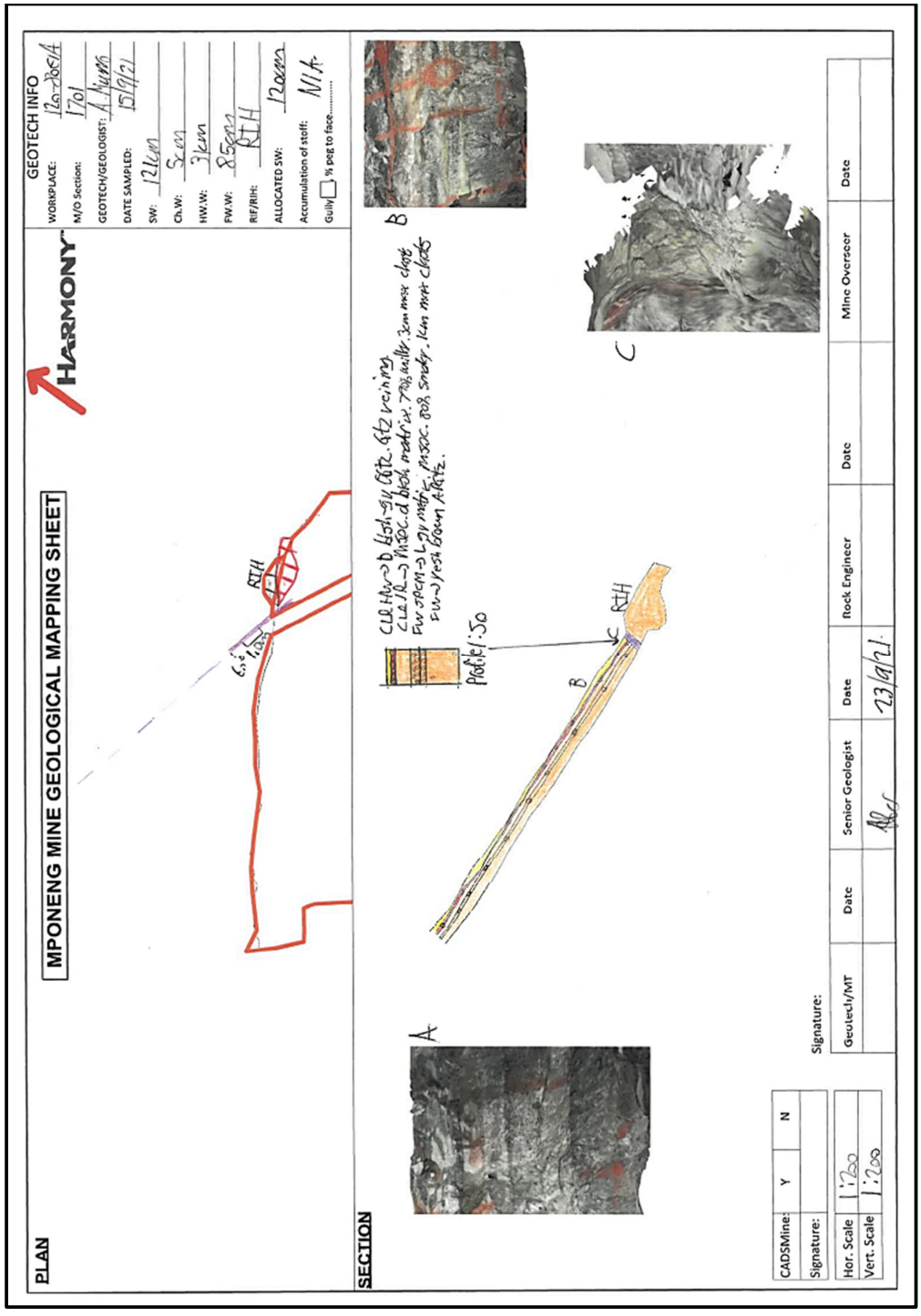


Figure 0-27: Mapping report of the CLR's 120-80 E1A panel from 15 September 2021.

On 7 October 2021, it was scanned again. Figure 0-28 shows a reduction in SW from 121cm to 99cm. This resulted in an increased area of reef in the hanging wall.

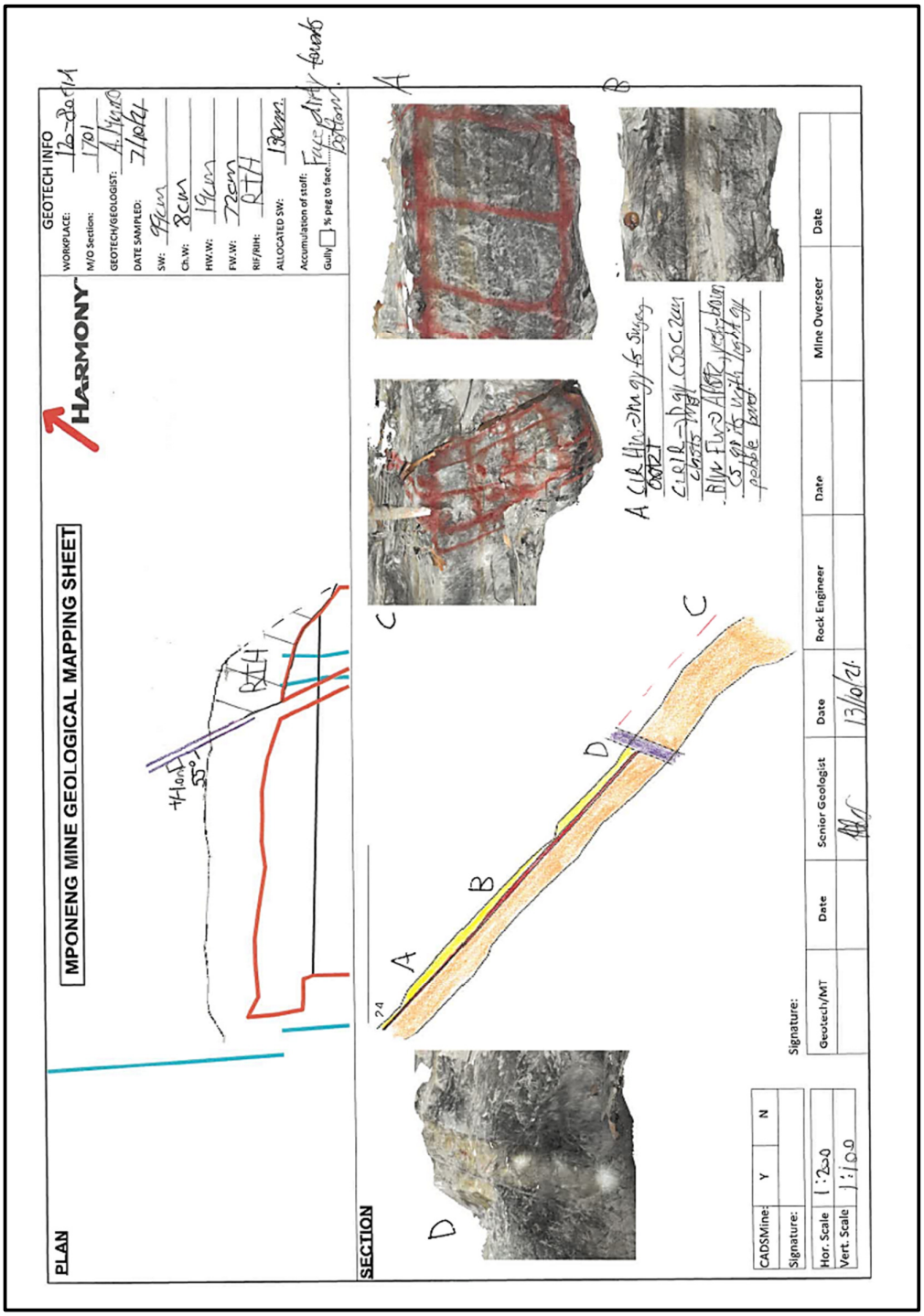


Figure 0-28: Mapping report of the CLRs from 7 October 2021.

Figure 0-29 is the sampling report of 120-80 E1A panel of the CLR from 8 November 2021, the sampling report shows one fault in this panel, and the geologist scanned this same panel on 12 November 2021 and picked up three faults in this same panel.

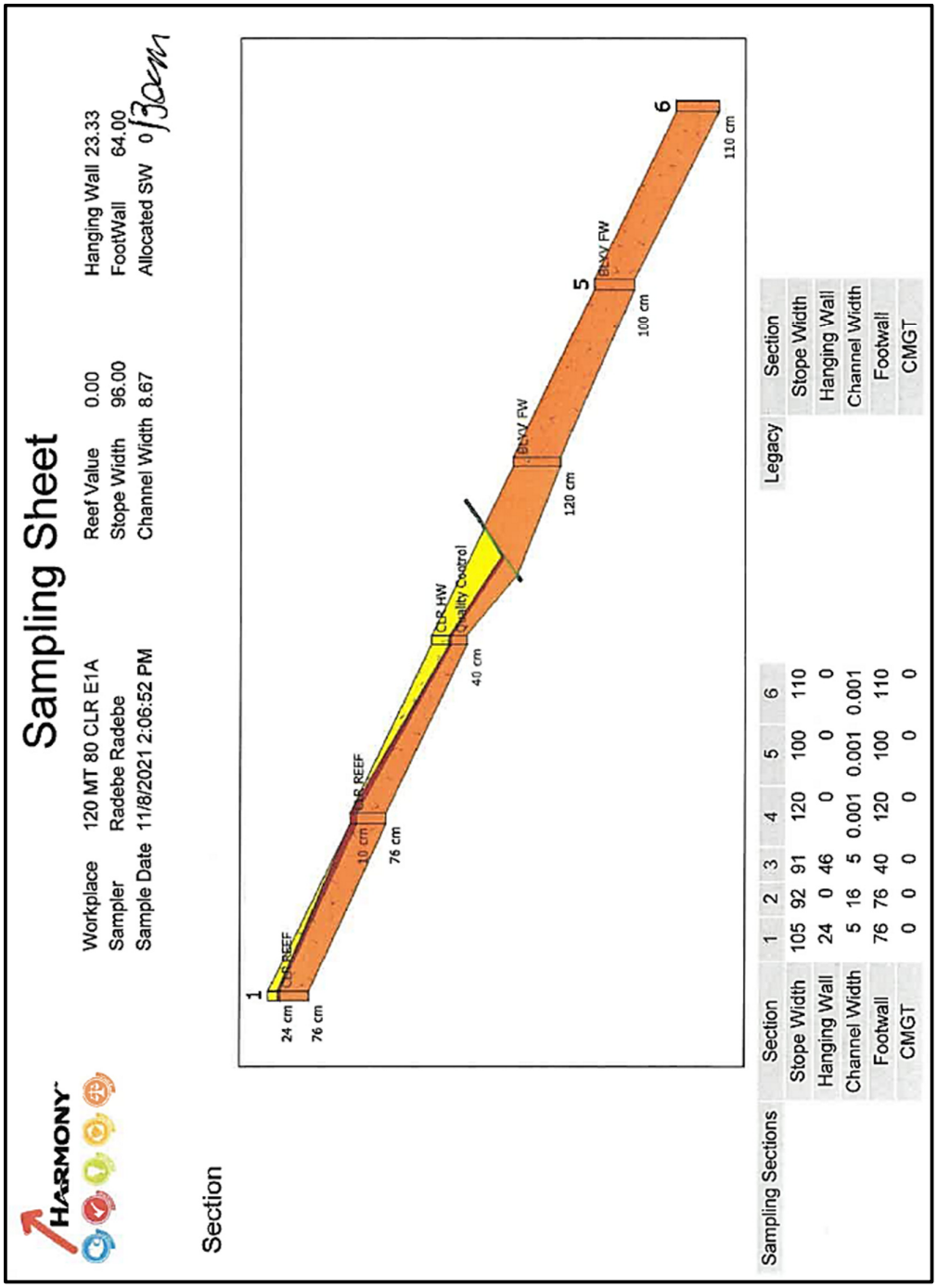


Figure 0-29: Sampling report of the panel of the CLRs 120-80 E1A from 8 November 2021.

Figure 0-30 is the mapping report from the CLR's 120-80 E1A panel that was scanned on 12 November 2021.

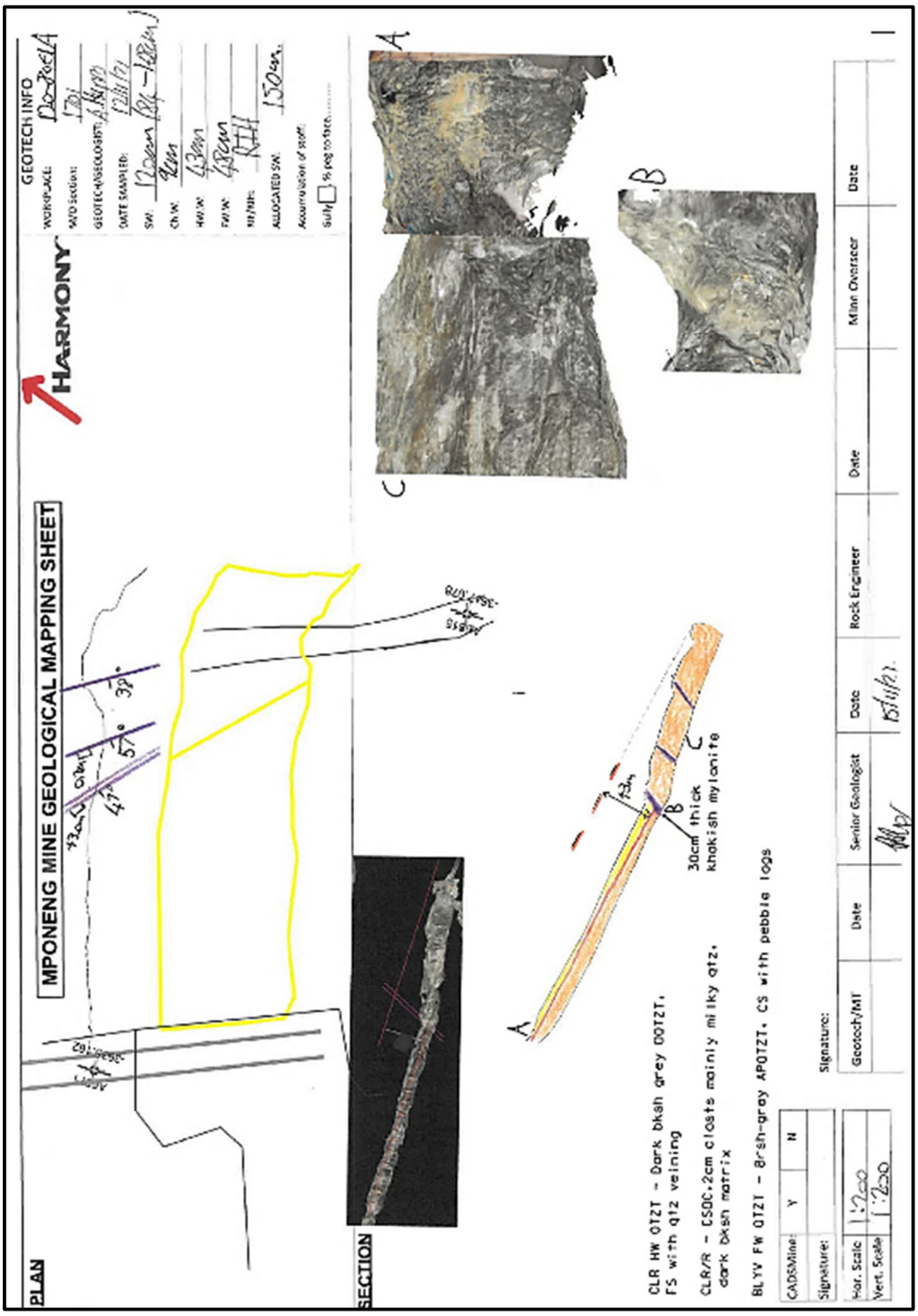


Figure 0-30: Mapping report of the CLR's 120-80 E1A panel from 12 November 2021.

This scan shows an increase in SW from 99cm to 120 cm; the geologist observed three faults in this panel. The one fault projected the reef 3 m up into the hanging wall. The scanned section view shown in Figure 0-30Figure 0-30 gives a total view of the stope panel. In contrast, normally, only a portion of the face would be presented in a photograph. The problem is that it is unclear which part of the stope panel is represented by the photo image shown on a mapping report.

1.23 Section Summary

As the disadvantages and advantages of each scanner and scanning application are mentioned, it is evident that the most suitable combination of 3D LiDAR scanner and 3D LiDAR scanning application is the 3D Scanner application and Apple iPhone Pro Max. This is due to the combination of accuracy in geological mapping in an underground environment.

Therefore, this is the most reliable combination to utilise for geological mapping. However, more investigation is required to decide on using scanners in the future to get the desired results compared to conventional survey measuring.

MINE THREE-DIMENSIONAL SCANNING WORKFLOWS

1.24 Section Overview

A 3D workflow was designed for the geological mapping staff to use and another workflow for the production team. The main difference between these two workflows is the intended purpose of use. For example, the geologist needs to geo-reference the underground scan to fit on survey pegs. In contrast, the production team may only need to view the scanned image of the stope face.

1.25 Geological Scanning Workflow

The Geological Scanning Workflow can be described as the geologist's process of capturing and reporting geological information in the scanning process. Figure 0-1 illustrates this process.

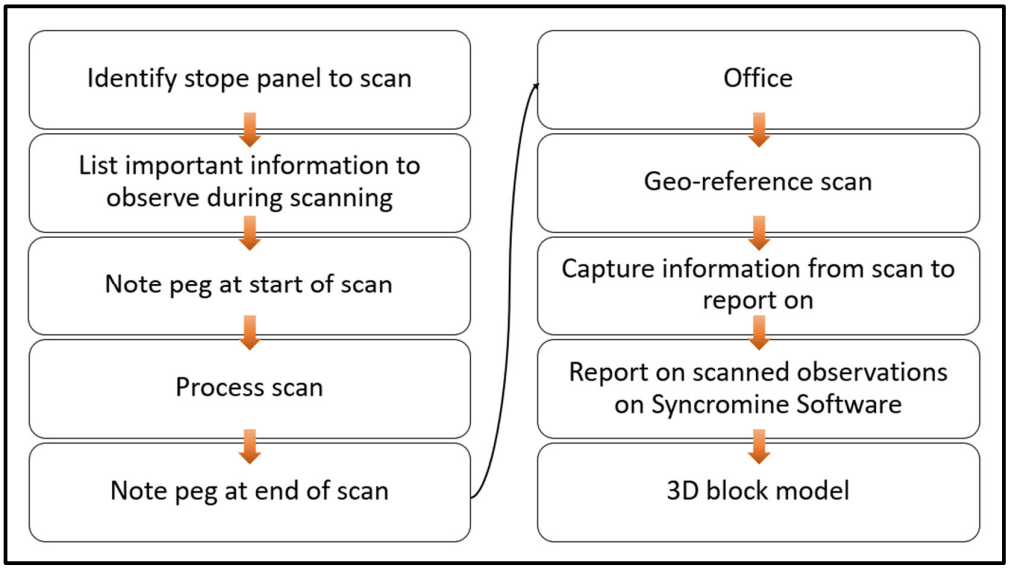


Figure 0-1: Geological Scanning Workflow.

The scanning process starts on the surface, where the geologist identifies which stope panel they plan to visit and scan during the shift. The geologist will then note what important information to be aware of when capturing the scan. This will include the following information:

- Stope width;
- Rock formation;
- The behaviour of ore (rolls in the reef);
- Reef in the hanging and reef in the footwall; and
- Faults and dykes.

Once the geologist returns to the office from underground, they will download the scan from the iPhone to the mine's server for relevant departments to view. The next step involves the geo-referencing of the scan. To do this, the geologist will load the survey pegs used during the

scan in the Deswik CAD software. Deswik CAD 'Modifying' tools are then used to geo-reference the scan to fit the requisite survey pegs. Once the scan has been geo-referenced correctly, the top view with the hanging wall, the footwall and the geological features are captured from the scanned image. Next, Deswik CAD tools are used to measure the average SW of the stope panel. The geological mapping report will then be completed on Syncromine software with special recommendations for the production team. Finally, the geological features that were captured from the scan are fed into the 3D geological model.

1.26 Production Scanning Workflow

The Production Scanning Workflow can be described as the production team capturing important production-related information during the scanning process. For example, this information may include the blasting advance, rock engineering support information, or equipment requirements for future planning; Figure 0-2 illustrates this process.

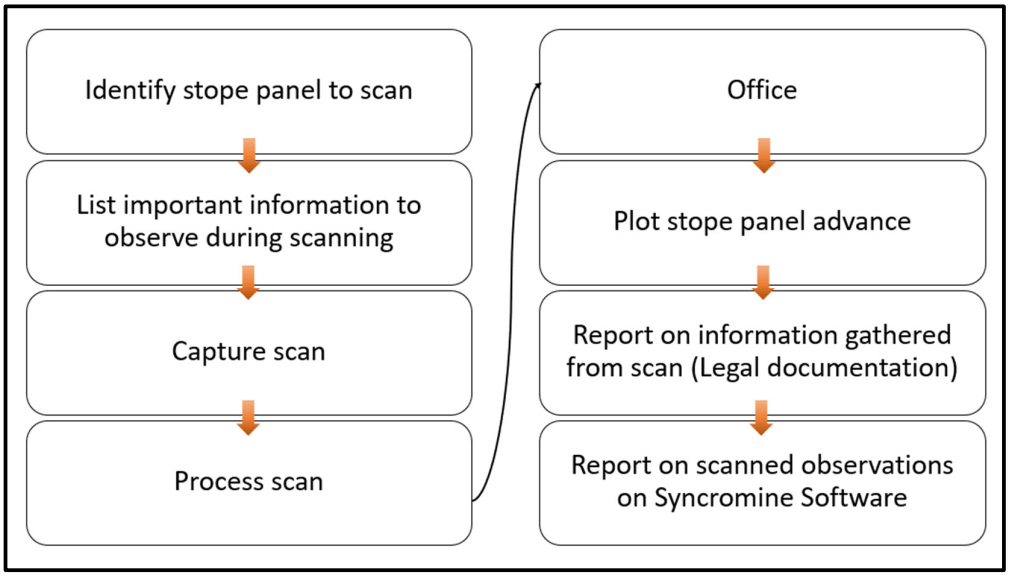


Figure 0-2: Production Scanning Workflow.

Geo-referencing is not required for the Production Scanning Workflow, this is because the production team requires different information from the scans than the geologists need.

1.27 Section Summary

The 3D scanning method of capturing geological data requires less time and energy to produce accurate 3D geological block models than traditional methods of capturing geological stope mapping. The data is also processed in a much shorter time and is readily available to the entire mining department for analysis and observation. This allows for increased time spent on mine planning and guidance of the production team for blasting. Communication also becomes more straightforward as a digital reference with exact images is displayed and can be viewed by all team members. In

contrast, previously, a geologist would need to explain their way of capturing data first. In addition, this method allows for an increased frequency of data capturing. Therefore, the production team can be informed of any issues before the next blast commences.

CONCLUSIONS AND RECOMMENDATIONS

This research has presented six chapters, which cover the following:

- Chapter 1, the introduction chapter, gave background to the research conducted to identify orebody dilution in an ultra-deep gold mine in South Africa. Problem statement: Dilution destroys the economic value of mining operations. In addition, mining and processing costs rise due to dilution from unwanted waste mining. For this reason, Mponeng Mine aims to reduce grade dilution by controlling the SW was, on average, 12% greater than ASW at Mponeng Mine;
- Chapter 2 was an overview of how resource estimation relies on 3D modelling. Two-dimensional geological mapping captured with tapes and clinometers is difficult to convert to 3D geological models. Mining accuracy can be improved by providing 3D geological models more often;
- Chapter 3 discusses how various scanning applications were tested to see how light might affect the quality of scans underground at Mponeng Mine. To test these scanners, DigiMine was chosen. The third step was to determine what scanning applications were most useful;
- Chapter 4 outlines the methodology that integrated quantitative and qualitative data. In the experimental phase, various scanners were tested at Wits DigiMine before going underground at Mponeng Mine. A 3D LiDAR scanner was tested for durability and practicality

in underground working stopes. Scans were downloaded from scanners and saved on a central server for all departments to access with free software (CloudCompare). Scans were georeferenced and imported into Deswik CAD;

- According to the results chapter, the best combination of a 3D LiDAR scanner and 3D LiDAR scanning application is the Apple iPhone Pro Max since it maps underground geology accurately;
- The 3D scanning method of geological data capture requires less time and energy to produce accurate 3D geological block models than traditional methods. The data is also processed much faster and readily available to the entire mining department. This allows more time to be spent on mine planning and blasting guidance. Communication becomes easier as a digital reference with exact images is displayed and can be viewed by all team members. As a result, the production team will be notified before the next blast of the results of the more frequent data collection; and
- The final chapter concludes the study and makes recommendations for further research.

1.28 Introduction

The research was conducted to identify orebody dilution in an ultra-deep gold mine in South Africa. VCR is highly variable due to its unconformity with Witwatersrand Supergroup sediments. Typically, the orebody dips 18

degrees south and is 120 cm thick. Virgin stresses are predicted between 95 MPa and 135 MPa with a rock density of 2700 kg/m3. Virgin stresses provide a challenge for safe workplace support. Reef rolls on strike and dip. Mining heights must be adjusted constantly to avoid grade dilution. These findings may be helpful to other mining operations in similar areas and under similar conditions. 3D measurements of the orebody are required to plan a mine since mine planning decisions may be influenced by limited information. Innovative mining techniques could increase precision and decrease lags in relaying dilution information. Dynamic 3D details can help achieve this.

1.29 Summary of Chapters

Based on the literature review, 3D modelling is crucial for resource estimation. As of now, geological mapping (tapes and clinometers) is challenging to convert into 3D geological models or display on digital plans. The accuracy of 3D geological models increases mining precision and may increase the average grade. Mining accuracy and prediction can be improved by providing these models more often.

Although 3D laser scanning improves accuracy and efficiency in the mining industry, accurate survey control is still very relevant. Surfaces can be captured more quickly, and the reliance on traditional mapping methods can be reduced. Digital systems provide access to geospatial data to all production team members. A better estimation of ore grade can be achieved

by monitoring blasting. By using 3D scanners, mapping and scanning become more common, and preparation for blasting could be accelerated. Mponeng's narrow, tabular stopes are suitable for 3D scanning systems commonly used in mines.

Quantitative and qualitative data had to be integrated into the methodology. The experimental phase of the research used various specifications of scanners shortlisted in the first phase. Testing was conducted in a controlled environment (Wits DigiMine) before continuing underground at Mponeng Mine. 3D LiDAR scans were captured in underground working stops to test the scanner's durability and practicality. Scans were downloaded from scanners and saved on a central server so that all departments could access them. The scans were geo-referenced and pulled into Deswik CAD using free software such as CloudCompare.

1.30 Research Observations

3D modelling plays a critical role in determining resource estimation and mining costs. Accurate gold grade and mining prediction according to the mine plan informed by the geological block model is crucial to benefit from the predicted profits. High confidence in the accuracy of 3D geological models increases the precision of mining. It, therefore, results in a higher gold grade with regards to an SW that is controlled to prevent dilution if mining proceeds according to plan. The accuracy and prediction of mining

are further enhanced when these models are provided more frequently, specifically before blasting commences.

The Structure Sensor II was tested but found unsuitable for the intended underground applications due to the unavailability of a suitable software application. In addition, it is an add-on to the iPad, making it vulnerable to damage in underground use.

All scans are stored on a digital system whereby the data is always readily available to all members of the geological and production teams. Monitoring of blasted ore becomes a traceable process with higher confidence, which offers increased estimations regarding the gold called for. The frequency of scanning and face mapping increases because the time and effort required when utilising 3D scanners are lessened. Therefore, the entire pre-blasting planning and preparation process can be accelerated since data is readily available within a short period.

The iPad Pro was tested on the surface and in the DigiMine tunnel. Lighting and protecting the iPad Pro were identified as requirements before the underground testing at Mponeng Mine. The 3D Scanning App was identified as the most appropriate app for the scans. Testing was conducted at Mponeng Mine, which was successful. However, the iPad Pro is considered vulnerable to damage, so the iPhone 12 Pro was selected for further development.

1.31 Research Contributions

The time taken to capture the stope face surfaces and the maximum allowable area to be captured and saved will further categorise the value that specific scanner software offers.

It is evident from the research that the most suitable combination of the 3D LiDAR scanner and 3D LiDAR scanning application is the Apple iPhone Pro Max and the 3D Scanner application. This combination is ideally suited to capture acceptable results for geological mapping in an underground environment since it offers greater efficiency and observation of the mining process.

Results have shown a clear benefit from using the dynamic 3D scanning method as an option to capture stope mapping to inform the 3D geological block model. This is evident in the comparison shown in the report between measurements from the scanned image compared to measurements taken underground according to the traditional method using a tape and clinorule.

The rock mass stability is maintained over an area extending at least up to the sweeping line by ensuring the support performance criteria are met. Therefore, the geologist is not permitted to move between the stope face and stope support. Instead, scans must be captured within the supported area. The 5 m scanning range makes it possible to scan from a safe, supported position. The geologist does not need to go beyond the installed

stope support to measure SW or dip direction and from the stope face scan, this information can now be measured.

1.32 Recommendations for Future Research Work

It is recommended that the Apple iPhone Pro Max with the 3D Scanner application should be used in the future to capture 3D geological mapping of stope faces to inform the 3D geological block model dynamically. It is recommended that Deswik CAD software is to be used for geo-referencing of 3D scans and the subsequent creation of the mapping report for the production team. The geological structures captured from the 3D scans using Deswik CAD can then update the 3D geological model.

It is recommended to carry out more tests for robustness and durability and improve the iPhone casing for the scanner for protection and MHSA requirements. According to the MHSA, since the iPhone is a cellular phone, it must adhere to regulations in areas where flammable gas concentrations exceed 1.4% by volume. It is further recommended that Mponeng Mine purchase an iPhone casing that allows devices to be taken into Zone 1 hazardous areas.

It is recommended that the Apple iPhone Pro Max are used to capture the mapping of raises. The mapping information of raises is lost once they are ledged and equipped for stope mining. Samplers and geology assistants can be trained to use the Apple iPhone Pro Max to assist in capturing

information to assist in geological reporting. In addition, this will provide guidance to the production team. Further analysis could be done on recovery numbers to see if better reporting to production teams about SW reduces dilution.

New areas of research that could be investigated include using remote scanning technology. In underground mining operations, it is often difficult to extract data from areas that are difficult to access. Sandvik's fully autonomous aerial vehicle can fly itself through stope panels and underground accident areas, where there is no GPS, no line-of-sight or communications and, using a laser scanning sensor, map the stope panels to create a rich 3D point cloud (Sandvik AB, 2020).

1.33 Conclusions

It is concluded that the captured scans can be geo-referenced within an acceptable error margin in Deswik CAD software. The horizontal displacement between the measured peg and the measured point on the scan is 0.015. This is within the defined accuracy of 0,1 m as defined by the MHSA Chapter 17(14)(b). The time taken to capture the stope face surfaces and the maximum allowable area to be captured and saved will further categorise the value-specific scanner software offers.

Results have shown a clear benefit from using the dynamic 3D scanning method as an option to capture stope mapping to inform the 3D geological

block model. This is evident in the comparison shown in the report between measurements from the scanned image compared to measures taken underground according to the traditional method using a tape and distometer.

Because scans do not take long to capture in the workplace, this has an added safety aspect as mine personnel can spend less time on the face and thus reduce the probability of accidents and injuries. Mine personnel can spend less time on the stope face as technology has enabled remote scanning of workplaces.

REFERENCE LIST

3D Printing Systems South Africa, 2021. *Structure Sensor (Mark 2) is now available.* [Online]
Available at: https://3dprintingsystems.co.za/product/structure-sensor/
[Accessed 20 November 2021].

3D Scan Expert, 2019. *Structure Sensor Mark II features higher resolution & outdoor scanning.* [Online]
Available at: https://3dscanexpert.com/structure-sensor-mark-ii-features-higher-resolution-outdoor-scanning/
[Accessed 20 November 2021].

Academic library, 2022. *Laser Triangulation.* [Online]
Available at: https://ebrary.net/133047/engineering/laser_triangulation
[Accessed 16 August 2022].

Ahamad, N. & Ojha, S. K., 2015. *The practical application of laser scanning in a mining environment.* [Online]
Available at: https://www.ResearchGate.net/publication/301229691
[Accessed 11 September 2021].

Allan, A., 2022. *Basic Sensors in iOS.* [Online]
Available at: https://www.oreilly.com/library/view/basic-sensors-in/9781449309480/ch04.html
[Accessed 11 September 2022].

Anderson, N. & Gall, K., 2020. *An underground mapping to implicit modeling workflow.* [Online]
Available at: https://www.deswik.com/wp-content/uploads/2020/01/An-underground-mapping-to-implicit-modeling-workflow.pdf
[Accessed 06 September 2021].

AngloGold Ashanti, 2020. *Mponeng Mine stoping width performance.* Carletonville(Gauteng): AngloGold Ashanti. Internal company document.

AngloGold Ashanti, 2020. *Mponeng Mine stoping width performance,* Carletonville: AngloGold Ashanti. Internal company document.

Aniwaa Pte. Ltd., 2021b. *Occipital Canvas overview.* [Online]
Available at: https://www.aniwaa.com/product/3d-scanners/occipital-canvas/
[Accessed 25 November 2021].

Aniwaa Pte. Ltd., 2021. *The 8 best 3D scanning apps for smartphones in 2021 (free!).* [Online]
Available at: https://www.aniwaa.com/buyers-guide/3d-scanners/best-3d-scanning-apps-smartphones/
[Accessed 27 November 2021].

Apple Inc., 2021a. *Room Capture - Structure SDK.* [Online]
Available at: https://apps.apple.com/us/app/room-capture-structure-sdk/id916501905
[Accessed 26 November 2021].

Apple Inc., 2021b. *Scanner - Structure SDK.* [Online]
Available at: https://apps.apple.com/us/app/scanner-structure-sdk/id891169722
[Accessed 23 November 2021].

Apple Inc., 2021c. *Scaniverse - LiDAR 3D Scanner.* [Online]
Available at: https://apps.apple.com/us/app/scaniverse-lidar-3d-scanner/id1541433223
[Accessed 26 November 2021].

Apple Inc., 2021d. *3d Scanner App™.* [Online]
Available at: https://apps.apple.com/us/app/3d-scanner-app/id1419913995#?platform=ipad
[Accessed 27 November 2021].

Apple Inc., 2021e. *Polycam - LiDAR & 3D Scanner.* [Online]
Available at: https://apps.apple.com/us/app/polycam-lidar-3d-scanner/id1532482376
[Accessed 27 November 2021].

Apple Inc., 2021f. *SiteScape - LiDAR 3D Scanner.* [Online]
Available at: https://apps.apple.com/us/app/sitescape-lidar-3d-scanner/id1524700432
[Accessed 27 November 2021].

Apple Inc., 2022. *iPhone 12 Pro Max, iPhone 12 mini, and HomePod mini available to order Friday.* [Online]
Available at: https://www.apple.com/ke/newsroom/2020/11/iphone-12-pro-max-iphone-12-mini-and-homepod-mini-available-to-order-friday/
[Accessed 4 September 2022].

Architectural CGI, 2016. *3D modeling things youve got know.* [Online]
Available at: https://archicgi.com/product-cgi/3d-modeling-things-youve-got-know/
[Accessed 6 September 2021].

Arrival 3D, Inc., 2022. *360-Degree panoramic images.* [Online]
Available at: https://arrival3d.com/panoramic-images/
[Accessed 21 August 2022].

Art.Illinois.edu, 2021. *Using the Structure Sensor with the iPad Air.* [Online]
Available at: https://web.faa.illinois.edu/app/uploads/sites/6/2021/05/Structure-Sensor-Scanning-Guide.pdf
[Accessed 23 November 2021].

Aspose Pty Ltd., 2021b. *PDF File Format - What is a PDF file?.* [Online]
Available at: https://docs.fileformat.com/pdf/
[Accessed 25 November 2021].

Auret, J., 2010. *New markings for Ex equipment.* [Online]
Available at: https://www.ee.co.za/wp-content/uploads/legacy/Vector%202010/Markings%20of%20ex%20equipment.pdf
[Accessed 18 September 2022].

Balasubramanian, A., 2017. *Geological mapping procedures.* [Online]
Available at: https://www.ResearchGate.net/publication/313799558
[Accessed 9 September 2021].

BeLight Software Ltd., 2021. *How to Use Room Scanner in Live Home 3D for iPhone and iPad.* [Online]
Available at: https://www.livehome3d.com/useful-articles/how-to-use-

room-scanner-in-live-home-3d-for-iphone-and-ipad
[Accessed 22 December 2021].

Birch, C., 2014. New systems for geological modelling–black box or best practice?. *The Journal of The Southern African Institute of Mining and Metallurgy,* December, 114(12), pp. 995, 1000.

Birch, C., 2018. Geological mapping and modelling training in the University of the Witwatersrand Mine Tunnel, South Africa.. *Journal of the Southern African Institute of Mining and Metallurgy,* August, 118(8a3), pp. 809, 813.

Birch, C., 2021. *Photo - Occipital Structure Sensor (Mark II),* Johannesburg: University of Witwatersrand.

Birch, C., 2021. *Ultimaker S5 printer,* Johannesburg: University of Witwatersrand.

Blaauw, F. & Trevarthen, N., 1987. *Mineral Resource Management: An overview of an Integrated Graphics Based System.* Welkom, APCOM 87, pp. 255-257.

CameraStuff, 2006. *[77046] Godox LEDM150 Mobile LED Video Light with Smartphone Bracket.* [Online]
Available at: https://www.camerastuff.co.za/shop/77046-godox-

ledm150-mobile-led-video-light-with-smartphone-bracket.html
[Accessed 5 January 2022].

Canon medical systems USA, inc., n.d.. *Computed Tomography.* [Online]
Available at: https://us.medical.canon/products/computed-tomography/
[Accessed 2022 August 2022].

CGI Furniture, 2022. *3D File Format for Furniture CGI.* [Online]
Available at: https://cgifurniture.com/3d-file-format-10-types/
[Accessed 11 September 2022].

Chanderman, L., Dohm, C. & Minnitt, R., 2017. 3D geological modelling and resource estimation for a gold deposit in Mali. *Journal of the Southern African Institute of Mining and Metallurgy,* February, 117(n2a10), pp. 190,197.

CloudCompare, 2015. *AirPhotoSE.* [Online]
Available at:
https://www.cloudcompare.org/doc/wiki/index.php/AirPhotoSE
[Accessed 11 September 2022].

CloudCompare, 2020. *3D point cloud and mesh processing software Open Source Project.* [Online]

Available at: https://www.cloudcompare.org/

[Accessed 05 December 2021].

Daehnke, A., Van Zyl, M. & Roberts, M., 2001. Review and application of stope support design criteria. *The Journal of The South African Institute of Mining and Metallurgy,* June, X(3), p. 145.

Datamine, 2019. *STRAT3D.* [Online]

Available at: https://www.dataminesoftware.com/wp-content/uploads/2019/12/Strat3D_Standard-Web.pdf

[Accessed 06 September 2021].

Datamine, 2021a. *Datamine PixPro Photogrammetry.* [Online]

Available at: https://www.dataminesoftware.com/solutions/photogrammetry-solution-pixpro/

[Accessed 06 September 2021].

Datamine, 2021b. *Fusion Geological Data Management Solution*. [Online]

Available at: https://www.dataminesoftware.com/solutions/fusion-geological-data-management/

[Accessed 06 September 2021].

Datamine, 2021c. *Resources and Reserves.* [Online]

Available at: https://www.dataminesoftware.com/sector/resources-

and-reserves/

[Accessed 02 December 2021].

Datamine, 2022a. *MineMapper 3D.* [Online]

Available at:

https://www.dataminesoftware.com/solutions/minemapper-3d-mine-mapping/

[Accessed 2 October 2016].

Datamine, 2022b. *About Datamine.* [Online]

Available at: https://www.dataminesoftware.com/about-us/

[Accessed 16 September 2021].

Department of Mineral Resources and Energy, 2021. *The prevention of flammable gas explosions in mines other than coal mines.* [Online]

Available at:

https://www.gov.za/sites/default/files/gcis_document/202104/44427gon326.pdf

[Accessed 10 September 2022].

Digital Preservation Home, 2020. *Polygon File Format (PLY) Family.*

[Online]

Available at:

https://www.loc.gov/preservation/digital/formats/fdd/fdd000501.shtml

[Accessed 11 September 2022].

Diversified Communications, 2022. *Speed Breakthrough in Time-of-Flight Laser Scanning from Leica Geosystems.* [Online]
Available at: https://www.geoweeknews.com/news/speed-breakthrough-in-time-of-flight-laser-scanning-from-leica-geosystems
[Accessed 16 August 2022].

Dominy, S. C. & Platten, I. M., 2012. Grade control geological mapping in underground gold vein operations.. *Applied Earth Science (Trans. Inst. Min. Metall. B),* 20 October, 121(2), pp. 97-103.

Donnelly, L., 2008. Communication in geology: a personal perspective and lessons from volcanic, mining, exploration, geotechnical, police and geoforensic investigations. *The Geological Society of London,* 4 June, 305(2), pp. 5-14.

E-Architect, 2020. *Measured Building Survey Using 3D Laser Scanning Equipment.* [Online]
Available at: https://www.e-architect.com/articles/measured-building-survey-using-3d-laser-scanning-equipment
[Accessed 17 August 2022].

Ebrahim, M. A., 2011. *3D Laser scanners: History, applications, and future.* [Online]
Available at:
https://www.ResearchGate.net/publication/267037683_3D_laser_sca

nners_history_applications_and_future

[Accessed 23 October 2021].

Esri, 2021. *ArcMap.* [Online]

Available at:

https://desktop.arcgis.com/en/arcmap/latest/extensions/geostatistical-analyst/understanding-geostatistical-analysis.htm#:~:text=Geostatistical%20methods%20are%20based%20on,the%20accuracy%20of%20these%20predictions.

[Accessed 16 August 2022].

ExNor AS, n.d.. *iPhone 13, 12, 12 Pro ATEX/ IECEX Zone 1.* [Online]

Available at: https://exnor.no/product/iphone-atex-iecex-zone-1/

[Accessed 11 September 2022].

Fallara, F., Legault, M. & Rabeau, O., 2006. 3-D Integrated Geological Modeling in the Abitibi Subprovince (Québec, Canada): Techniques and Applications. *Exploration and Mining Geology,* 15(1-2), p. 27.

FARO, 2014. *FARO® Laser Scanner Focus 3D. The perfect instrument for 3D documentation and surveying.* [Online]

Available at:

https://ats.se/pdf/faro/FARO_Laser_Scanner_Focus3D_X_Brochure.pdf

[Accessed 10 December 2022].

File-Extension.info, 2022. *PSZ File Extension.* [Online]
Available at: https://www.file-extension.info/format/psz
[Accessed 11 September 2022].

Funkner, M., 2021. *Polycam 3D Scanning App Review – LiDAR, Photo Mode, Polycam for Web.* [Online]
Available at: https://3dwithus.com/polycam-3d-scanning-app-review-lidar-vs-photo-mode
[Accessed 27 November 2021].

Gallagher, W., 2021. *How to get more from Apple's Measure app..* [Online]
Available at: https://appleinsider.com/articles/21/03/13/how-to-get-more-from-apples-measure-app
[Accessed 20 November 2021].

Geodetic Systems, Inc., 2020. *Basics of Photogrammetry – Contents.* [Online]
Available at: https://www.geodetic.com/basics-of-photogrammetry/
[Accessed 21 August 2022].

Google, 2022. *CSV file: Definition.* [Online]
Available at: https://support.google.com/google-ads/answer/9004364?hl=en
[Accessed 15 August 2022].

GSMArena.com, 2021a. *Apple iPad Pro 11.* [Online]
Available at: https://www.gsmarena.com/apple_ipad_pro_11_(2021)-10865.php
[Accessed 22 December 2021].

GSMArena.com, 2021b. *Compare specs.* [Online]
Available at: https://www.gsmarena.com/compare.php3?idPhone1=10237&idPhone2=10136
[Accessed 20 November 2021].

GSMArena.com, 2021c. *Sensors - definition.* [Online]
Available at: https://www.gsmarena.com/glossary.php3?term=sensors
[Accessed 20 November 2021].

Harmony Gold Mining Company Limited., 2020. *Briefing book.* [Online]
Available at: https://www.harmony.co.za/invest/presentations/2020/send/160-2020/3617-briefing-book-may-2020
[Accessed 15 September 2022].

Harmony, 2022. *Mponeng.* [Online]
Available at: https://www.harmony.co.za/business/sa/mponeng
[Accessed 15 August 2022].

Higgins, S., 2020. *NavVis.* [Online]
Available at: https://www.navvis.com/blog/how-slam-affects-the-accuracy-of-your-scan-and-how-to-improve-it
[Accessed 15 May 2021].

iF Design, 2022. *Leica BLK2GO Imaging laser scanner.* [Online]
Available at: https://ifdesign.com/en/winner-ranking/project/leica-blk2go/282008
[Accessed 19 November 2022].

IGI Global, 2022. *What is Poisson Surface Reconstruction.* [Online]
Available at: https://www.igi-global.com/dictionary/poisson-surface-reconstruction/56464
[Accessed 20 August 2022].

Information Commissioner's Office, 2015. *What is spatial information?.* [Online]
Available at: https://ico.org.uk/media/for-organisations/inspire-regulations-1-0.pdf
[Accessed 06 September 2021].

IoT ONE, 2022. *Inertial Measurement Unit (IMU).* [Online]
Available at: https://www.iotone.com/term/inertial-measurement-unit/t298
[Accessed 19 November 2022].

iPhoneTricks.org, 2021. *iPhoneTricks.org.* [Online]
Available at: https://www.iphonetricks.org/how-to-3d-scan-places-and-objects-with-iphone-12-pro/
[Accessed 27 November 2021].

iStore, 2021. *Buy iPad Pro 11-inch Wi-Fi 256 GB / Apple M1 / Space Grey.* [Online]
Available at: https://www.istore.co.za/ipad-pro-11-inch-wi-fi-256gb-apple-m1-space-grey
[Accessed 22 December 2021].

Johnstone, W., 2003. *Effective multi-dimensional orebody modelling: A key component of the mining value chain.* Johannesburg, South African Institute of Mining and Metallurgy, pp. 325-326.

Lee, S. & Choi, S., 2019. Analyzing the stability of underground mines using 3D point cloud data and discontinuum numerical analysis.. *Multidisciplinary Digital Publishing Institute,* 13 February, 11(4), pp. 11-19.

Leica Geosystems, 2019. *Leica BLK2GO Reality capture handheld.* [Online]
Available at: https://www.archi-tech.co.za/_files/ugd/9139a5_c93787146cfa466a90ef0d2956029045.

pdf

[Accessed 20 August 2022].

Leica-geosystems, 2022. *Leica-geosystems_LG16013480_TS07_3M,* Midrand: Leica-geosystems.

Leonida, C., 2016. *The Intelligent Miner.* [Online] Available at: https://theintelligentminer.com/2020/09/16/mining-and-3d-modelling-technology/

[Accessed 16 September 2021].

Lisle, R., Brabham, P. & Barnes, J., 2011. *Basic Geological Mapping.* Fifth Edition ed. Chichester(West Sussex): John Wiley & Sons, Ltd..

Malan, D. & Basson, F., 1998. Ultra-deep mining: The increased potential for squeezing conditions. *The Journal of the South African Institute of Mining and Metallurgy,* [online] 98(07), p. p.353.

Manzi, M., Hein, K., Durrheim, R. & King, N., 2014. The Ventersdorp Contact Reef model in the Kloof Gold Mine as derived from 3D seismics, geological mapping and exploration borehole datasets.. *International Journal of Rock Mechanics and Mining Sciences,* Volume 66, p. 97.

Math Open Reference, 2011. *Normal.* [Online]
Available at: https://www.mathopenref.com/normal.html
[Accessed 19 November 2022].

Mayo Foundation for Medical Education and Research (MFMER), 2022. *CT scan.* [Online]
Available at: https://www.mayoclinic.org/tests-procedures/ct-scan/about/pac-20393675
[Accessed 17 August 2022].

Medical Device Network, 2022. *GE's SIGNA 7.0T MRI Scanner.* [Online]
Available at: https://www.medicaldevice-network.com/projects/ges-signa-7-0t-mri-scanner/
[Accessed 17 August 2022].

Mijic, N., 2015. *Calibration of the terrestrial laser scanner.* Dubrovnik, RIM 2015.

Miller, S., Hashemian, A., Gillihan, R. & Helms, E., 2022. A Comparison of Mobile Phone LiDAR Capture and Established Ground Based 3D Scanning Methodologies. *SAE Technical Paper,* 29 March.p. 12.

Mine Health and Safety Council, 1996. *Mine Health and Safety Act.* [Online]
Available at:

https://www.dmr.gov.za/Portals/0/Resource%20Center/Mine%20Health%20and%20Safety%20Act%20and%20its%20Regulations/MHS%20Regulations_Chapter%2017_GG%2034308.pdf?ver=2018-03-13-015328-043
[Accessed 14 September 2022].

Mine Health and Safety Council, 2018. *Mine Health and Safety Act, 1996 (Act No. 29 of 1996) and Regulations.* [Online]
Available at:
https://www.mhsc.org.za/sites/default/files/public/publications/Mine%20Health%20and%20Safety%20Act%2029%20of%201996%20and%20Regulations%20Final%20Booklet.pdf
[Accessed 10 September 2022].

Mining Patch Associates, 2017. *Mining software.* [Online]
Available at: http://www.miningsoftware.org/portfolio-posts/surpac/
[Accessed 16 October 2021].

Moberg, J., 2017. *Accuracy, performance and challenges with a low cost 3d scanning platform.* Stockholm: KTH Royal Institute Of Technology.

Morris, A. S. & Langari, R., 2012. *Sensitivity Drift.* [Online]
Available at:

https://www.sciencedirect.com/topics/engineering/sensitivity-drift [Accessed 4 November 2021].

Moyo, A., 2018. *Wits, Sibanye create R27.5m DigiMine facility.* [Online] Available at: https://www.itweb.co.za/content/WnpNgM2A2oj7VrGd [Accessed 12 September 2022].

Mponeng Mine, 2021. *Mapping report 120-85 RSE 2.pdf,* Carletonville: Harmony Gold. Internal company document.

Munro, A., 2022. *HILTI Distometer,* Carlrtonville. Internal company document: Harmony.

Nagel, S., 2022. *Brass spad with numbered copper disc.* Carletonville: Harmony.

National Institutes of Health, n.d.. *Glossary of Terms.* [Online] Available at: https://www.nibib.nih.gov/science-education/glossary [Accessed 17 August 2022].

O'Reilly Media, Inc., 2022. *Signed and unsigned numbers.* [Online] Available at: https://www.oreilly.com/library/view/introduction-to-digital/9780470900550/chap2-sec009.html#:~:text=Unsigned%20binary%20numbers%20are%2C%

20by,to%20FF16%20in%20hexadecimal.

[Accessed 3 September 2022].

Occipital, Inc., 2020a. *Structure SDK (iOS) Release Notes.* [Online]
Available at: https://support.structure.io/article/623-sdk-release-notes
[Accessed 23 November 2021].

Occipital, Inc., 2020b. *How do I save files after using Scanner and Room Capture?.* [Online]
Available at: https://support.structure.io/article/150-how-do-i-save-files-after-scanning
[Accessed 26 November 2021].

Occipital, Inc., 2020c. *Can I use Structure Sensor (Mark II) or Structure Core for industrial purposes.* [Online]
Available at: https://support.structure.io/article/405-can-i-use-structure-sensor-mark-ii-or-structure-core-for-industrial-purposes
[Accessed 20 November 2021].

Occipital, Inc., 2020d. *What is the difference between the original Structure Sensor and Structure Sensor (Mark II)?.* [Online]
Available at: https://support.structure.io/article/397-what-is-the-difference-between-the-original-structure-sensor-and-structure-sensor-mark-ii
[Accessed 20 November 2021].

Occipital, Inc., 2021a. *Capture spaces in 3D with an iPad or iPhone.* [Online]
Available at: https://canvas.io/
[Accessed 25 November 2021].

Occipital, Inc., 2021b. *I need higher accuracy than 1-2%. Can I submit my own dimensions to improve accuracy?.* [Online]
Available at: https://support.canvas.io/article/198-how-to-submit-manual-dimensions-to-canvas
[Accessed 25 November 2021].

Occipital, Inc., 2021c. *The fast-track Scan-to-BIM workflow for Revit.* [Online]
Available at: https://canvas.io/export-revit
[Accessed 25 November 2021].

Occipital, Inc., 2021d. *The easy button for as-built 2D drawings.* [Online]
Available at: https://canvas.io/export-2d-drawings
[Accessed 25 November 2021].

Occipital, Inc., 2021e. *Structure SDK.* [Online]
Available at: https://structure.io/developers
[Accessed 23 November 2021].

Occipital, Inc., 2021f. *Simple, precise 3D scanning for orthotics and prosthetics.* [Online]
Available at: https://structure.io/use/orthotics-prosthetics
[Accessed 02 December 2021].

Optron group, 2018. *ZEB Revo RT.* [Online]
Available at: https://optron.com/geoslam/wp-content/uploads/2020/05/ds_zebrevort.pdf
[Accessed 20 August 2022].

Optron Group, 2018. *ZEB Revo RT Real-Time Handheld Scanner.* [Online]
Available at: https://optron.com/geoslam/products/zeb-revo-rt/
[Accessed 19 November 2022].

Oracle Corporation, 2010. *Chapter 7 Object File Format.* [Online]
Available at: https://docs.oracle.com/cd/E19683-01/817-3677/chapter6-46512/index.html
[Accessed 10 September 2022].

Orefind, 2017. *Orefind's 3D geological models created with Leapfrog implicit geological modelling software.* [Online]
Available at: http://www.orefind.com/media/leapfrog-models
[Accessed 28 December 2021].

Pandey, S., 2022. *Ore body modelling- concepts and techniques,* San Francisco: Academia.

Pepkor Trading Ltd. Pty., 2022. *Apple iPad Pro 11 inch Wi-Fi 256GB Space Grey.* [Online]
Available at: https://www.incredible.co.za/apple-ipad-pro-11-inch-wi-fi-256gb-space-grey
[Accessed 10 September 2022].

Pethe, A., 2008. *Super resolution 3d scanning using spatial light modulator and band correction modulator and band correction,* Kentucky: University of Kentucky.

Poniewierski, J., 2019. *Block model knowledge for mining engineers – an introduction,* Brisbane: Deswik.

Prerna, R. & Singh, C. K., 2015. Evaluation of LiDAR and image segmentation based classification techniques for automatic building footprint extraction for a segment of Atlantic County, New Jersey. *Geocarto International,* 2 September.pp. 4-5.

Reality Capture Review, 2018. *Preview: 3D Room Scanning with canvas & structure sensor.* [Online]
Available at: https://3dscanexpert.com/canvas-3d-room-scanning-

structure-sensor/

[Accessed 10 September 2022].

Resources Computing International Ltd, n.d.. *G-EXEC geological data handling system.* [Online]

Available at: https://www.mcjones.org/System_R/g-exec.html

[Accessed 15 August 2022].

RIEGL Laser measurement systems, 2020. *RIEGL VZ-6000 datasheet.* [Online]

Available at: http://www.riegl.com/uploads/tx_pxpriegldownloads/RIEGL_VZ-6000_Datasheet_2020-09-14.pdf

[Accessed 21 August 2022].

Roberts, M. & Schweitzer, J., 1999. Geotechnical areas associated with the Ventersdorp Contact Reef, Witwatersrand Basin, South Africa. *The Journal of The South African Institute of Mining and Metallurgy,,* 99((03)), p. 159.

Rock Mapper Helpdesk, 2022. *Georeference Point Cloud in CloudCompare.* [Online]

Available at: https://help.rockmapper.net/support/solutions/articles/51000252974-

georeference-point-cloud-in-cloudcompare

[Accessed 3 September 2022].

Rodin4D, 2021. *3D scanners Structure Sensor Mark II.* [Online]

Available at: https://www.rodin4d.com/en/structure-sensor/

[Accessed 20 November 2021].

Rogers, W. & Kanchibotla, S., 2013. Blast modelling. In: *Rock fragmentation by blasting.* Boca Raton(Florida): CRC Press is an imprint of Taylor & Francis Group, an Informa business, p. 263.

Russell, T. & Stacey, T., 2019. Using laser scanner face mapping to improve geotechnical data confidence at Sishen mine. *Journal of the Southern African Institute of Mining and Metallurgy,* January, 119(1), pp. 11-20.

Sandvik AB, 2020. *Innovation - Flying underground.* [Online]

Available at:

https://www.home.sandvik/en/stories/articles/2020/09/exyn-drones/

[Accessed 11 December 2022].

SCCS Survey, 2015. *Leica FlexLine TS07 Manual Total Station.* [Online]

Available at: https://www.sccssurvey.co.uk/leica-flexline-ts07-manual-total-station.html

[Accessed 22 November 2021].

SCCS Survey, 2022. *Leica RTC360 Laser Scanner.* [Online]
Available at: https://www.sccssurvey.co.uk/leica-rtc360-laser-scanner.html
[Accessed 21 August 2022].

Seequent Limited, n.d.. *Our story.* [Online]
Available at: https://www.seequent.com/company/mission-purpose/our-story/
[Accessed 16 September 2021].

Septarini, A., Soeksmantono, B. & Wikantika, K., 2013. *Lidar application study to calculate mine excavation volume.* Bandung, ResearchGate, pp. 1-5.

Sharpened Productions, 2021a. *.DAE File Extension.* [Online]
Available at: https://fileinfo.com/extension/dae
[Accessed 25 November 2021].

Sharpened Productions, 2021b. *.DXF File Extension.* [Online]
Available at: https://fileinfo.com/extension/dxf
[Accessed 27 November 2021].

Sharpened Productions, 2021c. *.GLB File Extension.* [Online]
Available at: https://fileinfo.com/extension/glb
[Accessed 27 November 2021].

Sharpened Productions, 2021d. *GLTF File Extension.* [Online]
Available at: https://fileinfo.com/extension/gltf
[Accessed 27 November 2021].

Sharpened Productions, 2021e. *.JPG File Extension.* [Online]
Available at: https://fileinfo.com/extension/jpg
[Accessed 26 November 2021].

Sharpened Productions, 2021f. *.LAS File Extension.* [Online]
Available at: https://fileinfo.com/extension/las
[Accessed 26 November 2021].

Sharpened Productions, 2021g. *.MTL File Extension.* [Online]
Available at: https://fileinfo.com/extension/mtl
[Accessed 26 November 2021].

Sharpened Productions, 2021h. *.OBJ File Extension.* [Online]
Available at: https://fileinfo.com/extension/obj
[Accessed 26 November 2021].

Sharpened Productions, 2021i. *.PLY File Extension.* [Online]
Available at: https://fileinfo.com/extension/ply
[Accessed 27 November 2021].

Sharpened Productions, 2021j. *.PNG File Extension.* [Online]
Available at: https://fileinfo.com/extension/png
[Accessed 27 November 2021].

Sharpened Productions, 2021k. *.PTS File Extension.* [Online]
Available at: https://fileinfo.com/extension/pts
[Accessed 27 November 2021].

Sharpened Productions, 2021l. *.STL File Extension.* [Online]
Available at: https://fileinfo.com/extension/stl
[Accessed 27 November 2021].

Sharpened Productions, 2021m. *.USDZ File Extension.* [Online]
Available at: https://fileinfo.com/extension/usdz
[Accessed 27 November 2021].

Sharpened Productions, 2021n. *.XYZ File Extension.* [Online]
Available at: https://fileinfo.com/extension/xyz
[Accessed 27 November 2021].

Sketchfab, 2021a. *Occipital Room Capture Mesh.* [Online]
Available at: https://sketchfab.com/3d-models/occipital-room-capture-mesh-3023b241350a40cc80064ba8ea453532
[Accessed 26 November 2021].

Sketchfab, 2021b. *Popular 3D models.* [Online]
Available at: https://sketchfab.com/scaniverse
[Accessed 26 November 2021].

South VI Instruments, n.d.. *Total Station N70.* [Online]
Available at: http://www.southsurvey.co.za/N70.html
[Accessed 22 November 2021].

Sphinx, n.d.. *Estimating Surface Normals in a PointCloud.* [Online]
Available at:
https://pcl.readthedocs.io/projects/tutorials/en/latest/normal_estimation.html
[Accessed 20 August 2022].

SRK Consulting (UK) Limited, 2012. *Mineral resource estimate for the Kagem emerald deposit of Gemfields resources PLC, Zambia,* City and County of Cardiff: SRK Consulting (UK) Limited 2011.

Staiger, R., 2003. *Terrestrial laser scanning technology, systems and applications.* Marrakech, 2nd FIG Regional Conference.

Taubin, G., Moreno, D. & Lanman, D., 2014. *3D scanning for personal 3D printing: Build your own desktop 3D scanner,* Vancouver: ResearchGate,

TC Join TechCrunch, 2021. *Occipital's Structure Sensor Mark II is a smaller and much improved 3D scanner for your iPad.* [Online]
Available at: https://techcrunch.com/2019/07/24/occipitals-structure-sensor-mark-ii-is-a-smaller-and-much-improved-3d-scanner-for-your-ipad/
[Accessed 20 November 2021].

Techopedia Inc., 2022. *LCD Projector.* [Online]
Available at: https://www.techopedia.com/definition/17178/lcd-projector
[Accessed 19 November 2022].

Thess, F., 2022. *Scaniverse - LiDAR scans with your iPhone.* [Online]
Available at: https://www.specularfilms.com/post/scaniverse-lidar-scans-with-your-iphone
[Accessed 11 September 2022].

Trebuňa, P., Mizerák, M. & Rosocha, L., 2018. 3D Scaning – technology and reconstruction. *International Scientific Journal about Simulation,* 15 September, 4(3), pp. 3-5.

University of the Witwatersrand, 2020. *About DigiMine.* [Online]
Available at: https://www.wits.ac.za/wmi/digimine/about-digimine/
[Accessed 13 August 2022].

University of the Witwatersrand, n.d.. *MRM Overview - Sampling, Geological Modelling and Resource Modelling,* Johannesburg: University of Witwatersrand.

V. I. Instruments, 2022. *7736-VI INSTRUMENTS-N7-SPECIAL-V1,* Johannesburg: V. I. Instruments.

Vollgger, S. A., Cruden, A. R., Ailleres, L. & Cowan, E. J., 2015. Regional dome evolution and its control on ore-grade distribution: Insights from 3D implicit modelling of the Navachab gold deposit, Namibia. *Elsevier B.V. ScienceDirect,* September, Volume 69, pp. 268-264.

Wang, W. L. J., Wang, C., Luo, B. & Zhang, C., 2021. DV-LOAM: Direct Visual LiDAR Odometry and Mapping. *Molecular Diversity Preservation International - Remote Sensing,* 23 August, 13(16), pp. 14, 21, 35.

Wilson, M., 2020. *What is a LiDAR scanner, the iPhone 12 Pro's camera upgrade, anyway?.* [Online]
Available at: https://global.techradar.com/en-za/news/what-is-a-lidar-scanner-the-iphone-12-pros-rumored-camera-upgrade-anyway
[Accessed 20 November 2021].

Wolfram Research, Inc., 2022. *Least Squares Fitting.* [Online]
Available at: https://mathworld.wolfram.com/LeastSquaresFitting.html
[Accessed 20 August 2022].

WordPress.com., 2011. *Braindering with ASCII files.* [Online]
Available at: https://brainder.org/tag/ply/
[Accessed 11 September 2022].

Xingwana, L., 2016. Monitoring ore loss and dilution for mine-to-mill integration in deep gold mines: A survey-based investigation. *Journal of the Southern African Institute of Mining and Metallurgy,* February, 116(2), p. 149.

Yashchuk, V. V., 2009. *Optimal measurement strategies for effective suppression of drift errors,* California: Lawrence Berkeley National Laboratory.

Zola, A. & Fontecchio, M., 2021. *Spatial data.* [Online]
Available at: https://searchsqlserver.techtarget.com/definition/spatial-data
[Accessed 06 September 2021].